UNIVERSIDADE FEDERAL DE SANTA CATARINA
CAMPUS FLORIANÓPOLIS
PROGRAMA DE PÓS-GRADUAÇÃO EM ENGENHARIA DE AUTOMAÇÃO E SISTEMAS

Ivan Francisco Yupanqui Tello

Contribution to State Estimation of Semilinear Parabolic Distributed Parameter Systems with Applications to Transport Reaction Systems

Mons
2021

Ivan Francisco Yupanqui Tello

Contribution to State Estimation of Semilinear Parabolic Distributed Parameter Systems with Applications to Transport Reaction Systems

Tese submetida ao Programa de Pós-Graduação em Engenharia de Automação e Sistemas da Universidade Federal de Santa Catarina e pela Instituição Université de Mons em regime de cotutela para a obtenção do título de Doutor em Engenharia de Automação e Sistemas.
Orientador: Prof. Daniel Coutinho, Dr. (UFSC),
Prof. Alain Vande Wouwer, Dr. (UMONS)

Mons
2021

Ficha de identificação da obra elaborada pelo autor,
através do Programa de Geração Automática da Biblioteca Universitária da UFSC.

Yupanqui Tello, Ivan Francisco
Contribution to State Estimation of Semilinear Parabolic Distributed Parameter Systems with Applications to Transport Reaction Systems / Ivan Francisco Yupanqui Tello ; orientador, Daniel Coutinho, orientador, Alain Vande Wouwer, 2022.
153 p.

Tese (doutorado) - Universidade Federal de Santa Catarina, Centro Tecnológico, Programa de Pós-Graduação em Engenharia de Automação e Sistemas, Florianópolis, 2022.

Inclui referências.

Trabalho elaborado em regime de co-tutela.

1. Engenharia de Automação e Sistemas. 2. Sistemas de Parâmetros Distribuídos. 3. Sistemas de Reação de Transporte. 4. Estimação de Estado. 5. Equações Diferenciais Parciais. I. Coutinho, Daniel. II. Vande Wouwer, Alain III. Universidade Federal de Santa Catarina. Programa de Pós Graduação em Engenharia de Automação e Sistemas. IV. Título.

Ivan Francisco Yupanqui Tello

Contribution to State Estimation of Semilinear Parabolic Distributed Parameter Systems with Applications to Transport Reaction Systems

O presente trabalho em nível de doutorado foi avaliado e aprovado por banca examinadora composta pelos seguintes membros:

Prof. Gustavo de Andrade, Dr.
Instituição Universidade Federal de Santa Catarina-UFSC

Laurent Dewasme, Dr.
Instituição Université de Mons-UMONS

Prof. Nicolas Gillis, Dr.
Instituição Université de Mons-UMONS

Prof. Joseph Winkin, Dr.
Instituição Université de Namur-UNAMUR

Prof. Thomas Meurer, Dr.
Instituição Christian-Albrechts-Universität zu Kiel-CAU

Certificamos que esta é a **versão original e final** do trabalho de conclusão que foi julgado adequado para obtenção do título de Doutor em Engenharia de Automação e Sistemas.

Documento assinado digitalmente

Werner Kraus Junior
Data: 21/01/2022 16:04:16-0300
CPF: 531.085.239-53
Verifique as assinaturas em https://v.ufsc.br

Coordenação do Programa de
Pós-Graduação

Documento assinado digitalmente

Daniel Ferreira Coutinho
Data: 21/01/2022 15:30:19-0300
CPF: 379.169.980-68
Verifique as assinaturas em https://v.ufsc.br

Prof. Daniel Coutinho, Dr.
Orientador

Prof. Alain Vande Wouwer, Dr.
Orientador

Mons, 2021.

I dedicate my work to my family.

ACKNOWLEDGEMENTS

I would like to express my sincere gratitude to my supervisors Dr. Daniel Coutinho and Dr. Alain Vande Wouwer for their appreciable inspiration, support and patience throughout my research and acting as a mentors to my overall professional development. The critical reviews and recommendations that they provided for the improvement of my articles and presentations were very valuable. They were great supervisors and it was a great pleasure to have the opportunity to work under their supervision.

Special gratitude to the members of the jury of my thesis, Prof. Gustavo Andrade (Universidade Federal de Santa Catarina), president of the jury and Dr. Laurent Dewasme (Université de Mons), secretary, Prof. Nicolas Gillis (Université de Mons), Prof. Thomas Meurer (Christian-Albrechts-Universität zu Kiel) and Prof. Joseph Winkin (Université de Namur). I would like to give special thanks to all them for their insightful comments about the thesis manuscript.

To my family, words cannot fully express how deeply grateful I am for all of your love and support. For my wife, my parents and sisters, thank you for believing in me and for encouraging me to pursue this path. Without all of your patience and empathy, I would not have been able to see this through. I hope to have made you proud.

“The men who have succeeded are men who have chosen one line and stuck to it.”
(Andrew Carnegie)

RESUMO

Os sistemas de reação de transporte são descritos por equações diferenciais parciais parabólicas semilineares (PDEs) e são fundamentais em aplicações onde os processos de difusão devem ser considerados explicitamente. O problema de estimação de estado com base em medições distribuídas no domínio não é trivial. Neste trabalho, abordamos esse problema para uma determinada classe de sistemas de reação de transporte. Para realizar essa tarefa, propomos estratégias de projeto do observador no quadro de ambas as abordagens de agrupamento inicial e tardia.

Em relação à abordagem de agrupamento inicial para o projeto do observador de estado, usamos o Método dos Resíduos Ponderados (MWR), que abrange o método de colocação ortogonal, para derivar um modelo de ordem reduzida aproximado, expresso como um conjunto de equações diferenciais ordinárias (ODEs) sujeito às restrições algébricas. Em seguida, um método de projeto baseado em Lyapunov é proposto para o modelo de ordem reduzida que fornece condições de projeto suficientes em termos de desigualdades matriciais lineares padrão (LMIs) visando a convergência exponencial do erro de estimativa com uma taxa de decaimento prescrita. O desempenho do observador é ainda melhorado por meio de um algoritmo *off-line* do posicionamento ótimo dos sensores considerando a parametrização da matriz de saída de ordem reduzida.

Com respeito à abordagem de agrupamento tardio, em primeiro lugar, estudamos a representação em operadores de semigrupo que nos leva ao uso das propriedades de decomposição espectral relacionadas aos operadores diferenciais parabólicos. Assim, objetivamos obter condições de síntese de observador de estado suficientes com base nas propriedades locais de lipschitz das funções do vetor de taxa de reação considerando um ganho de injeção de tipo modal. Em segundo lugar, o método de projeto baseado em Lyapunov é proposto para a estabilização da dinâmica do erro de estimação. A abordagem usa matrizes definidas positivas para parametrizar uma classe de funcionais de Lyapunov que são positivos no espaço das funções integráveis quadradas de Lebesgue. Assim, as condições de estabilidade podem ser expressas como um conjunto de restrições LMI que podem ser resolvidas numericamente usando programação de soma de quadrados (SOS) e ferramentas de programação semi-definida (SDP).

Ao longo dos capítulos desta tese, todas essas técnicas e métodos propostos são aplicados e testados numericamente aos casos representativos de processos de reatores tubulares bioquímicos. Os resultados da simulação apoiam a eficácia dos projetos sugeridos.

Finalmente, o problema de monitoramento de propagação do COVID-19 é abordado na parte de aplicação desta tese. Em particular, abordamos a estimação de estado do modelo compartimental modelado por um sistema de equações diferenciais parciais, que descreve a propagação da doença infecciosa em uma população hospedeira. O método de projeto baseado em Lyapunov e parametrização polinomial das variáveis de decisão é usado para derivar um problema de programação semi-definida cuja

solução fornece os ganhos de injeção do observador de estado do tipo Luenberger. Experimentos numéricos são apresentados para ilustrar a eficiência do método.

Palavras-chave: Sistemas de parâmetros distribuídos. Sistemas de transporte-reação. Estimativa de estado. Equações diferenciais parciais parabólicas semi-lineares.

RESUMO EXPANDIDO

Introdução

Os processos de reação de transporte são caracterizados pelo acoplamento de fenômenos de advecção, difusão e reação, e estão presentes em muitos processos científicos e industriais sendo fundamentais em aplicações da química, biologia, meteorologia, epidemiologia, dinâmica de fluidos e em outras áreas das ciências aplicadas. Os processos de reação de transporte são modelados por equações diferenciais parciais (PDEs) e junto com muitos outros (como os sistemas modelados por equações integrais e equações diferenciais de retardo) são chamados de sistemas de parâmetros distribuídos (DPSs). A estimação de estado de sistemas modelados por PDEs é um problema particularmente delicado em vista da dimensionalidade infinita do sistema e pelo fato de que dispor de um conjunto grande de sensores é fisicamente e economicamente inviável. Nesse caso, os estados internos devem ser estimados com base no modelo matemático e nas medições (disponíveis) fornecidas por sensores localizados em posições estratégicas no domínio espacial.

Objetivos

O objetivo fundamental desta Tese é desenvolver técnicas de síntese de observadores de estado com vistas a estimar as variáveis de estado de certa classe de sistemas de reação de transporte para fins de realimentação e/ou monitoramento. Motivado pelo fato de que a dinâmica deste último é descrita por sistemas semilineares de PDEs, que podem ser formulados como uma equação diferencial semilinear em um espaço de estados de dimensão infinita, várias técnicas no quadro das abordagens de agrupamento inicial e tardia da teoria de sistemas são descritas e/ou desenvolvidas e aplicadas a este modelo. Para atingir o objetivo principal, são definidos os seguintes objetivos específicos: (i) obter um modelo reduzido aproximado utilizando o método de colocação ortogonal da classe de sistemas de interesse e estudar o seu grau de precisão com respeito à seleção dos pontos de colocação, (ii) projetar um observador de estado baseado em Lyapunov do modelo de ordem reduzida que garanta a convergência exponencial da dinâmica do erro de estimação, (iii) estudar as propriedades espectrais do operador diferencial multivariável de segunda ordem relacionadas a sistemas de reação de transporte e as propriedades de Lipschitz da função taxa de reação, a fim de obter condições suficientes para o projeto de observador de estado modal, (iv) projetar um observador de estado baseado na teoria de Lyapunov do sistema de PDEs semilineares descrevendo a classe de sistemas de reação de transporte de interesse usando parametrização polinomial de tal forma que os parâmetros do observador possam ser obtidos por meio da solução de um programa de soma de quadrados (SOSs), (v) testar numericamente as metodologias de estimação de estado desenvolvidas em aplicações de processos bioquímicos de referência.

Metodologia

Neste trabalho abordamos o problema de estimação de estado para uma determinada classe de sistemas de reação de transporte. Para realizar essa tarefa, propomos estratégias de projeto do observador usando as abordagens de agrupamento inicial e tardia. Assim, métodos de projeto baseado em Lyapunov e na teoria de semigrupos são propostos para a estabilização da dinâmica do erro de estimação. As condições de

estabilidade podem ser expressas como um conjunto de restrições LMI que podem ser resolvidas numericamente usando ferramentas padrão de programação semi-definida (SDP).

Resultados e Discussão

Esta tese é uma tentativa de fornecer uma estrutura tratável para processos multi-estados considerando medições distribuídas no domínio espacial. As técnicas de estimação de estado propostas reduzem significativamente a complexidade da análise de estabilidade da dinâmica do erro usando condições de setor algébrico local para representar a dinâmica do erro como um sistema de tipo Lure. Ao longo dos capítulos desta tese as técnicas e métodos propostos são aplicados e testados numericamente aos casos representativos de processos de reatores tubulares bioquímicos onde os resultados da simulação apoiam a eficácia dos projetos sugeridos. Finalmente, o problema de monitoramento da propagação do COVID-19 é abordado no capitulo final desta tese, em particular, abordamos a estimação de estado do modelo compartimental modelado por um sistema de equações diferenciais parciais, que descreve a propagação da doença infecciosa em uma população hospedeira. O método de projeto baseado em Lyapunov com parametrização polinomial das variáveis de decisão é usado para derivar um problema programação semi-definida cuja solução fornece os ganhos de injeção do observador de estado do tipo Luenberger. Experimentos numéricos são apresentados para ilustrar a eficiência do método.

Considerações Finais

As técnicas propostas nesta tese foram elaboradas à luz de uma exploração motivada de abordagens reconhecidas e amplamente utilizadas na literatura da teoria de sistemas. Assim, o problema de estimação de estado foi abordado em uma estrutura unificadora combinando (i) técnicas de redução de modelo, (ii) teoria de semigrupos, (iii) teoria de Lyapunov e (iv) programação semi-definida e de soma de quadrados. Tendo em vista os estudos anteriores registrados na literatura, as técnicas propostas de projeto fornecem inovações importantes, compreendendo (i) o projeto sistemático através da utilização de ferramentas de programação semi-definidas para calculas os parâmetros dos observadores de estado de sistemas multi-estado, (ii) aprimoração da convergência através da otimização dos posicionamentos dos sensores e das condições iniciais do observador projetado. Essas características de projeto foram possíveis devido a uma combinação frutífera das ferramentas matemáticas e computacionais para programação semi-definida, bem como métodos de análise e projeto.

Palavras-chave: Sistemas de parâmetros distribuídos. Sistemas de transporte-reação. Estimativa de estado. Equações diferenciais parciais parabólicas semi-lineares.

ABSTRACT

Transport–reaction systems are described by semilinear parabolic partial differential equations (PDEs) and are fundamental in applications where diffusion processes must be considered explicitly. The state estimation problem on the basis of some in-domain distributed measurements is non-trivial. In this work we address this problem for a certain class of transport-reaction systems. To achieve this task, we propose observer design strategies in the frame of both early and late lumping approaches.

Regarding the early lumping approach for the state observer design, we use the Method of Weighted Residuals (MWR), that encompasses the orthogonal collocation method, to derive an approximate reduced-order model, expressed as a set of ordinary differential equations (ODEs) subject to algebraic constraints. Then, a Lyapunov-based design method is proposed for the reduced-order model which provides sufficient design conditions in terms of standard linear matrix inequalities (LMIs) aiming at the exponential convergence of the estimation error with a prescribed decay rate. The observer performance is further improved through an offline optimal sensor placement algorithm considering a parameterized reduced-order output matrix.

Concerning the late lumping approach, firstly, we studied the operator semi-group representation which lead us to the use of the spectrum-decomposition properties related to parabolic differential operators. Thus we aimed at obtaining sufficient state observer synthesis conditions based on the local lipschitz properties of the reaction rate vector functions considering a modal output injection gain. Secondly, a Lyapunov based design method is proposed for the stabilization of the estimation error dynamics. The approach uses positive definite matrices to parameterize a class of Lyapunov functionals that are positive in the space of Lebesgue square integrable functions. Thus, the stability conditions can be expressed as a set of LMI constraints which can be solved numerically using sum of squares (SOS) and standard semi-definite programming (SDP) tools.

Throughout the chapters of this thesis, all these proposed techniques and methods are applied and tested numerically to the representative cases of biochemical tubular reactor processes. Simulation results support the effectiveness of the suggested designs.

Finally, the COVID-19 spread monitoring problem is addressed in the application part of this thesis. In particular, we tackle the state estimation of the compartmental model based on partial differential equations (PDEs) which describes the spread of the infectious disease in a host population. A Lyapunov based design method with SOS and polynomial parameterization of the decision variables is used to derive a SDP problem whose solution provides the injection gains of the Luenberger type state observer, Numerical experiments are presented to illustrate the method efficiency.

Keywords: Distributed parameter systems. Transport-reaction systems. State estimation. Semi-linear parabolic partial differential equations.

LIST OF FIGURES

LIST OF TABLES

ABBREVIATIONS

ODEs	Ordinary differential equations.
PDEs	Partial differential equations.
LPSs	Lumped parameter systems.
DPSs	Distributed parameter systems.
POD	Proper orthogonal decomposition.
SDP	Semidefinite programming.
LMIs	Linear matrix inequalities.
SOSs	Sum of squares.
a.c	Absolutely continuous.

LIST OF SYMBOLS

$\mathbb{N}$	Set of Natural numbers.
$\mathbb{R}$	Set of Real numbers.
$\mathbb{R}^+$	Set of Real positive numbers.
$\mathbb{R}^{m\times n}$	Vector space of m-by-n real matrices.
$\mathbb{S}^n$	Set of all real symmetric matrices of dimension n-by-n.
I_n	Identity matrix of size n.
$0_{m\times n}$	Matrix of zeros of size $m \times n$.
$\otimes$	Kronecker product.
δ_{nm}	Kronecker delta of the arguments n and m.
A^T	Transpose of the matrix A.
A^{-1}	Inverse of the matrix A.
$A > 0$	$A \in \mathbb{S}^n$ and is positive definite.
$A \geq 0$	$A \in \mathbb{S}^n$ and is semi-positive definite.
$A < 0$	$A \in \mathbb{S}^n$ and is negative definite.
$A \leq 0$	$A \in \mathbb{S}^n$ and is semi-negative definite.
$\mathrm{He}\{\cdot\}$	Hermitian operator, $\mathrm{He}\{A\} = A + A^T$.
$\mathrm{vec}\,(A)$	Column vector by vertically stacking the columns of the matrix A.
$\mathrm{diag}\,(\cdots)$	Block-diagonal matrix.
$\lambda_{\max}(A)$	Largest eigenvalue of matrix A.
$\sigma_{\max}(A)$	Largest singular value of matrix A.
∂_t	Partial time differential operator.
∂_z	First order partial space differential operator with respect to z .
∂_z^2	Second order partial space differential operator with respect to z.
∇_z	Gradient vector operator with respect to $z \in \mathbb{R}^{n_z}$.
Δ_z	Laplace operator with respect to the cartesian coordinate system defined by $z \in \mathbb{R}^{n_z}$.
Ω	A domain $\Omega \subset \mathbb{R}^2$, i.e. a connected, open subset of $\mathbb{R}^2$.
$\overline{\Omega}$	Closure of Ω.
$\partial\Omega$	Boundary of Ω.
$\mathcal{H}$	Infinite dimensional Hilbert state space.
$\langle\cdot,\cdot\rangle_{\mathcal{H}}$	$\langle u, v\rangle_H$, inner product of u and v in $\mathcal{H}$.
$\|\cdot\|_{\mathcal{H}}$	$\|x\|_{\mathcal{H}}$, norm of x in $\mathcal{H}$.
$\mathbf{L}_2^{n_x}(a,b)$	Hilbert space of square Lebesgue integrable real vector valued functions on the interval $(a,b) \in \mathbb{R}$, i.e. $\mathbf{L}_2^{n_x}(a,b) = \left\{ x : (a,b) \to \mathbb{R}^{n_x} : \left(\int_a^b x^T(z)x(z)dz \right)^{\frac{1}{2}} < \infty \right\}$.

$\mathbf{L}_2^{n_x}(\Omega)$	Hilbert space of square Lebesgue integrable real vector valued functions on the region $\Omega \in \mathbb{R}^2$, i.e. $\mathbf{L}_2^{n_x}(\Omega) = \left\{ x : \Omega \to \mathbb{R}^{n_x} : \left(\int_\Omega x^T(z)x(z)d\Omega \right)^{\frac{1}{2}} < \infty \right\}$.
$\mathbf{C}[a, b]$	Class of continuous functions from $[a, b]$ to $\mathbb{R}$.
$\mathbf{C}([a, b]; \mathcal{H})$	Class of continuous functions from $[a, b]$ to $\mathcal{H}$.
$\mathbf{C}^1([a, b]; \mathcal{H})$	Class of continuously differentiable functions from $[a, b]$ to $\mathcal{H}$.
$\mathcal{A}$	State linear operator.
$\mathcal{C}$	Output linear operator.
$\ker\mathcal{A}$	Kernel of the operator $\mathcal{A}$.
$\text{ran}\mathcal{A}$	Range of the operator $\mathcal{A}$.
$\mathcal{D}(\mathcal{A})$	Domain of the operator $\mathcal{A}$.
$\mathcal{S}_\mathcal{A}(t)$	C_0-semigroup generated by the operator $\mathcal{A}$.
$\sigma(\mathcal{A})$	Spectrum of the operator $\mathcal{A}$.
$\mathcal{L}(\mathcal{H}_1, \mathcal{H}_2)$	Space of all linear, bounded operators from $\mathcal{H}_1$ to $\mathcal{H}_2$.
$\mathcal{L}(\mathcal{H})$	Space of all linear, bounded operators from $\mathcal{H}$ to $\mathcal{H}$.
$Z_m(z)$	Vector of monomials up to degree m, i.e. $Z_m(z) = \begin{bmatrix} 1 & z & \cdots & z^{m-1} & z^m \end{bmatrix}^T$.
$\{\ell_n(z) : n = 1, ..., N\}$	Lagrange basis polynomials with interpolation nodes $0 = z_1 < z_2 < \cdots < z_{N-1} < z_N = 1$ and where $\ell_n(z) = \prod_{\substack{m=1 \\ m \neq n}}^{N} \frac{z - z_m}{z_n - z_m}$, $n = 1, ..., N$.
$\mathbf{P}_N^{(\alpha,\beta)}$	N-th degree monic Jacobi polynomial with parameters α and β.

CONTENTS

1 INTRODUCTION

For many physical systems, states, inputs, and outputs may depend on a spatial variable, which defines a position in one-dimensional or multidimensional space. These systems are modeled by partial differential equations (PDEs) and along with many others (like systems modeled by integral equations and delay differential equations) are called distributed parameter systems (DPSs). They differ from lumped parameter systems (LPSs), modeled by ordinary differential equations (ODEs), in the non-spatial dependence of their states, inputs and outputs. Studies on parameter identification, control and state estimation of processes modeled by PDEs are relatively recent but plentiful.

The time and space dependence makes the analysis of systems modeled by PDEs more complex than in the lumped-parameter case. In addition, depending on the type of boundary conditions, these systems can be more or less difficult to analyze. On-line state estimation of DPSs modeled by PDEs is particularly a delicate problem in view of the system dimensionality and the fact that providing a comprehensive set of sensors is either physically impossible or too costly (A. VANDE WOUWER et al., 2000). In such a case, the internal states have to be estimated on the basis of the mathematical model and (available) online measurements provided by sensors located at strategic positions in the spatial domain. In general, measurements for PDE systems are either in domain (provided by sensors located inside the domain of the PDE system and they may be of pointwise or piecewise type) or boundary (provided by sensors located at the boundary of the PDE system).

1.1 STATE OF THE ART

Many seemingly distinct phenomena found in different fields of research in science and engineering can be mathematically formalized by PDEs with mixed or homogeneous boundary conditions arising from chemical and physical principles (e.g., conservation laws as well as mass, energy and momentum balances). Thus, there exists need for accurate models to design algorithms for control, observation or diagnostic of failures for PDE systems leading to a growing interest in PDE control and systems theory in the last decade. At the same time, the progress in computational and applied mathematics combined with the availability of rapidly increasing computer power steadily extend the range of real life applications that can be numerically solved. These developments lead to new challenges in the field of state estimation and control of PDE systems. In particular, we can cite several works related to the application of PDE theory in different fields of application.

- **Industrial processes**. A significant number of applications of PDE theory arises

in industrial process control. Perhaps one of the largest number of reported applications have been to heating and cooling problems (LONG et al., 2016; NGUYEN; TENNO, 2016) as well as fluid heat exchangers (MAIDI; CORRIOU, 2020; XU; DUBLJEVIC, 2016). Other major areas of applications are to biochemical reactors and similar processes (CHEN, Y. et al., 2015; LAO et al., 2014; DELATTRE, Cedric et al., 2004; BOUBAKER et al., 1998) characterized by chemical conversion, internal heat generation or consumption, and strong nonlinearities in their kinetics. Other applications of PDE theory are reported in a number of other areas of process control. For instance, polymer processing operations (LOPEZ-GOMEZ et al., 2007), control of plasmas (MAVKOV et al., 2017), nuclear reactor control (CHAUDHURI, 1972), and for a scattered variety of other process control applications (YEBI; AYALEW, 2015; KOTSUR, 2015) a number of studies have appeared.

- **Mechanical systems**. A second area of application of PDE theory is to mechanical systems problems such as bridge, towers and vehicle modeling and control design (XING; LIU, J., 2020; KIRCHER; ZHANG, K. M., 2016; LE FLOCH et al., 2016), and the control of platforms, flexible structures and robots; see, e.g., (BARTECKI, 2013; WU, F.; YILDIZOGLU, 2005; YANG, H. et al., 2015). The main problems in this area seem to be the design of these structures so that they are stable under dynamic disturbances as well as the identification of parameters and dynamic state so that structural feedback controllers may be developed.

- **Resource recovery and environmental systems**. Another major area of applications of PDE theory is the resource recovery and environmental problems. Resource recovery applications include identification of under ground oil, water and coal reservoirs (EWING et al., 1994; OMOSEBI; IGBOKOYI, 2016). The quality of the environment is another important area in which PDE theory has found important applications. One can cite the management of water quality, modeling, prediction and control of atmospheric pollution (FERRAGUT et al., 2013) and control of forest and meadow fires (SÉRO-GUILLAUME et al., 2008).

- **Epidemiological models**. Another interesting new area in PDE theory is the modeling of spatial spread of infectious diseases. Studies reported on epidemiology involve the mathematical modeling of the distribution effects in the mechanism of transmission of the contagion, and this has led to a number of both quantitative and qualitative predictions in the infectious diseases dynamics (LOTFI et al., 2014; HUANG, W. et al., 2010).

1.1.1 State estimation of PDE systems

The problem of designing observers for DPSs modeled by PDEs has been an active field of research over the last years. Thus, the literature related to the subject matter is very rich. These works have widely different approaches, symbolisms, measurement processes and boundary conditions associated with them. As classical surveys systematizing the various techniques in this field, one can cite those by (FUJII, 1980), or a more recent book (BANKS; KUNISCH, 2012) where a broad class of estimation techniques for DPSs is presented.

For the purpose of implementing observer and controller design techniques for PDE systems, the dimension of the system must be reduced. This process is called lumping and there are two kinds of lumping (A. VANDE WOUWER; ZEITZ, 2009; RAY, 1981): early lumping and late lumping, which are summarized in the following.

1.1.1.1 Early lumping

In the early lumping approach the PDE system is first approximated by a finite-dimensional system (obtained by model reduction methods) for which the observer is designed. Model reduction may be considered as some of the fundamental issues for the DPSs modeling. In this context, within the time–space separation framework, different approaches and methods arise according to the combination of proper model reduction approaches and spatial basis functions selection. The method of weighted residuals (MWR) (FINLAYSON, 2013) is the most often used method for model reduction. The accuracy and efficiency of MWR depend on appropriately choosing the basis and weighted functions. Many methods have been proposed based on the selection of weighting functions. The most popular approaches appear to be Galerkin and collocation methods (FINLAYSON, 2013). On the other hand, selection of spatial basis functions is critical to the model reduction, and has a great impact in the modeling performance. The spatial basis functions can be classified into analytical and data-based functions. In general, there are four major approaches, the finite difference method (FDM) (MITCHELL; GRIFFITHS, 1980), the finite element method (FEM) (BRENNER et al., 2008), the spectral method (BOYD, J. P., 2001) and the Karhunen-Loève (KL) method (PARK; CHO, 1996). For different applications, different modeling methodologies can be formulated through an integration of proper spatial basis functions and model reduction approaches.

Recently, several works have addressed the state estimation problem of DPSs considering early lumping based approaches such as (KATZ; FRIDMAN, 2020; MARKO et al., 2018; WU, H.-N. et al., 2016). In the context of spatially distributed sensing, the sensor placement problem is of particular interest, since the observer performance directly depends on the proper allocation of sensors available for on-

line measurement. There are several approaches addressing the sensor placement problem in distributed systems, for instance, one can cite the classic works in (A. VANDE WOUWER et al., 2000; ALONSO et al., 2004; DEMETRIOU, 2005) and a more recent paper in (GUNDER et al., 2018). Therein, different approaches were proposed in order to improve the performance with respect to a certain optimization index or a specific desired feature.

1.1.1.2 Late lumping

In the late-lumping approach the distributed nature of the system model is maintained for the observer design, the resulting observer is infinite dimensional, which is then lumped for implementation purposes. This approach theoretically leads to better estimation results since no approximation of the model is made, nevertheless it requires the manipulation of more sophisticated mathematical tools and methods.

Observer synthesis of DPSs is based on semigroup theory, Lyapunov approach and the use of the backstepping technique, which are detailed below.

- **Synthesis based on the semigroup theory**. The study of operator semigroups is a mature area of functional analysis which is still very active. In this framework, The DPS is described by an abstract ODE which involves a sum of linear and/or nonlinear operators (semigroup operators) defined in Hilbert or Banach spaces. The study of observation operators for such systems is relatively more recent. Crucial to the developments of these studies are the concepts of admissibility, observability and detectability (JACOB; PARTINGTON, 2004; TUCSNAK; WEISS, 2009; CHEN, W.; TU, 1995). The state observer is an extension of the well-known lumped parameter Luenberger observer theory to an infinite dimensional system described by a semigroup operator and its infinitesimal generator (CURTAIN; ZWART, 2020; VRIES et al., 2007).

  Concerning the design of observers for semilinear PDEs using the abstract infinite dimensional description, the dissipativity-based observer design (SCHAUM et al., n.d.) provides an effective mean for dealing with complex nonlinearities yielding local and global convergent results through the use of modal measurement injection approach as addressed in (CURTAIN; ZWART, 2020).

- **Synthesis based on the Lyapunov method**. In the Lyapunov-based observer synthesis, the convergence of the observer is established by analyzing the stability of the estimation error dynamics using an appropriate Lyapunov functional. Stability conditions are expressed as linear matrix inequality (LMI) constraints, which are numerically solved using standard interior-point algorithms and whose solution provides the output injection operator of the observer. This approach can be found in (FRIDMAN, 2013a, 2013b; CASTILLO et al., 2013) for first order

hyperbolic systems and in (FRIDMAN; ORLOV, 2009; YANG, Y.; DUBLJEVIC, 2014; SCHAUM, Alexander et al., 2014; GAHLAWAT; PEET, Matthew M, 2016a; LIU, Y.-Q. et al., 2018) for second order parabolic systems.

Recently, Sum-of-Squares (SOS) optimization methods have been applied to the parametrization of positive Lyapunov functionals using SOS polynomials, which renders the problem of searching for solutions for the observer gain convex. More importantly, with such parametrization of positive operators, the solutions may be searched using semidefinite programming using recently developed numerical tools (PAPACHRISTODOULOU et al., 2013). Examples of these works can be found in (PAPACHRISTODOULOU; PEET, Matthew Monnig, 2006; GAHLAWAT; PEET, Matthew M, 2016a, 2016b).

- **Synthesis based on the backstepping technique**

  In the backstepping technique, an invertible integral Volterra type transformation is used to match the state estimation error dynamics to a target system having the desired stability properties. This technique requires the determination of the integral kernel defined on a limited domain and which is a solution of a set of PDEs that can be solved numerically or in some cases analytically. By principle of equivalence, the proof of the stability of the target system allows to conclude on the stability of the estimation error dynamics.

  The strength of this approach lies in its structural simplicity and a fairly wide field of application for various classes of systems modeled by PDEs. For systems governed by parabolic PDEs defined on a one-dimensional (1D) spatial domain, a systematic observer design approach using boundary sensing is introduced in (SMYSHLYAEV; KRSTIC, 2005). Recently, the backstepping-based observer design was presented in (TSUBAKINO; HARA, 2015) for reaction-diffusion processes with spatially varying reaction coeffient and a certain weighted average of the state over the spatial domain as measured output. In (JADACHOWSKI et al., 2011, 2015), backstepping-based observer design was addressed for reaction-diffsion processes evolving in multidimensional spatial domains. In (MIRANDA et al., 2010), the backstepping-based design for parabolic processes was applied by adopting a nonconventional target system for the error dynamics, embedding certain discontinuous output injection terms.

  More recently, multivariable systems of coupled PDEs were considered in the backstepping-based boundary control and observer design settings. The most intensive efforts of the current literature seem however to be oriented towards coupled processes of transport type (VAZQUEZ et al., 2008, 2011; MOURA et al., 2013; BACCOLI; PISANO, 2015; LIU, B.-N. et al., 2016).

1.2 MOTIVATION

Nowadays, transport-reaction systems have launched applications in chemistry, biology, meteorology, epidemiology, fluid dynamics, and other fields of applied sciences. Transport-reaction processes are characterized by the coupling of advection, diffusion and reaction phenomena, and are pervasive in many scientific and industrial processes. The advection–reaction–diffusion equation is one of the most pertinent areas of study in applied mathematics. The combination of these three components in a mathematical model puts a strong impact on the theory of PDEs and gives rise to rethink the corresponding models in the light of the physical properties of a governing phenomenon.

Successful control and/or monitoring of this kind of processes requires online information about the relevant process variables. In most cases, it is not possible to have full access to these key variables due to economical or physical reasons and/or the fact that not all variables can be measured. In such a case, the internal states have to be estimated using a state observer.

1.3 PROBLEM DEFINITION

This thesis is particularly concerned with the synthesis of state observers for a class of one-dimensional multivariable transport-reaction systems described by the following semilinear PDE system:

$$\partial_t x(z,t) = D\partial_z^2 x(z,t) - \mathcal{V}\partial_z x(z,t) - \mathrm{K}\; x(z,t) + B\; u_d(t) + G\; r\left(x(z,t)\right) \tag{1}$$

for $(z,t) \in (0,1) \times (0,\infty)$, subject to the Robin boundary conditions

$$\begin{array}{rcl} M_{\alpha_0}\partial_z x(0,t) + M_{\beta_0} x(0,t) & = & u_0(t) \\ M_{\alpha_1}\partial_z x(1,t) + M_{\beta_1} x(1,t) & = & u_1(t) \end{array} \tag{2}$$

for $t \in [0,\infty)$ and initial condition

$$x(z,0) = x_0(z) \tag{3}$$

where

$$x(\cdot,t) = \begin{bmatrix} x_1(\cdot,t) & \cdots & x_{n_x}(\cdot,t) \end{bmatrix}^T \in \mathbf{L}_2^{n_x}(0,1)$$

denotes the state variable,

$$u_d(t) = \begin{bmatrix} u_{d,1}(t) & \cdots & u_{d,n_x}(t) \end{bmatrix}^T \in \mathbb{R}^{n_x}$$

is a known distributed exogenous input and

$$u_0(t) = \begin{bmatrix} u_{0,1}(t), & \cdots & u_{0,n_x}(t) \end{bmatrix}^T \in \mathbb{R}^{n_x}$$
$$u_1(t) = \begin{bmatrix} u_{1,1}(t) & \cdots & u_{1,n_x}(t) \end{bmatrix}^T \in \mathbb{R}^{n_x}$$

are the boundary known exogenous inputs at $z = 0$ and $z = 1$, respectively. The matrices $D = diag(d_i)$, $\mathcal{V} = diag(\upsilon_i)$, $\mathrm{K} = diag(\kappa_i)$ and $B = diag(b_i)$, $\forall i \in 1, ..., n_x$ are matrices of constant entries denoting the diffusion, superficial velocity, linear source and shaping distributed input coefficients respectively, $G \in \mathbb{R}^{n_x \times n_r}$ is the stoichiometric-kinetic gain matrix and $r(\cdot) : \mathbf{L}_2^{n_x}(0,1) \to \mathbf{L}_2^{n_r}(0,1)$ the vector of reaction rates. $M_{\alpha_0} = diag(\alpha_{0,i})$, $M_{\beta_0} = diag(\beta_{0,i})$, $M_{\alpha_0} = diag(\alpha_{1,i})$ and $M_{\beta_1} = diag(\beta_{1,i})$, $\forall i \in 1, ..., n_x$ are matrices of constant entries denoting the coefficients related to the Robin boundary conditions.

In order to ensure the well-posedness of the governing equations and the observer design problem for (1)–(2) , the following conditions are assumed to be held

- $d_i > 0$ for $i = 1, \ldots, n_x$.
- $r(\cdot) : \mathbf{L}_2^{n_x}(0,1) \to \mathbf{L}_2^{n_r}(0,1)$ is locally Lipschitz continuous in x, i.e., there exists a positive constant $l^r = l^r(\rho)$ where $\rho > 0$ such that

$$\|r(x) - r(\hat{x})\| \leq l^r \|x - \hat{x}\| \tag{4}$$

  holds for all $x, \hat{x} \in \mathbf{L}_2^{n_x}(0,1)$ with $\|x\|, \|\hat{x}\| \leq \rho$.

1.3.1 Output measurement

The measurement vector for the PDE system (1)-(2) is defined as follows

$$y(t) = \begin{bmatrix} \int_0^1 c_1(z)\mathbf{c}_1^T x(z,t)dz \\ \vdots \\ \int_0^1 c_{n_y}(z)\mathbf{c}_{n_y}^T x(z,t)dz \end{bmatrix} \in \mathbb{R}^{n_y} \tag{5}$$

where $c_j(z)$ describes the distribution of the measurement at the j-th position over the spatial domain $[0, 1]$.

Measurement sensors in a number of practical problems are only placed at a finite number of discrete points or partial areas of the spatial domain. Different functional forms $c_j(z)$ will lead to different forms of local measurement (WANG, J.-W. et al., 2016). For instance, the choice

$$c_j(z) = \delta(z - \zeta_j) \tag{6}$$

corresponds to pointwise measurement at the positions ζ_j, $j \in \mathbb{N}_y$, and the functional form

$$c_j(z) = \frac{1}{2\varepsilon_j} 1_{[\zeta_j-\varepsilon_j,\zeta_j+\varepsilon_j]} \tag{7}$$

with

$$1_{[\zeta_j-\varepsilon_j,\zeta_j+\varepsilon_j]} = \begin{cases} 1, & \zeta_j - \varepsilon_j \leq z \leq \zeta_j + \varepsilon_j, \\ 0, & \text{elsewhere} \end{cases} \tag{8}$$

produces n_y zones of piecewise uniform sensing in the interval $[\zeta_j - \varepsilon_j, \zeta_j + \varepsilon_j]$. These cases are illustrated in Figures 1 and 2.

Figure 1 – Distributed pointwise measurements.

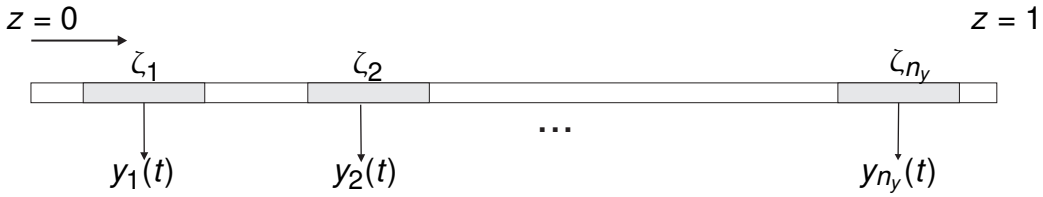

Figure 2 – Distributed piecewise measurements

.

Remark 1.1. *The boundary measurement case corresponds to the pointwise measurement case at* $z = 0$ *and/or* $z = 1$*.*

1.4 BENCHMARK APPLICATION

Transport-reaction systems described by (1)-(2) are used to represent a wide range of systems found in science and engineering applications. For numerical validation purposes of the state estimation techniques studied and developed in this work, we focus on benchmark applications related to biochemical tubular reactors model.

1.4.1 Biochemical tubular reactors

Industrial chemical processes typically rely on process models for design, monitoring, control and optimization. Distributed chemical reaction systems correspond to processes involving reactions with phases that are not well mixed, thus resulting in spatial dependencies. Tubular reactors (FRIEDLY, 1972) are a prime example

of such systems. The dependent variables of these models are typically concentrations and temperatures. These variables, which depend on time and spatial coordinates, are described by partial differential equations (PDEs) consisting of material and heat balances that couple the effects of advection, reaction, diffusion, conduction, and initial and boundary conditions. The coupling in time and space makes the analysis of distributed reaction systems more complex. In addition, depending on the type of boundary conditions, these systems can be more or less difficult to analyze (PARULEKAR; RAMKRISHNA, 1984).

System description

In single-phase one-dimensional tubular reactors, the concentrations and temperature are functions of the spatial coordinate ξ and the time τ. It is assumed that the inlet of the system is located at $\xi = 0$ and ξ is positive along the reactor length. Since the concentrations and the temperature vary with the spatial coordinate, the concentration and temperature gradients might lead to significant diffusion when the flow of material is not dominated by advection. Hence, the general formulation of the material and energy balances for a single-phase one-dimensional tubular reactor considers the system from the standpoint of an advection-diffusion-reaction problem.

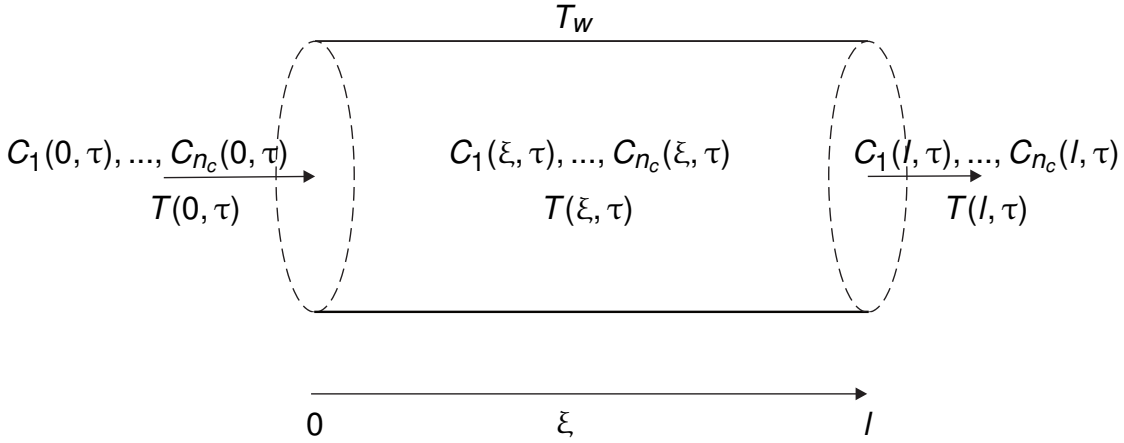

Figure 3 – Nonisothermal tubular reactor.

Let us consider a single-phase one-dimensional tubular reactor as schematized in Figure 3 which is characterised by an axial dispersion. Then the dynamical model is readily derived by using mass and energy balances and can be written as the following coupled set of parabolic PDEs,

$$\partial_\tau x(\xi,\tau) = \overline{D}\partial^2_\xi x(\xi,\tau) - \overline{\mathcal{V}}\partial_\xi x(\xi,\tau) - \overline{K}x(\xi,\tau) + \overline{B}_d u_d(\tau) + \overline{G}\ r\left(x(\xi,\tau)\right) \quad (9)$$

for $(\xi,\tau) \in (0,l)\times(0,\infty)$, subject to the Danckwerts boundary conditions (DANCKWERTS, 1953)

$$\begin{aligned} \overline{D}\partial_\xi x(0,\tau) &= \overline{\mathcal{V}}(x(0,\tau) - x_{in}(\tau)) \\ \partial_\xi x(l,\tau) &= 0. \end{aligned} \tag{10}$$

with

$$\begin{aligned} x(\xi,\tau) &= \begin{bmatrix} C_1(\xi,\tau) & \cdots & C_{n_c}(\xi,\tau) & T(\xi,\tau) \end{bmatrix}^T \\ x_{in}(t) &= \begin{bmatrix} C_{1,in}(\tau) & \cdots C_{n_c,in}(\tau) & T_{in}(\tau) \end{bmatrix}^T \\ u_d(\tau) &= \begin{bmatrix} 0 & \cdots 0 & T_w(\tau) \end{bmatrix}^T \end{aligned}$$

and

$$\begin{aligned} D = diag(d_a\, I, \frac{\lambda_a}{\rho_p c_p}),\ \mathcal{V} = diag(\upsilon I, \epsilon\upsilon\frac{\rho_g c_{pg}}{\rho c_p}),\ K = diag(0, -\frac{2k_w}{r_d \rho c_p}), \\ B_d = diag(0, \frac{2k_w}{r_d \rho c_p}),\ G = \begin{bmatrix} G_r & -\frac{\Delta H}{\rho c_p} \end{bmatrix}^T \end{aligned} \tag{11}$$

where T is the temperature (K), $C_1, ..., C_{n_c}$ are the reactant concentrations (mol/m^3), T_w the coolant temperature (K), T_{in} the inlet temperature (K), $C_{1,in}, ..., C_{n_c,in}$ the inlet reactant concentrations (mol/m^3), τ (s) and ξ (m) the time and space variables, $\lambda_a/(\rho c_p)$ and d_a the axial energy and mass dispersion coefficients (m^2/s), υ the fluid velocity (m/s), l the reactor length (m), ΔH the reaction heat (kcal), ρ the fluid density (kg/m^3), c_p the specific heat (kcal/kgK), r the reaction rate vector (m^3/s), r_d the reactor radius (m), k_w the heat removal rate (kcal/m^{2}sK).

Using the chemical process engineering parametrization

$$\begin{aligned} z = \frac{\xi}{l},\quad t = \frac{\tau\upsilon}{l}, \\ P_e = \frac{l\upsilon}{D},\quad P_{eT} = \frac{l\epsilon\upsilon\rho_g cp_g}{\lambda},\quad L_e = \frac{\epsilon\rho_g cp_g}{\rho c_p}, \\ D_a = \frac{l}{\upsilon},\ \beta = -\frac{\Delta H}{\rho c_p},\quad \eta = \frac{2k_w}{r_d \rho c_p}\frac{l}{\upsilon} \end{aligned} \tag{12}$$

the system modeled by (9)-(10) take the form of (1)-(2) by considering

$$
\begin{aligned}
x(z,t) = \begin{bmatrix} C_1(z,t) & \cdots & C_{n_c}(z,t) & T(z,t) \end{bmatrix}^T,\ u_d = \begin{bmatrix} 0 & T_w \end{bmatrix}^T,\\
u_0(t) = \begin{bmatrix} C_{1,in}(t) & \cdots & C_{n_c,in}(t) & T_{in}(t) \end{bmatrix}^T,\ u_1(t) = 0,\\
D = diag(\frac{1}{Pe} I, \frac{L_e}{P_{eT}}),\ \mathcal{V} = diag(I, L_e),\ K = diag(0, -\eta),\\
B = diag(0, \eta),\ G = \begin{bmatrix} -D_a G_r & \beta D_a \end{bmatrix}^T,\\
M_{\alpha_0} = diag(\frac{1}{Pe} I, \frac{1}{P_{eT}}),\ M_{\beta_0} = -I,\ M_{\alpha_1} = I,\ M_{\beta_1} = 0. \qquad (13)
\end{aligned}
$$

For more details on the model derivation, see e.g. ((FEYO DE AZEVEDO et al., 1990; DOCHAIN, 1994)) which contain a number of older references including seminal papers like (LANGMUIR, 1908; DANCKWERTS, 1953).

The estimation problem corresponding to tubular biochemical reactors consists of inferring the concentration and temperature profiles from temperature and/or concentration measurements.

1.5 OBJECTIVES

The fundamental objective of this Thesis is to develop techniques for the synthesis of state observers in view to estimate the state variables of transport-reaction systems described by (1)-(2) for feedback and/or monitoring purposes. Motivated by the fact that the dynamics of the latter are described by semilinear systems of PDEs, which can be formulated as a semilinear differential equation on an infinite-dimensional state-space, several techniques in the frame of the early and late lumping approaches of system theory are described and/or developed, and applied to this model.

In order to achieve the main objective, the following specific objectives are defined:

- To obtain an approximated reduced model using the Method of Weighted Residuals of the class of systems of interest and to study its degree of accuracy with respect of the selection of the collocation points.
- To design a Lyapunov-based state observer of the reduced order model which ensures the exponential convergence of the estimation error dynamics.
- To study the spectral properties of the multivariable second order differential operator related to transport reaction systems and the Lipschitz properties of the reaction rate function in order to obtain sufficient conditions for the modal state observer design.

- To design a Lyapunov-based state observer of the semilinear PDEs describing the class of transport reaction systems of interest based on polynomial parametrization and whose parameters may be obtained via the solution of a SOSs program.
- To test numerically the developed state estimation methodologies in benchmark biochemical processes applications.

1.6 CONTRIBUTIONS

This thesis is an attempt to provide a tractable framework for the state estimation of multi-state transport-reaction process described by semilinear PDE systems considering various in-domain distributed measurements. The proposed techniques significantly reduces the stability analysis complexity of the state estimation error dynamics by using local Lipschitz and algebraic sector conditions to represent the error dynamics as a Lure system. It should be noticed that the methodology to be presented concerns a large class of semilinear PDE systems within which the applications related to the state estimation of biochemical tubular reactors models are very representative as industrial process applications, moreover the observer synthesis for the SEIR-type distributed model describing the spatial spread of COVID-19 plays an important role for epidemic outbreak forecasting and/or conception of early warning systems in the context of all advantages that the use of one state estimator can provide with respect to the mere simulation of the actual dynamics (faster convergence from any initial condition, robustness).

1.6.1 Publications

Some chapters of the present thesis are contained in the following conference papers and articles.

[1] Ivan Francisco Yupanqui Tello, Daniel Coutinho, and Alain Vande Wouwer. Extended kalman filter design for semilinear distributed parameter systems with application to anaerobic digestion. *SYSTEM THEORY, CONTROL AND COMPUTING JOURNAL*, 1(1):95–103, 2021.

[2] Ivan Francisco Yupanqui Tello, Daniel Coutinho, Joseph Winkin, and Alain Vande Wouver. Observer design for chemical tubular reactors based on system linearization. In *2020 European Control Conference (ECC)*, pages 1141–1146. IEEE, 2020.

[3] Ivan Francisco Yupanqui Tello, Alain Vande Wouver, and Daniel Coutinho. Extension of kalman filtering to semilinear pde systems-application to pulp and paper.

In *2020 24th International Conference on System Theory, Control and Computing (ICSTCC)*, pages 813–818. IEEE, 2020.

[4] Ivan Francisco Yupanqui Tello, Alain Vande Wouver, and Daniel Coutinho. LMI observer design for a class of tubular reactors. In *2020 24th International Conference on System Theory, Control and Computing (ICSTCC)*, pages 570–575. IEEE, 2020.

[5] Ivan Francisco Yupanqui Tello, Alain Vande Wouver, and Daniel Coutinho. Observer design for linear parabolic pde systems. In *39th Benelux Meeting on Systems and Control*, pages 37–37. University of Groningen, 2020.

[6] Ivan Francisco Yupanqui Tello, Alain Vande Wouver, and Daniel Coutinho. Backstepping observer design for a tubular catalytic cracking reactor. In *Computer Aided Process Engineering (CAPE) Forum 2019*, pages 62–62, 2019.

[7] Ivan Francisco Yupanqui Tello, Daniel Coutinho, and Alain Vande Wouver. Early Lumping Observer Design and Sensor Placement for Transport-Reaction Systems. In *Journal of Process Control*, *first review*.

[8] Ivan Francisco Yupanqui Tello, Daniel Coutinho, and Alain Vande Wouver. Observer Design for Multivariable Transport-Reaction Systems based on Spatially Distributed Measurements. In *Systems and Control Letters*, *in submitted*.

[9] Ivan Francisco Yupanqui Tello, Daniel Coutinho, and Alain Vande Wouver. Observer Design for Multivariable Transport-Reaction Systems based on Spatially Distributed Measurements. In *Mathematics*, *submitted*.

1.7 THESIS ORGANIZATION

The focus of this thesis is the online state estimation of transport-reaction systems. In particular, the state estimation and observer design techniques are addressed via the early and late lumping approach, and along with the development, formulation, they are explored within the following chapters.

Chapter 2 focuses on the synthesis of finite-dimensional observers for the class of transport-reaction systems of interest. Firstly, the mathematical model described by semilinear PDEs system is approximated using the orthogonal collocation method yielding a differential-algebraic system of equations (DAEs). Then, a Lyapunov-based

design method is proposed for the approximated reduced-order model which provides sufficient design conditions in terms of standard linear matrix inequalities (LMIs) aiming at the exponential convergence of the estimation error with a prescribed decay rate. The observer performance is further improved through an offline optimal sensor placement algorithm considering a parameterized reduced-order output matrix. Finally, a case study related to a nonisothermal tubular reactor is presented to demonstrate the observer performance as well as the advantages of the proposed sensor placement optimization scheme.

In Chapter 3, we are interested in the modal-based observer synthesis problem. The spectral decomposition of the infinite dimensional Hilbert state space let us to extend the modal analysis to transpot-reaction systems described by coupled 1-D semi-linear parabolic PDEs systems with multiple in-domain measurements and state dependent nonlinearities. The local lipschitz property assumption of the reaction rate function let us to set two synthesis conditions ensuring the exponential stability of the state estimation error.

Chapter 4 is devoted to the Lyapunov-based design method for the state observer synthesis of the class of transport-reaction systems of interest. The Lyapunov functions is parametrized by sum-of-squares polynomials. In addition, the output injection matrix gain is parametrized by polynomials with prescribed degree. In particular, we use the representation of the error dynamics as a Lure system considering an intrinsic sector condition related to the rate reaction function and the estimation error state. The observer synthesis guarantees a prescribed decay rate of convergence which is obtained through the solution of an appropriately formulated SOS program. A case study related to a nonisothermal tubular reactor is presented to demonstrate the observer performance as well as the advantages of the proposed formulation.

Chapter 5 is dedicated to the state estimation for the compartmental model based on partial differential equations (PDEs) which describes the spread of the infectious disease in a host population. Local exponential stability and robustness with respect to variation rates are ensured by an appropriate choice of the observer gains, through the use of the theory of Lyapunov stability. Numerical experiments are presented to illustrate the method efficiency.

Figure 4 shows the research roadmap that contains the different methods approached throughout the chapters of this thesis.

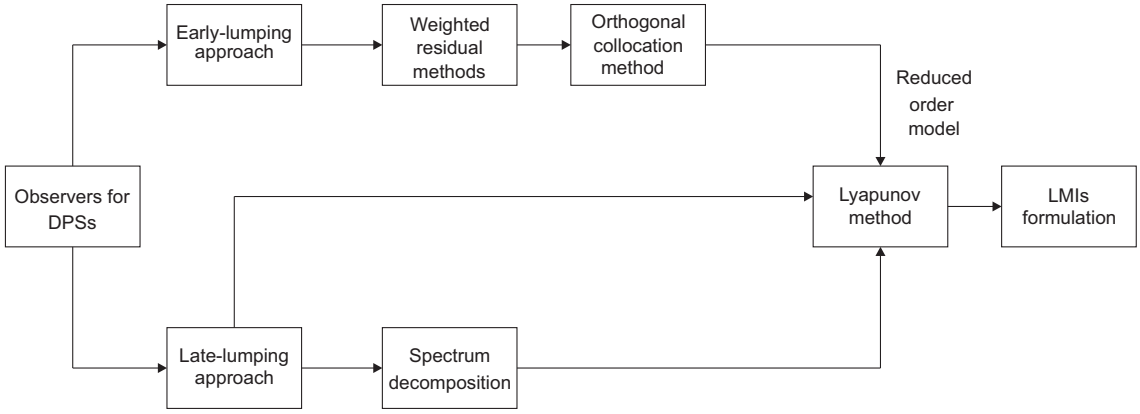

Figure 4 – Research roadmap of the thesis.

2 INSTRUMENTAL TOOLS

In this chapter, we present some mathematical definitions and preliminary results that will be used in the sequel. This chapter begins by presenting some results on the well-posedness, stability and model reduction of PDE systems. We also provide a brief review of Semi-Definite Programming (SDP) and SOS (Sum of Squares) tools which are the main instruments for the computational synthesis of state observers in this thesis. To simplify the presentation and discussion, the PDE systems of interest are written specifically to represent a general class of second-order, semilinear systems. Thus, we consider the following (abstract) differential equations on a Hilbert space $\mathcal{H}$

$$\partial_t x(z,t) = \mathcal{A}x(z,t) + F(x(z,t)), \quad x(z,0) = x_0(z) \in \mathcal{H} \tag{14}$$

for $(z,t) \in \Omega \times (0,\infty)$ and where $\mathcal{A}$ is a differential linear operator on $\mathcal{H}$, $F(\cdot)$ is a nonlinear function from $\mathcal{H}$ into itself and the following condition is assumed to be hold

- $F(\cdot) : \mathcal{H} \to \mathcal{H}$ is locally Lipschitz continuous, i.e., there exists a positive constant $l^F = l^F(\rho)$ where $\rho > 0$ such that

$$\|F(x) - F(\hat{x})\| \leq l^F \|x - \hat{x}\| \tag{15}$$

  holds for all $x, \hat{x} \in \mathcal{H}$ with $\|x\|, \|\hat{x}\| \leq \rho$.

To see how this abstract representation can be used to analyze PDEs, let us go through the following example

The Semilinear Heat Equation. Consider a heated metal bar of unit length, in which the two ends of the bar are insulated so that there is no heat flux. The heat distribution over the rod is described by the following semilinear PDE

$$\partial_t x(z,t) = \partial_z^2 x(z,t) - x^3(z,t) \tag{16}$$

for $(z,t) \in (0,1) \times (0,\infty)$, subject to the Neumann boundary conditions

$$\begin{aligned} \partial_z x(0,t) &= 0 \\ \partial_z x(1,t) &= 0 \end{aligned} \tag{17}$$

for $t \in [0,\infty)$ and initial condition

$$x(z,0) = x_0(z). \tag{18}$$

In order to use the abstract form (14), we take $\Omega = (0,1)$ and hence $\mathcal{H} = \mathbf{L}_2(0,1)$ as the state space and the trajectory segment $x(\cdot,t) \in \mathcal{H}$ as the state. Now it suffices to define

$$\begin{aligned} \mathcal{A}x(z,t) &= \partial_z^2 x(z,t) \\ \mathcal{D}(\mathcal{A}) &= \{x(z,t) \in \mathcal{H} : \ x(z,t),\ \partial_z x(z,t) \ \text{ are absolutely continuous,} \\ &\qquad\qquad \partial_z^2 x(z,t) \in \mathcal{H} \ \text{ and } \ \partial_z x(0,t) = 0, \ \ \partial_z x(1,t) = 0 \Big\} \\ F(x) &= -x^3. \end{aligned} \tag{19}$$

2.1 LINEAR PDE SYSTEMS

In the case where $F = 0$, the well-posedness problem of (14) is tied to $\mathcal{A}$ being the generator of a strongly continuous semigroup denoted C_0-Semigroup (CURTAIN; ZWART, 2020; PAZY, 2012). Let $\mathcal{L}(\mathcal{H})$ be the space of bounded linear operators on a Hilbert space $\mathcal{H}$.

Definition 2.1. *A strongly continuous semigroup (C_0-semigroup) is an operator-valued function $\mathcal{S}(t) : [0,\infty) \to \mathcal{L}(\mathcal{H})$ that satisfies the following properties:*

- $\mathcal{S}(0) = \mathcal{I}$ *(identity operator);*
- $\mathcal{S}(t+s) = \mathcal{S}(t)\mathcal{S}(s)$, $t \geq 0, \ s \geq 0$*;*
- $\mathcal{S}(t)x_0 \to x_0$, *as* $t \to 0^+ \ \ \forall x_0 \in \mathcal{H}$.

Theorem 2.1. *A C_0-semigroup $\mathcal{S}(t)$ on a Hilbert space $\mathcal{H}$ has the following properties:*

- $\|\mathcal{S}(t)\|$ *is bounded on every finite subinterval of* $[0,\infty)$*;*
- *If* $\omega_0 = \inf_{t>0} \frac{\log\|\mathcal{S}(t)\|}{t}$, *then* $\omega_0 = \lim_{t\to\infty} \frac{\log\|\mathcal{S}(t)\|}{t} < \infty$*;*
- $\forall \omega > \omega_0$, *there exists a constant* M_ω *such that* $\forall t \geq 0$, $\|\mathcal{S}(t)\| \leq M_\omega e^{\omega t}$.

The constant ω_0 is called the growth bound of the semigroup.

Definition 2.2. *The infinitesimal generator $\mathcal{A}$ of a C_0-semigroup on the Hilbert space $\mathcal{H}$ is defined by*

$$\mathcal{A}x = \lim_{t\to 0^+} \frac{\mathcal{S}(t)x - x}{t} \tag{20}$$

whenever the limit exists; the domain of $\mathcal{A}$, $\mathcal{D}(\mathcal{A})$, being the set of elements $x \in \mathcal{H}$ for which the limit exists.

Theorem 2.2. *Let $\mathcal{S}(t)$ be a C_0-semigroup on the Hilbert space $\mathcal{H}$ with infinitesimal generator $\mathcal{A}$. Then the following results hold:*

- *For* $x_0 \in \mathcal{D}(\mathcal{A})$, $\mathcal{S}(t)x_0 \in \mathcal{D}(\mathcal{A})\ \forall\ t \geq 0$*;*
- $\frac{d^n}{dt^n}(\mathcal{S}(t)x_0) = \mathcal{A}^n\mathcal{S}(t)x_0 = \mathcal{S}(t)\mathcal{A}^n x_0$ *for* $x_0 \in \mathcal{D}(\mathcal{A}^n)$, $n \in \mathbb{N}$, $t > 0$*;*
- $\mathcal{S}(t)x_0 - x_0 = \int_0^t S(\sigma)Ax_0 d\sigma$ *for* $x_0 \in \mathcal{D}(\mathcal{A})$*;*
- $\mathcal{A}$ *is a closed linear operator and* $\mathcal{D}(\mathcal{A})$ *is dense on* $\mathcal{H}$*.*

Sufficient and necessary conditions for a closed, densely defined operator $\mathcal{A}$ on a Hilbert space to be the infinitesimal generator of a C_0-semigroup satisfying $\|\mathcal{S}(t)\| \leq e^{\omega t}$ are:

$$\begin{aligned} \mathrm{Re}(\langle \mathcal{A}x, x\rangle) &\leq \omega\|x\|^2 \quad \textit{for} \quad x \in \mathcal{D}(\mathcal{A}); \\ \mathrm{Re}(\langle \mathcal{A}^* x, x\rangle) &\leq \omega\|x\|^2 \quad \textit{for} \quad x \in \mathcal{D}(\mathcal{A}^*). \end{aligned}$$

Cauchy problem in a Hilbert space

let $\mathcal{A}$ be a differential operator which is the infinitesimal generator of a C_0-semigroup $\mathcal{S}(t)$ on $\mathcal{H}$. Let us also consider the following homogenous Cauchy problem

$$\begin{aligned} \dot{x}(t) &= \mathcal{A}x(t), \quad t \geq 0, \\ x(0) &= x_0 \in \mathcal{D}(\mathcal{A}). \end{aligned} \tag{21}$$

It can be easily seen from Theorem 2.2 that the classical solution of this problem is given by:

$$x(t) = S(t)x_0. \tag{22}$$

Stability is one of the most important aspects of systems theory. In this section, by stability we mean exponential stability. This property can be characterized by many criteria. Here, we present the criteria for verifying the exponential stability of a linear PDE system which is directly related to the stability of the C_0-semigroup $\mathcal{S}(t)$.

Stability of Semigroups

Definition 2.3. *A* C_0*-semigroup,* $\mathcal{S}(t)$*, on a Hilbert space* $\mathcal{H}$ *is exponentially stable if there exist positive constants* M *and* α *such that*

$$\|\mathcal{S}(t)\| \leq Me^{-\alpha t}, \quad \forall t \geq 0. \tag{23}$$

The α *is called the decay rate, and the supremum over all possible values of* α *is the stability margin of* $\mathcal{S}(t)$*. We say that* $\mathcal{S}(t)$ *is* β*-exponentially stable if (23) holds for* $-\alpha < \beta$*, i.e., its stability margin is at least* $-\beta$*.*

Remark 2.1. *The growth bound ω_0 defined in Theorem 2.1 is the opposite of the stability margin (CURTAIN; ZWART, 2020).*

Important criteria for exponential stability of a C_0-semigroup are given in the following theorem.

Theorem 2.3. *Let $\mathcal{S}(t)$ be a C_0-semigroup on a Hilbert space $\mathcal{H}$, and let $\mathcal{A}$ be its infinitesimal generator. Then the following assertions are equivalent:*

- *$\mathcal{S}(t)$ is exponentially stable;*
- *The solution to the abstract Cauchy problem for any $x_0 \in \mathcal{D}(\mathcal{A})$,*

$$\dot{x}(t) = \mathcal{A}x(t),\ t \geq 0,\quad x(0) = x_0, \tag{24}$$

  tends to zero exponentially fast as $t \to \infty$;

- *For every $x \in \mathcal{H}$, there exists a positive constant $\gamma_x < \infty$ such that*

$$\int_0^\infty \|\mathcal{S}(t)x\|^2 dt \leq \gamma_x; \tag{25}$$

- *There exists a positive operator $\mathcal{P} \in \mathcal{L}(\mathcal{H})$ such that*

$$\langle \mathcal{A}x, \mathcal{P}x\rangle + \langle \mathcal{P}x, \mathcal{A}x\rangle = -\langle x, x\rangle,\quad \forall x \in \mathcal{D}(\mathcal{A}). \tag{26}$$

  The expression in (26) is often referred as the (infinite dimensional) Lyapunov equation.

In general, it is not feasible in infinite dimensions to examine exponential stability via the spectrum of the operator as the following inequality always holds

$$sup(Re(\lambda), \lambda \in \sigma(A)) \leq \lim_{t\to\infty} \frac{log\|\mathcal{S}(t)\|}{t} = \omega_0. \tag{27}$$

Riesz-spectral operators

Here, a convenient representation for large classes of linear partial differential systems of both parabolic and hyperbolic types is introduced. Riesz spectral operators allow for non-self-adjoint operators whose eigenvectors may not be orthogonal, but do form a Riesz basis.

Definition 2.4. *A sequence of vectors $\{\phi_n :\ n \geq 1\}$ in a Hilbert space $\mathcal{H}$ forms a Riesz basis for $\mathcal{H}$ if the following two conditions hold:*

- *$\overline{span}\{\phi_n\} = \mathcal{H}$;*

- *There exist positive constants m and M such that for arbitrary* $N \in \mathbb{N}$ *and arbitrary scalars* α_n, $n = 1, ..., N$, *such that*

$$m \sum_{n=1}^{N} |\alpha_n|^2 \leq \| \sum_{n=1}^{N} \alpha_n \phi_n \|^2 \leq M \sum_{n=1}^{N} |\alpha_n|^2. \tag{28}$$

Definition 2.5. *Suppose that* $\mathcal{A}$ *is a linear, closed operator on a Hilbert space,* $\mathcal{H}$*, with simple eigenvalues* $\{\lambda_n : n \geq 1\}$ *and suppose that the corresponding eigenvectors* $\{\phi_n : n \geq 1\}$ *form a Riesz basis in* $\mathcal{H}$*. If the closure of* $\{\lambda_n : n \geq 1\}$ *is totally disconnected, then we call* $\mathcal{A}$ *a Riesz-spectral operator.*

By totally disconnected we mean that no two points $\lambda, \mu \in \overline{\{\lambda_n : n \geq 1\}}$ can be joined by a segment lying entirely in $\overline{\{\lambda_n : n \geq 1\}}$. Then, Definition 2.5 covers the case where $\mathcal{A}$ has finitely many accumulation points.

Theorem 2.4. *Suppose that* $\mathcal{A}$ *is a Riesz-spectral operator with simple eigenvalues* $\{\lambda_n, n \geq 1\}$ *and corresponding eigenvectors* $\{\phi_n : n \geq 1\}$*. Let* $\{\psi_n : n \geq 1\}$ *be the eigenvectors of* $\mathcal{A}^*$ *such that* $\langle \phi_n, \psi_m \rangle = \delta_{nm}$*, then*

- *Every* $x \in \mathcal{H}$ *can be represented uniquely by*

$$x = \sum_{n=1}^{\infty} \langle x, \phi_n \rangle \psi_n; \tag{29}$$

- $\mathcal{A}$ *has the representation*

$$\mathcal{A}x = \sum_{n=1}^{\infty} \lambda_n \langle x, \psi_n \rangle \phi_n \tag{30}$$

for $x \in \mathcal{D}(\mathcal{A})$*, and*

$$\mathcal{D}(\mathcal{A}) = \{x \in \mathcal{H} : \sum_{n=1}^{\infty} |\lambda_n|^2 |\langle x, \psi_n \rangle|^2 < \infty\}; \tag{31}$$

- $\mathcal{A}$ *is the infinitesimal generator of a* C_0*-semigroup* $\mathcal{S}(t)$ *if and only if* $\sup_{n \geq 1} Re(\lambda_n) < \infty$ *and* $\mathcal{S}(t)$ *is given by*

$$\mathcal{S}(t)x = \sum_{n=1}^{\infty} e^{\lambda_n t} \langle x, \psi_n \rangle \phi_n; \tag{32}$$

- *The growth bound of the semigroup is given by*

$$\omega_0 = \sup_{n \geq 1} Re(\lambda_n). \tag{33}$$

Sturm-Liouville operators

Definition 2.6. *(DELATTRE, Cédric et al., 2003) Consider the differential operator defined as*

$$\mathcal{A} = \frac{1}{\rho(z)} \left(\partial_z(p(z)\partial_z) - q(z)\mathcal{I}\right), \tag{34}$$

where the functions $p(z),\ \rho(z) \in \mathbb{R}^+$ *are continuously differentiable and* $q(z) \in \mathbb{R}$ *is continuous on* $[0, 1]$*. Furthermore, the domain* $\mathcal{D}(\mathcal{A})$ *is given by*

$$\mathcal{D}(\mathcal{A}) = \Big\{ x \in \mathbf{L}_2(0,1) :\ x,\ \partial_z x \ \text{ are absolutely continuous, } \ \partial_z^2 x \in \mathbf{L}_2(0,1),$$
$$\alpha_0 \partial_z x(0) + \beta_0 x(0) = 0 \ \text{ and } \ \alpha_1 \partial_z x(1) + \beta_1 x(1) = 0 \Big\}$$

where $(\alpha_0, \beta_0) \neq (0,0)$ *and* $(\alpha_1, \beta_1) \neq (0,0)$ *then* $-\mathcal{A}$ *is said to be a Sturm-Liouville operator.*

The following result sets the connection between Sturm-Liouville and Riesz spectral operators.

Theorem 2.5. *(DELATTRE, Cédric et al., 2003) Any Sturm-Liouville operator is a Riesz-spectral operator.*

The immediate consequence of this result is that the properties of Riesz-spectral systems and operators (CURTAIN; ZWART, 2020) can be used in the analysis, control and observer design involving Sturm-Liouville operators, in particular for convection-diffusion-reaction systems.

2.2 SEMILINEAR PDE SYSTEMS

It is well-known (see e.g. (PAZY, 2012)) that, under the above assumptions, the Cauchy problem (14) admits a unique mild solution $x(z,t) \in \mathbf{C}^1([0,T];\mathcal{H}),\ T \in \mathbb{R}^+$ given by the integral representation

$$x(z,t) = \mathcal{S}(t)x_0(z) + \int_0^T \mathcal{S}(t-s)F(x(z,s))ds. \tag{35}$$

For the purpose of this thesis, we are interested in studying the exponential stability of the null steady state profile, i.e., $x_{eq}(z) = 0, \forall z \in \Omega$ satisfying $\mathcal{A}x_{eq} + F(x_{eq}) = 0$. Then $x_{eq}(z) = 0$ is exponentially stable in $\mathcal{H}$, if there exists positive scalars $\gamma,\ \rho,\ M$

$$\|x(z,t)\| < M\|x_0(z)\|e^{-\gamma t}, \quad \forall \|x_0(z)\| < \rho \tag{36}$$

and globally exponentially stable if this occurs for every initial condition $x_0(z) \in \mathcal{H}$ with finite norm.

We now turn to the basic tool for stability analysis in the time-domain for these systems, what is known as a Lyapunov functional. Given (14) a dynamical system on $\mathcal{H}$, a Lyapunov functional is a continuous real-valued function $V : \mathcal{H} \to \mathbb{R}^+$ such that

$$D^+[V(x(z,t))] = \lim_{h\to 0^+} \sup \frac{V(x(z,t+h)) - V(x(z,t))}{h} \leq 0, \tag{37}$$

for all $x(z,t)$ satisfying (35).

Notice that if $x(z,t) \in \mathbf{C}^1([0,T];\mathcal{H})$, $T \in \mathbb{R}^+$, then $D^+[V(x(z,t))] = \dot{V}(x(z,t))$. We have the following theorem

Theorem 2.6. *Suppose that $V : \mathcal{H} \to \mathbb{R}^+$ is a Lyapunov functional which satisfies $V(0) = 0$. Let a and b be positive scalars such that*

$$a\|x\| \leq V(x) \leq b\|x\| \tag{38}$$

for all $x \in \mathcal{H}$. Furthermore, suppose there exists $c > 0$ such that for all $t \geq 0$ the upper right-hand derivative of V defined in (37) *satisfies*

$$\dot{V}(x(z,t)) \leq -c\|x(z,t)\| \tag{39}$$

with $x(z,t)$ satisfying (35)*. Then*

$$\|x(z,t)\| \leq \sqrt{\frac{b}{a}}\|x_0(z)\|e^{-\frac{c}{b}t}, \quad t \geq 0. \tag{40}$$

Proof. For the proof of the above theorem, refer to (MEYER; PEET, Matthew M, 2015). □

2.3 SEMI-DEFINITE PROGRAMMING

We use Lyapunov functions parametrized by matrices and sum-of-squares polynomials for the analysis of parabolic PDEs. The search for such Lyapunov functions can be represented as Semi-Definite Programming (SDP) problems.

A SDP problem is an optimization problem of the form (BOYD, S. et al., 1994)

$$\begin{cases} \min\limits_{x\in\mathbb{R}^n} c^T x \\ \text{subject to :} \\ F(x) = F_0 + \sum_{i=1}^n x_i F_i \leq 0, \\ Ax = b \end{cases} \tag{41}$$

where $x \in \mathbb{R}^n$ is the vector of decision variables, and $c \in \mathbb{R}^n$, $b \in \mathbb{R}^k$, $A \in \mathbb{R}^{k\times n}$ and $F_i \in \mathbb{S}^n$, $i = 0, 1, \ldots, n$, are given. Since the cost function is linear and the constraints are affine, an SDP problem is a convex optimization problem. Nowadays, SDP

problems can be solved very efficiently utilizing, for instance, interior point methods (NESTEROV; NEMIROVSKII, 1994; ALIZADEH et al., 1998) where the optimal solution may be obtained in a polynomial number of iterations. A survey of the theory and applications of SDP problems can be found in (VANDENBERGHE; BOYD, S., 1996).

Usually, SDP problems are used to solve the feasibility problem: does there exist an $x \in R^n$ such that $F(x) \leq 0$? The inequality $F(x) \leq 0$ is linear in the search variables. Thus, the feasibility problem is known as a Linear Matrix Inequality (LMI). Any number of given LMIs can be cast as a single LMI. For example, LMIs $F(x) \leq 0$ and $G(x) \leq 0$ can be rewritten as

$$\begin{bmatrix} F(x) & 0 \\ 0 & G(x) \end{bmatrix} = \begin{bmatrix} F_0 & 0 \\ 0 & G_0 \end{bmatrix} + \sum_{i=1}^{n} x_i \begin{bmatrix} F_i & 0 \\ 0 & G_i \end{bmatrix} \leq 0. \tag{42}$$

It is important to emphasize that an LMI can be represented in several ways and hardly appears in a problem in the generic affine form as presented in (41). For example, given a matrix A and a matrix $Q > 0$, the matrix function $F(P) = A^T P + PA + Q$, which appears in various stability problems, is affine with respect to variable P and therefore the inequality $F(P) < 0$ is an LMI that can be easily rewritten in the affine form, where x is the vector containing the elements of the matrix P to be determined. The advantage of the affine generic representation of $F(x)$ in (41) is that every LMI can be rewritten in this way and therefore, most LMIs solvers algorithms are developed for this representation. However the conversion from an LMI to affine form is done by specialized LMI packages called parsers such as YALMIP (LOFBERG, 2004).

2.4 SUM-OF-SQUARES PROGRAMMING

In this thesis, we employ sum-of-squares (SOS) programming in some of our computational formulations. That is, we convert different analysis problems into a SOS program. SOS programming is developed as a consequence of the recent interest in sum of squares polynomials, partly due to the fact that these techniques provide convex relaxations for many hard problems such as global, constrained, and boolean optimization. In this section, we provide a quick overview on SOS tools, and present the general optimization problem in SOS programming

Definition 2.7. *A polynomial $p : \mathbb{R}^n \to \mathbb{R}$ is SOS if there exist polynomials $g_i : \mathbb{R}^n \to \mathbb{R}$ such that*

$$p(\mathrm{z}) = \sum_{i=1}^{m} g_i^2(\mathrm{z}). \tag{43}$$

We use $p \in \Sigma_s$ to denote that p is SOS.

The importance of the SOS condition lies in the fact that it can be readily enforced using semidefinite programming. This fact is attributed to the following theorem.

Theorem 2.7. *A polynomial $p : \mathbb{R}^n \to \mathbb{R}$ of degree $2m$ is SOS if and only if there exists a positive semidefinite matrix Q such that*

$$p(\mathbf{z}) = Z_m^T(\mathbf{z})\ Q\ Z_m(\mathbf{z}) \tag{44}$$

where $Z_m(\mathbf{z})$ is a vector of monomials up to degree m.

Proof. For the proof, refer to (PARRILO, 2003). □

As hinted above, sums of squares techniques can be used to provide tractable relaxations for many hard optimization problems. A very general and powerful relaxation methodology, introduced in (PARRILO, 2000), is based on the Positivstellensatz, a central result in real algebraic geometry. Some approaches in this work can be interpreted as special cases of the practical application of this general relaxation method. The general optimization problem in SOS programming will be formulated as follows:

$$\begin{cases} \min_c\ w^T c \\ \text{where } c \text{ is a vector formed from the (unknown) coefficients of} \\ \text{polynomials} \quad p_i(z), \quad i = 1, ..., \hat{N}, \\ \text{sum of squares} \quad p_i(z), \quad i = \hat{N}+1, ..., N, \\ \text{such that} \\ a_{0,j}(z) + \sum_{i=1}^{N} p_i(z) a_{i,j}(z) = 0,\ j = 1, ..., \hat{J}, \\ a_{0,j}(z) + \sum_{i=1}^{N} p_i(z) a_{i,j}(z) \ \text{ are SOS},\ j = \hat{J}+1, ..., J. \end{cases} \tag{45}$$

In the above formulation, w is the vector of weighting coefficients for the linear objective function. The problem formulated above are quite general, and in specific cases reduce to well-known problems. In particular, notice that if all the unknown polynomials p_i are restricted to be constants, and the $a_{i,j}$, $b_{i,j}$ are quadratic forms, then we exactly recover the standard linear matrix inequality (LMI) problem formulation. The extra degrees of freedom in SOS programming are actually a bit illusory, as every SOSP can be exactly converted to an equivalent SDP problemm (PARRILO, 2000). Nevertheless, for several reasons, the problem specification outlined above has definite practical and methodological advantages, and establishes a useful framework within which many specific problems can be solved.

Algorithms for solving SOS programs are automated in MATLAB toolboxes such as SOSTOOLS (PAPACHRISTODOULOU et al., 2013) and YALMIP (LOFBERG, 2004), in which the SOS problem is parsed into an SDP formulation and the SDPs are solved by LMI solvers such as SeDuMi (STURM, 1999). In this thesis, we use the SOSTOOLS toolbox for the numerical experiments.

2.5 MODEL REDUCTION

Either for numerical simulation or for control and observer design, PDEs models are commonly reduced to a set of ODEs by using reduced order methods. Within the time–space separation framework, different approaches can be used based either on discretization or functional approximation, and combinations of the two. The method of weighted residuals (MWR) (FINLAYSON, 2013) is one of the most common methods for model reduction in reduced order modeling.

2.5.1 Method of weighted residuals (MWR)

MWR is a general method of obtaining approximate solutions for PDEs. The unknown solution is expanded in a set of trial functions, which are specified, but with adjustable constants (or functions), which are chosen to give the best solution to the PDE.

In general, applications with MWR have three important steps: choice of a trial function, choice of a criterion that involves the selection of weight functions to minimize the residual, and calculation of successive approximations. It has been shown that the choice of a criterion is not too crucial, especially for higher approximations (FINLAYSON, 2003). The choice of trial functions is more important, and some possibilities are discussed in this section.

In order to present MWR, consider the abstract formulation of the PDE system in (14) with $\mathcal{H} = \mathbf{L}_2(\Omega)$. Thus, the unknown solution $x(z,t)$ is approximated by a function $x^*(z,t)$ and we write

$$x(z,t) \approx x^*(z,t) = \sum_{n=1}^{N} a_n(t)\phi_i(z) \tag{46}$$

where the set $\{\phi_n(z) : n = 1, ..., N\}$ constitutes a basis for a finite dimensional subspace of $\mathcal{H}$ and the a_n coefficients are functions of time. The approximate solution to the problem is then expressed in terms of the N trial functions, where the coefficients $a_n(t)$ must be defined in such a way that $x^*(z,t)$ is a good approximation to the solution of (14), i.e., $x^*(z,t) \in \mathcal{D}(\mathcal{A}),\ \forall t \geq 0$ and the residual

$$R(z,t) = \partial_t x^*(z,t) - \mathcal{A}x^*(z,t) - F(x^*(z,t)) \tag{47}$$

approaches to zero in some average sense over the spatial domain Ω by requiring that

$$\left\langle w_i(z), R(z,t) \right\rangle = 0, \quad i = 1, ..., N \tag{48}$$

where $\{w_i(z) : i = 1, ...N\}$ is a set of weighting functions to be chosen. The choice of weighting functions can lead to several different submethods. Let us discuss the two most used in systems theory:

1. Galerkin method – when the weighting functions $w_1(z), \ldots, w_N(z)$ are chosen to be the basis functions themselves, i.e.,

$$w_i(z) = \phi_i(z), \quad i = 1, 2, ..., N \tag{49}$$

then the technique is referred as the Galerkin method. This technique has the advantage that the residual is made orthogonal to each basis function and therefore is considered as the best solution possible in the space made up of the N functions $\phi_1, \ldots, \phi_N(z)$. Thus, as $N \to \infty$, the residual $R(z,t)$ tends to zero, because it will be orthogonal to every function in a complete set of functions.

2. Collocation methods – when $w_i(z)$ is chosen to be dirac functions $\delta(z-z_i)$, then (48) is applied to $R(z,t)$ yielding

$$R(z = z_i, t) = 0, \quad i = 1, \ldots, N, \tag{50}$$

and the differential equation is required to be solved exactly at N points on the spatial domain. The collocation method has been further refined in (FINLAYSON, 2013; STEWART, W.; SØRENSEN, 1980) and has been shown to be extremely powerful. The recent versions are called orthogonal collocation because orthogonal polynomials are used as the basis functions and the collocation points are specified automatically in an optimal way, for instance, the roots of the orthogonal polynomials (e.g., (LEFÈVRE et al., 2000)).

2.6 CONCLUDING REMARKS

This chapter is mainly aimed at presenting some fundamental concepts related to the well-posedness, stability and model reduction of PDE systems as well as a brief review of Semi-Definite Programming (SDP) and SOS (Sum of Squares) tools which are the main instruments for the computational synthesis of state observers in this thesis. Notice that this chapter was limited to questions related to definitions and review of general methodologies and results. However, this constitutes a fundamental component for the comprehension of this work. The focus of the following chapters will be on the observer design problem for the class of transport-reaction systems of interest, and more particularly, on specific approaches used for solving this problem.

3 EARLY LUMPING OBSERVER DESIGN

In this chapter we address the design of finite-dimensional state estimators for the transport-reaction systems of interest. To accomplish this task, the PDE system is approximated using the standard method of weighted residuals (MWR) that actually encompasses several methods (Galerkin, collocation, subdomains, among others) to obtain the reduced order approximate model described by a set of ODEs with different degrees of accuracy. Particularly, the orthogonal collocation method is selected as method to derive a reduced order model described by a differential-algebraic system of equations (DAEs). Thus, the design procedure firstly results in a brief review study that aims to obtain a satisfactory reduced order model through the conventional analysis of selecting the appropriate location of the collocation points to guarantee accuracy and robustness.Later, a Lyapunov-based design method is proposed for the reduced-order model which provides sufficient design conditions in terms of standard linear matrix inequalities (LMIs) aiming the exponential convergence of the estimation error with a prescribed decay rate. The observer performance is further improved through an offline optimal sensor placement algorithm considering a parameterized reduced-order output matrix. A case study related to a nonisothermal tubular reactor is presented to demonstrate the observer performance as well as the advantages of the proposed sensor placement optimization scheme.

3.1 ORTHOGONAL COLLOCATION METHOD

Many of the rate functions involved in transport-reaction systems concern strong nonlinearities with respect to the state variables. Clearly, if the state variables are expanded in a series of functions and the method of weighted residuals (MWR) is applied, it would be difficult to derive the values of integrals involving the referred nonlinear terms. A quadrature method can be employed to ease this problem, however a more direct approach would be appropriate for control and state estimation applications. In the collocation method it is only necessary to evaluate the residual at the collocation points an that is why the orthogonal collocation method can be easily implemented, which has been first introduced in (VILLADSEN, JV; STEWART, Warren E, 1967). They discovered that collocation points chosen as the roots of orthogonal polynomials gave good results due to some attractive features of these polynomials. They also chose the trial functions as the Jacobi polynomials and picked the collocation points as the corresponding zeros of these polynomials. Thereafter, many researchers used it to solve a variety of nonlinear problems in chemical engineering (FINLAYSON, 2003, 2013; ALHUMAIZI, 2006; LEFÈVRE et al., 2000).

3.2 MODEL REDUCTION

We use the Lagrange interpolation polynomial to get an approximate solution of (1)-(3), that is

$$x_i^*(z,t) = \sum_{n=1}^{N} a_{i,n}(t)\ell_n(z), \quad i = 1, ..., n_x \tag{51}$$

where $x_i^*(z,t)$ denotes the approximation of $x_i(z,t)$, $N-1$ is the order of the reduction and $\ell_n(z)$ is the $(N-1)$-th order Lagrange interpolation polynomial defined by

$$\ell_n(z) = \prod_{\substack{m=1 \\ m\neq n}}^{N} \frac{z - z_m}{z_n - z_m}, \quad n = 1, ..., N \tag{52}$$

with $0 = z_1 < z_2 < \cdots < z_{N-1} < z_N = 1$ being the interpolation/collocation nodes in such a way that the set $\{z_m : m = 2, \cdots, N-1\}$ is chosen as the roots of the $(N-2)$-th degree monic Jacobi polynomial $\mathrm{P}_{N-2}^{(\alpha,\beta)}$ (LEFÈVRE et al., 2000).

The Lagrange polynomial has the property that

$$\ell_n(z_m) = \begin{cases} 1, & m = n \\ 0, & m \neq n \end{cases} \tag{53}$$

for $n = 1, \ldots, N$. Moreover, the set $\{\ell_n(z) : i = 1, ..., N\}$ is linearly independent and forms a basis for the space of polynomials of degree less than or equal to $N-1$ on the interval $[0, 1]$. Furthermore, in virtue of (53), it follows that

$$a_{i,n}(t) = x_i^*(z_n, t) = x_i(z_n, t); \quad i = 1, ..., n_x \text{ and } n = 1, ..., N, \tag{54}$$

which means that the approximate solution at nodes $z_1, \ldots, z_n$ are time-variant coefficients in equation (51).

Considering the approximate solution (51) for (1)-(3), the residual becomes

$$\begin{aligned} R_i(z,t) = &\sum_{n=1}^{N} \left[\dot{a}_{i,n}(t)\ell_n(z) - d_i a_{i,n}(t)\frac{d^2\ell_n}{dz^2}(z) + \upsilon_i a_{i,n}(t)\frac{d\ell_n}{dz}(z) + \mathrm{K}_i a_{i,n}\ell_n(z) \right] \\ &- b_i u_{d,i}(t) - G_i^T r\left(\sum_{n=1}^{N} a_{1,n}(t)\ell_n(z), \cdots, \sum_{n=1}^{N} a_{n_x,n}(t)\ell_n(z) \right), \quad i = 1, ..., n_x. \end{aligned} \tag{55}$$

The residual equations associated to the orthogonal collocation method are produced by

$$\int_0^1 R_i(z,t)\delta(z - z_m)dz = R_i(z_m, t) = 0; \quad i = 1, ..., n_x, \quad m = 1, ..., N. \tag{56}$$

Thus, from (55) and (56), it follows that

$$\dot{a}_{i,m}(t) = \sum_{n=1}^{N} \left[d_i \frac{d^2\ell_n}{dz^2}(z_m) - \upsilon_i \frac{d\ell_n}{dz}(z_m) \right] a_{i,n}(t) - \kappa_i a_{i,n}(t) + b_i u_{d,i}(t) + G_i^T r\left(a_{1,m}(t), \cdots, a_{n_x,m}(t)\right); \quad (57)$$

$i = 1, ..., n_x$, $m = 1, ..., N$. Additionally, the boundary conditions in (2) set

$$\sum_{n=1}^{N} \alpha_{0,i} a_{i,n}(t) \frac{d\ell_n}{dz}(z_1) + \beta_{0,1} a_{i,1}(t) = u_{0,i}(t) \quad (58)$$

$$\alpha_{1,i} a_{i,N}(t) + \sum_{n=1}^{N} \beta_{1,i} a_{i,n}(t) \frac{d\ell_n}{dz}(z_N) = u_{1,i}(t), \quad (59)$$

$i = 1, ..., n_x$.

Defining L_1, L_2 as the matrices of, respectively, first and second order derivatives of Lagrange polynomials evaluated at the collocation points, that is:

$$(\mathsf{L}_1)_{m,n} = \frac{d\ell_n}{dz}(z_m), \quad (\mathsf{L}_2)_{m,n} = \frac{d^2\ell_n}{dz^2}(z_m); \quad m, n = 1, ..., N. \quad (60)$$

We can express (57)-(59) in the following state space representation

$$\dot{a}(t) = Aa(t) + B_d u_d(t) + G_a\, r_a(a(t)) \quad (61)$$

$$B_b a(t) = u_b(t) \quad (62)$$

where

$$a(t) = \begin{bmatrix} a_{1,1}(t) & \cdots & a_{1,N}(t) & \cdots & a_{n_x,1}(t) & \cdots & a_{n_x,N}(t) \end{bmatrix}^T \in \mathbb{R}^{Nn_x},$$

$$u_b(t) = \begin{bmatrix} u_{0,1}(t) & u_{1,1}(t) & \cdots & u_{0,n_x}(t) & u_{1,n_x}(t) \end{bmatrix}^T \in \mathbb{R}^{2n_x},$$

and the corresponding system matrices are defined as

$$A = \mathrm{diag}\left(A_1, ..., A_{n_x}\right), \quad A_i = d_i \mathsf{L}_2 - \upsilon_i \mathsf{L}_1 - \kappa_i I_N, \quad i = 1, ..., n_x,$$

$$B_d = \mathrm{diag}\left(B_{d,1}, ..., B_{d,n_x}\right), \quad B_{d,i} = \overrightarrow{1}_N\, b_i, \quad i = 1, ..., n_x,$$

$$B_b = \mathrm{diag}\left(B_{b,1}, ..., B_{b,n_x}\right),$$

$$B_{b,i} = \begin{bmatrix} \alpha_{0,i}\frac{d}{dz}\ell_1(z_1) & \cdots & \alpha_{0,i}\frac{d}{dz}\ell_N(z_1) \\ \alpha_{1,i}\frac{d}{dz}\ell_1(z_N) & \cdots & \alpha_{1,i}\frac{d}{dz}\ell_N(z_N) \end{bmatrix} + \begin{bmatrix} \beta_{0,i} & \cdots & 0 \\ 0 & \cdots & \beta_{1,i} \end{bmatrix}, \; i = 1, ..., n_x,$$

$$G_a = \begin{bmatrix} I_N \otimes G_1^T \\ \vdots \\ I_N \otimes G_{n_x}^T \end{bmatrix}, \qquad r_a(a) = \begin{bmatrix} r\left(a_{1,1}, ..., a_{n_x,1}\right) \\ \vdots \\ r\left(a_{1,N}, ..., a_{n_x,N}\right) \end{bmatrix}. \tag{63}$$

Likewise, we can also obtain the reduced-order characterization of the output measurement (5). It is described as

$$y_a(t) = Ca(t) \tag{64}$$

where

$$C = \text{diag}(\mathbf{c}_1^T, ..., \mathbf{c}_{n_y}^T) \begin{bmatrix} I \otimes \int_0^1 c_1(z)\mathbf{l}(z)dz \\ \vdots \\ I \otimes \int_0^1 c_{n_y}(z)\mathbf{l}(z)dz \end{bmatrix} \tag{65}$$

and

$$\mathbf{l}(z) = \begin{bmatrix} \ell_1(z) & \cdots & \ell_N(z) \end{bmatrix}. \tag{66}$$

3.2.1 Interpolation error minimization

In searching the approximated solution in the form of (51), we actually look, at each fixed time t, for the $(N-1)$th order polynomial which interpolates the unknown exact solution at the N collocation points $(z_1, ..., z_N)$. The following Cauchy's result (see (DAVIS, 1975)), gives an upper error bound for such approximations.

Let us define the interpolation error by:

$$e^*(z,t) = x(z,t) - x^*(z,t)$$

where $x^*(z,t)$ is the approximate solution whose components are described by (51). Assuming that the unknown solution $x(z,t)$ is sufficiently continuously differentiable, we have that

$$e^*(z,t) = w(z)\frac{\partial_z^{N+1} x(\epsilon(z),t)}{(N+1)!} \tag{67}$$

where

$$w(z) = \prod_{m=1}^{N}(z - z_m) \tag{68}$$

and $\epsilon(z) \in [0, 1]$. Hence, we aim at selecting the interior collocation points $z_2, ..., z_{N-1}$ that minimizes the interpolation error in (67). Without any a priori knowledge on the behaviour of the exact solution, this problem reduces to find the $z_2, ..., z_{N-1}$ such that $\|w(\cdot)\|_\infty$ is minimal.

Equation (67) suggests that we can handle the effect of large variations (typically, due to the presence of 'hot spots' i.e. large and concentrated variations in the spatial profiles of the state variables) on the interpolation error by choosing suitable collocation points. Therefore, in (LEFÈVRE et al., 2000) it is suggested that the selection of the $N-2$ interior collocation points may be carried out through the solution of the following problem

$$\min_{z_1,...,z_N \in [0,1]} \left(\left\| \prod_{m=1}^{N} (z - z_m) w_\infty(z) \right\|_\infty \right) \tag{69}$$

where the weight $w_\infty(z)$ is supposed to be large around the hot spots, and small everywhere else which led us to keep the interpolation error small where it should be large.

The solution of the minimization problem in (69) is tackled in (LEFÈVRE et al., 2000). Therein, it is found that a satisfactory approximation result may be obtained with

$$w_\infty(z) = \sqrt{\sqrt{1 - z^2} w(z)}. \tag{70}$$

Thus, in the case where the collocation points $z_2, ..., z_{N-1}$ are the zeros of Jacobi polynomials $\mathbf{P}_{N-2}^{(\alpha,\beta)}$, we know that

$$w(z) = (1 - z)^\alpha (1 + z)^\beta. \tag{71}$$

Hence, it implies that using these collocation points, we will get an approximated solution which minimises an interpolation error weighted by the function,

$$\begin{aligned} w_\infty(z) &= \sqrt{\sqrt{1 - z^2}(1 - z)^\alpha (1 + z)^\beta} \\ &= (1 - z)^{\frac{2\alpha+1}{4}} (1 + z)^{\frac{2\beta+1}{4}} \end{aligned} \tag{72}$$

with $\alpha,\ \beta \geq -\frac{1}{2}$.

Many shapes may be reached with weight of the form in (72). They allow to emphasise the interpolation error from one side to the other of the transport-reaction system, according to the values of the tuning parameters α and β. A simple scaling of the weights $w(z)$ on $[0, 1]$ and short calculations show that these weighting functions reach their maximum in

$$z_{max} = \frac{1 + 2\beta}{2(\alpha + \beta + 1)}. \tag{73}$$

The dependence of z_{max} with respect to α and β is illustrated in Figure 5 for values of a ranging from $-\frac{1}{2}$ ('Chebyshev' or uniform weighting) to 2. It gives us an overall view where the weight error is more localized around in terms of the parameters α and β.

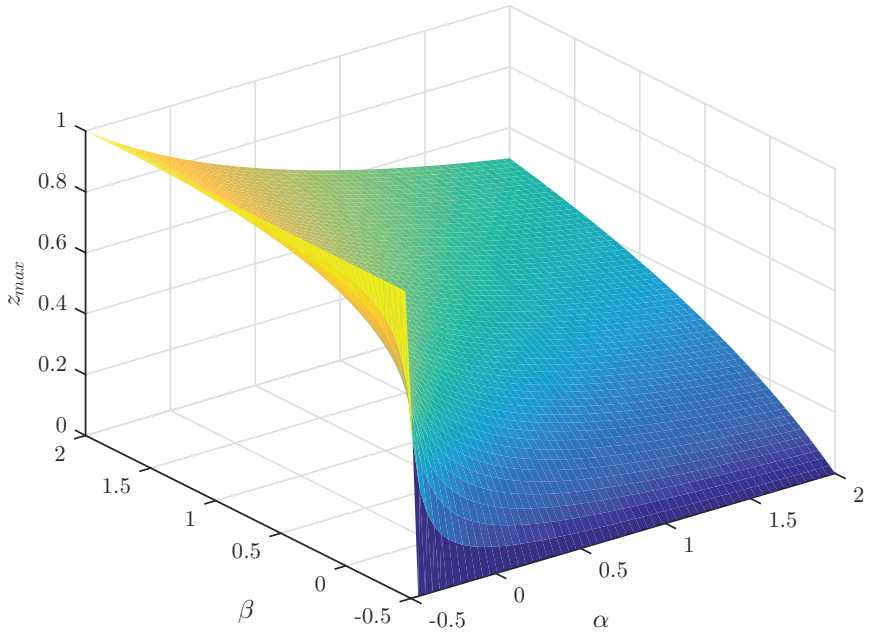

Figure 5 – z_{max} when α, β range from $[-\frac{1}{2}, 2]$.

3.2.2 Well-posedness of the reduced model

As $r_a(a)$ models the reactions function $r(x)$ and it is possibly highly non-linear since its components essentially depend, for instance, on the chosen kinetic models, hence a general theory on its behaviour cannot be made available. No general information on its structure, nor on its fastest variation rate, may be used to specify $r_a(a)$, due to the very large variety of reaction functions used in process engineering. However, In transport reaction systems, it may be supposed that it is differentiable, hence locally Lipschitzian. The following assumption will, therefore, holds in the following

$$\|r_a(a) - r_a(\hat{a})\| \leq l^a \|a - \hat{a}\| \tag{74}$$

where $l^a = l^a(\rho_a)$ with ρ_a being a positive scalar such that $\|a\| < \rho_a$ and $\|\hat{a}\| \leq \rho_a$. This assumption guarantees the global existence and uniqueness of a solution for equations (61)-(64).

The next result establishes what is often called 'the continuous dependence of the solution' (see e.g. (GOTTLIEB; ORSZAG, 1977)), relatively to system (61)-(62). It is

here generalised slightly in order to take into account the specific features of transport reaction systems

Theorem 3.1. *(LEFÈVRE et al., 2000) Let a perturbed problem be defined according to*

$$\dot{a_p}(t) = A a_p(t) + B_d u_d(t) + G_a\, r_a(a_p(t)) + \varpi(t) \tag{75}$$

$$B_b a_p(t) = u_b(t) \tag{76}$$

where the perturbation $\varpi(t)$ is assumed to be continuous. Then, the norm of the distance between the solution of the initial problem (61)-(62) and the perturbed problem (75)-(76) is upper bounded as follows

$$\|a_p(t) - a(t)\| \leq \varpi_0 e^{\vartheta t} + \varpi_\infty \frac{e^{\vartheta t} - 1}{\vartheta} \tag{77}$$

where $\varpi_\infty = \max_{t\in\mathbb{R}^+} \varpi(t)$, $\vartheta = l^a + \sigma_{max}(A)$.

Proof. see (LEFÈVRE et al., 2000). □

Equation (77) shows the continuous dependence of the (exact) solution of (61)-(62) to its data. Moreover, it bounds the fastest propagation of floating points errors we may expect, as well as the propagation of errors due to modelling, inaccurate parameters estimation, or approximate initial conditions. All these errors should be evaluated carefully, when dealing with model reduction of transport-reaction systems.

On the other hand the linear part of (61), representing the discretised transport component of the model, has always the same structure, and informations on it may be summarised in the matrix A. Thus, to improve the conditioning of the differential problem in (61)-(62), that is to minimise ϑ, tuning the position of collocation points may be an efficient strategy. There is no simple analytic expression for the largest singular value of A, since it strongly depends on the advection matrix $\mathcal{V}$, and on the diffusion matrix D, that is on operating conditions of the system. However, we may resort to efficient numerical methods to compute it in a range of collocation points.

Taking into account this conditioning problem, the position of collocation points has to be determined with two simultaneous criteria

1. it should minimise the theoretical interpolation error, relatively to a suitable choice of a weighting factor, related to the dynamics of the reactor model (see Section 3.2.1);

2. it should give a reasonable conditioning number, which allows the computed solution (numerical integration) to be representative of the theoretical accuracy of the reduction method.

3.3 STATE OBSERVER DESIGN

Considering the reduced order finite dimensional state space representation described in (61)-(64), the following extended Luenberger observer is proposed to estimate the state vector $a(t)$:

$$\begin{aligned} \dot{\hat{a}}(t) &= A\hat{a}(t) + B_d u_d(t) + G_a r_a(\hat{a}(t)) + L_o(\hat{y}_a(t) - y_a(t)) \\ B_b\hat{a}(t) &= u_b(t) \\ \hat{y}_a &= C\hat{a}(t) \end{aligned} \tag{78}$$

where $\hat{a}(t) \in \mathbb{R}^{Nn_x}$ is the observer state and $L_o \in \mathbb{R}^{Nn_x \times n_y}$ is the output injection gain. Hence, the estimation $\hat{x}_i(z,t)$ of $x_i(z,t)$ can be obtained from

$$\hat{x}_i(z,t) = \sum_{n=1}^{N} \hat{a}_{i,n}(t)\ell_n(z), \quad i = 1, ..., n_x. \tag{79}$$

Let

$$\tilde{a}(t) := a(t) - \hat{a}(t) \tag{80}$$

be the estimation error. Then, the output injection gain L_o is designed in order to ensure the stability of the estimation error dynamics, which is described by

$$\dot{\tilde{a}}(t) = (A + L_o C)\tilde{a}(t) + G_a\left[r_a(a(t)) - r_a(\hat{a}(t))\right] \tag{81}$$

$$B_b\tilde{a}(t) = 0. \tag{82}$$

where $r_a(a(t)) \in \mathbb{R}^{Nn_r}$ is defined according to (63).

Notice from (4) that $r_a(a(t))$ satisfies the following local Lipschitz condition

$$\|r_a(a(t)) - r_a(\hat{a}(t))\| \leq l^a \|a(t) - \hat{a}(t)\| \tag{83}$$

where $l^a = l^a(\rho_a)$ with ρ_a being a positive scalar such that $\|a\| < \rho_a$ and $\|\hat{a}\| \leq \rho_a$.

Based on the above condition, the function $\nu(t)$ defined as

$$\nu(t) := r_a(a(t)) - r_a(\hat{a}(t)) \tag{84}$$

and the the estimation error $\tilde{a}(t)$ satisfy different algebraic conditions (AÇIKMEŞE; CORLESS, 2011; ARCAK; KOKOTOVIĆ, 2001). In this work, we use a sector condition based on the boundedness of the Jacobian matrix of the nonlinear function $r_a(\cdot)$.

3.3.1 Sector Condition for $a(t)$ and $\nu(t)$

Suppose the two matrices $\Gamma_1,\ \Gamma_2 \in \mathbb{R}^{Nn_r \times Nn_x}$ are respectively constant matrices whose entries are the local lower and upper bound of the Jacobian matrix entries of $r_a(\cdot)$ defined as

$$\Gamma(a) := \nabla_a r_a(a) \tag{85}$$

Then, the Differential Mean Value Theorem (ZEMOUCHE et al., 2005) leads to the following inequality

$$\Gamma_1(a-\hat{a}) \leq r_a(a) - r_a(\hat{a}) \leq \Gamma_2(a-\hat{a}). \tag{86}$$

Notice that the above inequality can be cast in the following sector condition

$$(\nu(t) - \Gamma_1 \tilde{a}(t))^T (\Gamma_2 \tilde{a}(t) - \nu(t)) \geq 0 \tag{87}$$

or, equivalently, in the following quadratic form

$$\begin{bmatrix} \tilde{a}(t) \\ \nu(t) \end{bmatrix}^T \underbrace{\begin{bmatrix} \frac{\Gamma_1^T\Gamma_2 + \Gamma_2^T\Gamma_1}{2} & -\frac{\Gamma_1^T + \Gamma_2^T}{2} \\ -\frac{\Gamma_1+\Gamma_2}{2} & I \end{bmatrix}}_{M} \begin{bmatrix} \tilde{a}(t) \\ \nu(t) \end{bmatrix} \leq 0. \tag{88}$$

Remark 3.1. *The error dynamics in* (81)-(82) *with* (83) *can be represented as a Lure system as illustrated in Fig. 6, where the mapping from* $\tilde{a}(t)$ *to* $\nu(t)$ *satisfies the sector condition defined in* (88)*. Then, the sector condition can be embedded into the stability analysis by applying the S-Procedure (BOYD, S. et al., 1994).*

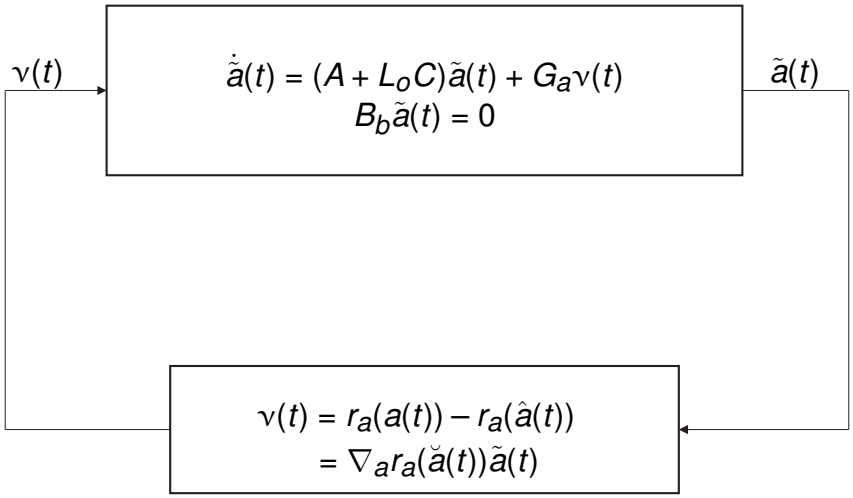

Figure 6 – Lure-System representation of the observer error system.

The following result provides an LMI based condition to the computation of the output injection gain L_o guaranteeing the local exponential stability of the estimation error dynamics while ensuring a lower bound on the estimation error decay rate.

Theorem 3.2. *Let γ be a given positive scalar. Suppose there exist matrices $P > 0$, with $P = P^T$, and W having appropriate dimensions, and scalars $\tau > 0$ and μ satisfying the following LMI:*

$$\begin{bmatrix} \text{He}\{PA\} + WC + C^T W^T + 2\gamma P - \mu B_b^T B_b & PG_a \\ G_a^T P & 0 \end{bmatrix} - \tau M < 0 \tag{89}$$

Then, the estimation error dynamics as defined in (81)-(82) *is locally exponentially stable with a guaranteed decay rate γ, where the observer gain is given by:*

$$L_o = P^{-1} W \, . \tag{90}$$

Proof. Suppose there exists a feasible solution (P, W, μ, τ) to (89) and consider the parametrization $W = PL_o$. Now, let

$$V(t) = \tilde{a}^T(t) P \tilde{a}(t) \tag{91}$$

be a Lyapunov function candidate to the estimation error dynamics defined in (81)-(82).

Next, notice that (89) can be cast as follows

$$\begin{bmatrix} \text{He}\{P(A + L_o C)\} + 2\gamma P & PG_a \\ G_a^T P & 0 \end{bmatrix} - \mu \begin{bmatrix} B_b^T \\ 0 \end{bmatrix} \begin{bmatrix} B_b^T \\ 0 \end{bmatrix}^T - \tau M < 0 \tag{92}$$

Thus, pre- and post-multiplying (92) by $\begin{bmatrix} \tilde{a}^T(t) & \nu^T(t) \end{bmatrix}$ and its transpose yields

$$\dot{V}(t) + 2\gamma V(t) < 0, \tag{93}$$

since

$$\begin{bmatrix} B_b & 0 \end{bmatrix} \begin{bmatrix} \tilde{a}(t) \\ \nu(t) \end{bmatrix} = 0 \;\text{ and }\; -\tau \begin{bmatrix} \tilde{a}(t) \\ \nu(t) \end{bmatrix}^T M \begin{bmatrix} \tilde{a}(t) \\ \nu(t) \end{bmatrix} \geq 0.$$

Then, from the comparison lemma (KHALIL, 2002), the dissipation inequality in (93) implies that

$$\|\tilde{a}(t)\| \leq \underbrace{\sqrt{\frac{\lambda_{max}(P)}{\lambda_{min}(P)}}\, \|\tilde{a}(0)\|}_{M_{\tilde{a}}} \, \text{e}^{-\gamma t} \tag{94}$$

for a sufficiently small ρ_0 such that $\|\tilde{a}(0)\| \leq \rho_0$, which completes the proof. □

The LMI-based observer design may return high observer gains which is usually undesirable in practical applications. Since we cannot directly restrict the observer gain L_o because it is not a decision variable in the LMI constraint, we resort to limit its norm.

To this end, suppose that χ is the maximum allowed norm for the observer gain L_o. Then, the following inequality holds

$$L_o^T L_o = W^T P^{-2} W \leq \chi I$$

From Schur complement, we obtain

$$\begin{bmatrix} \chi I & W^T \\ W & P^2 \end{bmatrix} \geq 0. \tag{95}$$

As (95) depends on the decision variable P quadratically, we propose the following relaxation

$$P - \theta I \geq 0 \qquad \begin{bmatrix} \chi I & W^T \\ W & \theta^2 I \end{bmatrix} \geq 0 \tag{96}$$

where $\theta > 0$ is a small positive scalar assigned by the designer.

3.3.2 Distributed state estimation error

Considering that the lumped parameter system described by (61)-(62) allow us to approximate accurately the distributed parameter system in (1)-(2) over the whole dimensionless spatial domain $z \in [0, 1]$ through the appropriate selection of the collocation points (LEFÈVRE et al., 2000) we can easily obtain from (94) that

$$\|x^*(z,t) - \hat{x}(z,t)\| \leq \underbrace{\sqrt{\lambda_{max}\left(\int_0^1 \mathrm{l}^T(z)\mathrm{l}(z)dz\right)}\sqrt{\frac{\lambda_{max}(P)}{\lambda_{min}(P)}}\|\tilde{a}(0)\|}_{M_e} \mathrm{e}^{-\gamma t}. \tag{97}$$

Since $x^*(z,t) = x(z,t) - e^*(z,t)$, the distributed estimation error $e(z,t) = x(z,t) - \hat{x}(z,t)$ is such that

$$\|e(z,t)\| \leq M_e \mathrm{e}^{-\gamma t} + \frac{\partial_z^{N+1} x(\epsilon(z),t)}{(N+1)!}\|w(z)\|, \quad \epsilon(z) \in [0,1]. \tag{98}$$

3.3.3 Sensors placement algorithm

In this section the sensor optimal placement problem is addressed by optimizing the lower bound γ on the estimation error decay rate with respect to sensor location candidates while ensuring an upper bound on the observer gain norm. Then, we first

parameterize the output matrix $C = C(\zeta_j)$, $\zeta_j \in Z$, as derived in (65), where Z corresponds to some specific set related to the pointwise measurements positions or otherwise the center points related to the distributed measurements intervals according to the description in Section 1.3.1 That is:

$$Z = \{\zeta_1, ..., \zeta_{n_y}\}. \tag{99}$$

In addition, it is assumed there exists a finite set

$$\mathfrak{Z} = \{Z_1, ..., Z_s\} \tag{100}$$

defining the sensor location candidates for a given specific practical application.

The reason for considering a finite set $\mathfrak{Z}$ is twofold. Firstly, due to practical design considerations, one rarely has the freedom to place sensors in more than a finite number of feasible locations; and secondly, one avoids considering a continuum of sensor locations which could lead to an infeasible optimization. Notice, by considering a finite set $\mathfrak{Z}$, one can apply simpler static optimization techniques leading to considerable computation savings.

In view of the above developments, the following algorithm for the observer design with optimal sensor location is proposed.

Algorithm 1.

1. Define the set of admissible sensor locations $\mathfrak{Z}$ implicitly assuming the feasibility of the problem for every $Z_i \in \mathfrak{Z}$.
2. Build the matrix $C = C(\zeta_j^{(i)})$, $\zeta_j^{(i)} \in Z_i$, as defined in (65) for each $Z_i \in \mathfrak{Z}$.
3. For each $Z_i \in \mathfrak{Z}$ and given θ_i and χ_i, $i = 1, \ldots, s$, such that the implementability of the observer is guaranteed, find the interval of feasibility $[0, \bar{\gamma}_i]$ related to the decay rate parameter γ in the Z-parameterized LMI conditions (89) and (96).
4. The optimal sensor location is determined via

$$Z^{opt} = \arg \max_{Z_i \in \mathfrak{Z}} \bar{\gamma}_i.$$

3.3.4 Optimal initial conditions

It is clear from (97) that the observer designer has two independent means for enhancing the condition that '$\|e(z,t)\| \to 0$ promptly'. First, the gain matrix L_o can be designed to make γ as large as possible which is accomplished by the sensor placement algorithm. Secondly, the value of $\hat{a}(0)$ can be designed to minimize the 'start-up error norm'

$$\|\tilde{a}(0)\| = \|a(0) - \hat{a}(0)\| \tag{101}$$

in some physically realizable sense. The design of $\hat{a}(0)$ to reduce or minimize (101) is a subject that has almost been completely ignored in state estimation applications. As a consequence, control engineers in industry usually set $\hat{a}(0) = 0$ in which case $\|\tilde{a}(0)\| = \|a(0)\|$. However, this choice does not reduce $\|\tilde{a}(0)\|$ as much as is physically possible. In particular, considering that $x(z,0)$ and hence $a(0)$ are unknown and by virtue of the triangular inequality $\|a(0)-\hat{a}(0)\| \leq \|a(0)\| + \|\hat{a}(0)\|$ which lead us to aim at minimizing $\|\hat{a}(0)\|$. Then the physically realizable design is related to meet the boundary conditions and the initial measurements $y(0)$ which is assumed to be known. Thus, the solution of the semidefinite programming (SDP) problem in (102) that can be solved by using conventional SOS (sum of squares) tools (PAPACHRISTODOULOU et al., 2013) provides a local optimal selection for $\hat{a}(0)$ and hence for $\hat{x}(z,0)$.

$$\begin{cases} \min \|\hat{a}(0)\| \\ \text{subject to} \\ B_b\hat{a}(0) = u(0) \\ C\hat{a}(0) = y(0) \\ \mathrm{I}(z)\begin{bmatrix} a_{i,1}(0) \\ \vdots \\ a_{i,N}(0) \end{bmatrix} \geq 0, \quad \forall z \in [0,1], \quad i = 1,...,n_x. \end{cases} \tag{102}$$

Remark 3.2. *Since we cannot directly implement the minimization of* $\|\hat{a}(0)\|$ *in* (102)*, we substitute it with the following equivalent convex relaxation*

$$\begin{cases} \textit{min } \vartheta \\ \textit{subject to} \\ \begin{bmatrix} \vartheta I & \hat{a}^T(0) \\ \hat{a}(0) & I \end{bmatrix} \geq 0. \end{cases} \tag{103}$$

3.4 CO_2 METHANATION IN A FIXED BED REACTOR

The dynamic hydrogenation of carbon oxides towards methane is becoming increasingly important. Besides hydrogen, synthetic methane offers the possibility to store large amounts of energy from renewable sources for long time periods in an already existing storage system, the natural gas grid. Carbon dioxide captured from the atmosphere, biogas plants, or flue gas emitted by large scale power plants can be converted with hydrogen from renewable energies via water electrolysis in the Sabatier

reaction:

$$CO_2 + 4H_2 \rightarrow CH_4 + 2H_2O. \tag{104}$$

Consider a laboratory-scale catalytic fixed-bed reactor in which the hydrogenation of small amounts of CO_2 to methane is accomplished according to (104). The model consists of two PDEs for the mass balance of CO_2 and the energy balance, respectively (DOESBURG; DE JONG, 1976):

$$\begin{aligned}
\partial_\tau[CO_2](\xi,\tau) &= D\partial_\xi^2[CO_2](\xi,\tau) - \upsilon\partial_\xi[CO_2](\xi,\tau) - r\left([CO_2](\xi,\tau), T(\xi,\tau)\right) \\
\partial_\tau T(\xi,\tau) &= \frac{\lambda}{\rho c_p}\partial_{\xi\xi} T(\xi,\tau) - \epsilon\upsilon\frac{\rho_g c_{pg}}{\rho c_p}\partial_\xi T(\xi,\tau) + \frac{2k_w}{r_d \rho c_p}(T_w - T) \\
&\quad + \frac{-\Delta H}{\rho c_p} r\left([CO_2](\xi,\tau), T(\xi,\tau)\right)
\end{aligned} \tag{105}$$

with

$$r\left([CO_2](\xi,\tau), T(\xi,\tau)\right) = k_r \frac{[CO_2](\xi,\tau) e^{-\frac{E}{RT(\xi,\tau)}}}{1 + k_C[CO_2](\xi,\tau)} \tag{106}$$

and the boundary conditions

$$\begin{aligned}
D\partial_\xi[CO_2](0,\tau) &= \upsilon\left([CO_2](0,\tau) - [CO_2]_{in}(\tau)\right) \\
\frac{\lambda}{\rho c_p}\partial_\xi T(0,\tau) &= \epsilon\upsilon\frac{\rho_g c_{pg}}{\rho c_p}(T(0,\tau) - T_{in}(\tau)) \\
\partial_\xi[CO_2](l,\tau) &= 0 \\
\partial_\xi T(l,\tau) &= 0
\end{aligned} \tag{107}$$

where T is the temperature (K), $[CO_2]$ is the reactant concentration (mol%), T_w the coolant temperature (K), T_{in} the inlet temperature (K), $[CO_2]_{in}$ the inlet reactant concentration (mol%), τ (s) and ξ (m) the time and space variables, $\lambda/(\rho c_p)$ and D the axial energy and mass dispersion coefficients (m^2/s), υ the fluid velocity (m/s), l the reactor length (m), ΔH the reaction heat (kcal), ρ the fluid density (kg/m^3), c_p the specific heat (kcal/kgK), r the reaction rate vector (m^3/s), r_d the reactor radius (m), k_w the heat removal rate ($kcal/m^2sK$), E the activation energy (kcal/mol), R the gas constant (kcal/molK).

Using the chemical process engineering parametrization

$$\begin{aligned}
z &= \frac{\xi}{l}, \quad t = \frac{\tau\upsilon}{l}, \\
P_e &= \frac{l\upsilon}{D}, \quad P_{eT} = \frac{l\epsilon\upsilon\rho_g cp_g}{\lambda}, \quad L_e = \frac{\epsilon\rho_g cp_g}{\rho c_p}, \\
D_a &= \frac{l}{\upsilon}, \quad \beta = -\frac{\Delta H}{\rho c_p}, \quad \eta = \frac{2k_w}{r_d \rho c_p}\frac{l}{\upsilon},
\end{aligned} \tag{108}$$

the system modeled by (105)-(107) take the form of (1)-(2) by considering

$$\begin{gathered} x(z,t) = \begin{bmatrix} [CO_2](z,t) & T(z,t) \end{bmatrix}^T,\ u_d = \begin{bmatrix} 0 & T_w \end{bmatrix}^T, \\ u_0(t) = \begin{bmatrix} [CO_2]_{in}(t) & T_{in}(t) \end{bmatrix}^T,\ u_1(t) = \begin{bmatrix} 0 & 0 \end{bmatrix}^T, \\ D = \operatorname{diag}\left(\frac{1}{Pe}, \frac{L_e}{P_{eT}}\right),\ \mathcal{V} = \operatorname{diag}(1, L_e),\ K = \operatorname{diag}(0, -\eta), \\ B = \begin{bmatrix} 0 & \eta \end{bmatrix}^T,\ G = \begin{bmatrix} -D_a & \beta D_a \end{bmatrix}^T, \\ M_{\alpha_0} = \operatorname{diag}\left(\frac{1}{Pe}, \frac{1}{P_{eT}}\right),\ M_{\beta_0} = -I,\ M_{\alpha_1} = I,\ M_{\beta_1} = 0. \end{gathered} \tag{109}$$

The corresponding definition of the system parameters and their respective numerical values are listed in Table 1.

Table 1 – Parameter values.

Parameter	**Value**	**Definition**
l	1	Reactor length
P_{eT}	5	Thermal Peclet number
P_e	5	Mass Peclet number
L_e	1	Lewis number
D_a	0.875	Damkohler number
η	13	Heat transfer coefficient
β	0.9571	Heat of reaction
$[CO_2]_{in}$	1	Inlet reactant concentration
T_{in}	1	Inlet temperature
T_w	1	Coolant temperature
k_r	3.2690×10^6	Constant
k_C	0.1	Constant
R	1.98×10^{-3}	Gas constant
E_a	$29.7 \times 10–3$	Activation energy

The section hereafter is devoted to the analysis of the influence of the collocation points on the accuracy and robustness of the reduced model related to this example by following the analysis developed in Sections 3.2.1 and 3.2.2.

3.4.1 Model reduction

According to the procedure presented in Section 3.2, the model reduction of the PDE system described by (105)-(107) leads to the set of ordinary differential equations in (61)-(62)

Now, the steady state solution of this reduced model will be computed and compared with steady state solution of the distributed parameters model. It exhibits a hot spot in the stationary temperature profile and allows us to apply a selection of collocation points which emphasises the behaviour of the reactor around this hot spot.

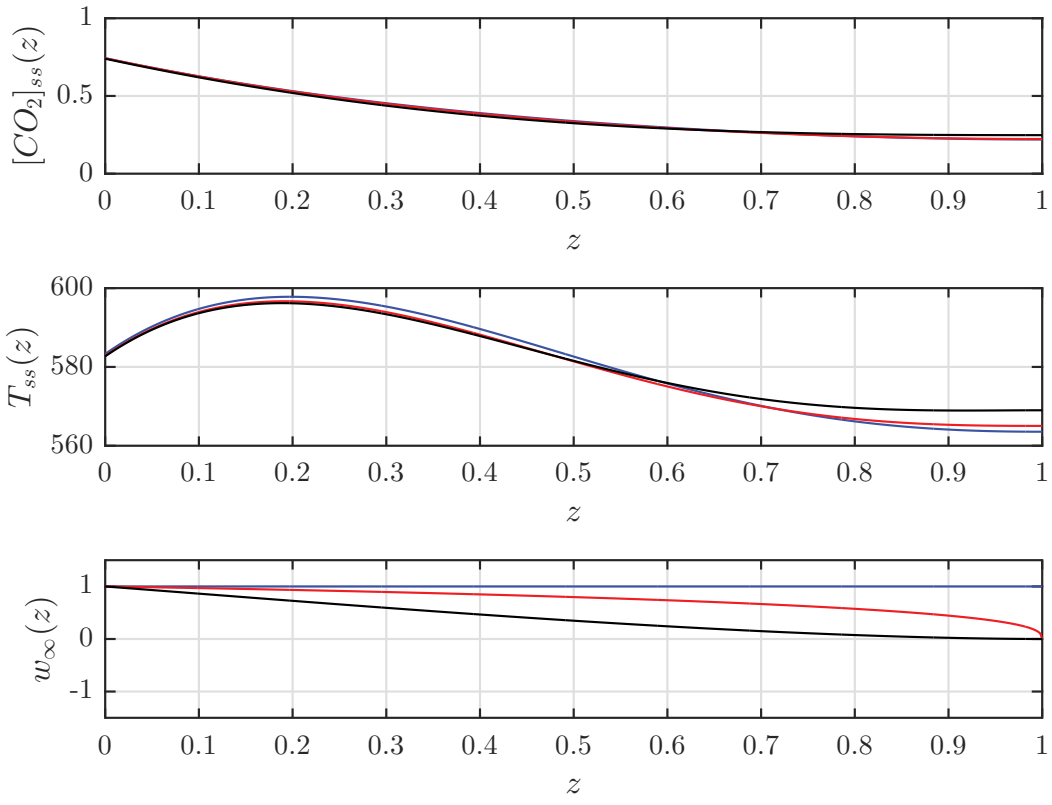

Figure 7 – Concentration and temperature stationary profiles and corresponding weights on the error with $(\alpha, \beta) = (-\frac{1}{2}, -\frac{1}{2})$ (blue lines), $(\alpha, \beta) = (\frac{1}{4}, -\frac{1}{3})$ (red lines) and $(\alpha, \beta) = (3, \frac{5}{18})$ (black lines).

From a first computation of the initial temperature and concentration profiles, it has been observed that the temperature exhibits a hot spot around $z = 0.1818$. Then the family of weights on the error defined in (72) which reach their maximal value in $z = 0.1818$ according to (73) has been selected. Equation (73) is, in this case, an equation with two unknowns, the Jacobi parameters α and β. Another equation between these two parameters may be obtained by choosing for instance any measure of the dispersion of the weight on the error around its maximal value. In Figure 7 hereafter, three cases have been compared, a uniform weight on the error with $(\alpha, \beta) = (-\frac{1}{2}, -\frac{1}{2})$, see the blue lines, $(\alpha, \beta) = (\frac{1}{4}, -\frac{1}{3})$, see the red lines and with $(\alpha, \beta) = (3, \frac{5}{18})$, see the black lines. The results confirm what the theory predicts. Indeed a weight highly localised around z_{max} gives excellent results around this point but causes the solution to diverge significantly away from this point. Note that in the chose example, there are only three interior collocation points and consequently the asymptotic equi-oscillation behaviour of the error is not reached yet.

It remains now to check if the designed weight which is suitable for error minimisation on the stationary profiles $(\alpha, \beta) = (\frac{1}{4}, -\frac{1}{3})$ leads also to a reasonable conditioning number and achieves stability of reduced transport component model.

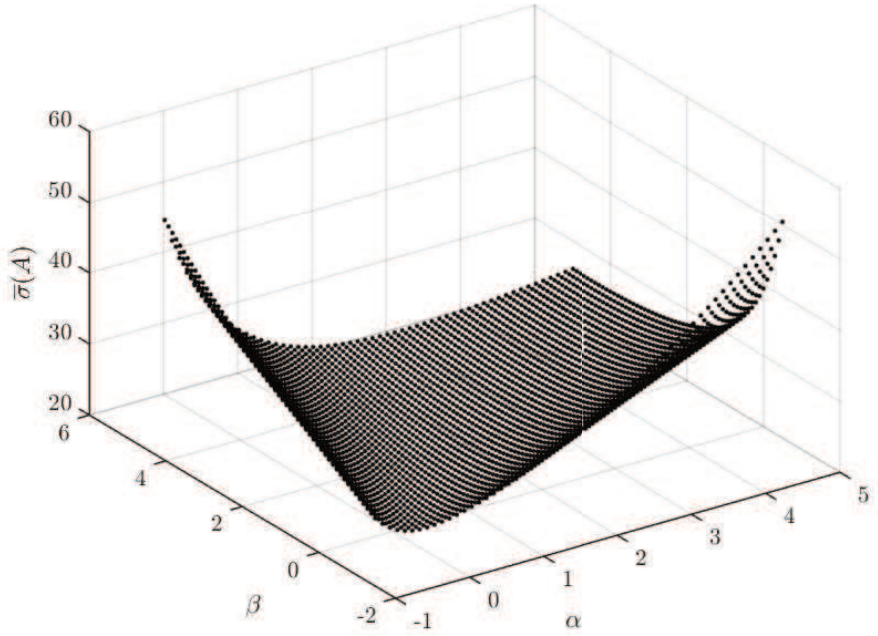

Figure 8 – Largest singular value $\overline{\sigma}(A)$ for three interior collocation points.

Thus, for three interior collocation points, the maximum singular value of the reduced transport component matrix is of the same magnitude for reasonable values of the Jacobi Parameters α and β as it is illustrated in Figure 8.

However this maximum singular value increases rapidly with the number of collocation points. Then, for large values of either α or β, a very large maximum singular value for the reduced transport component is obtained. Such a choice should be ruled out, since this largest singular value largely exceeds the value of the Lipschitz constant and speeds up the error propagation during the numerical integration of the reduced differential model.

3.4.2 Observer design

From this set-up, the rate function is defined as

$$r(x(z,t)) = \left[r\left([CO_2](z,t), [T](z,t)\right) \right] \tag{110}$$

and hence its Jacobian matrix is given by

$$\nabla_x r(x) = \begin{bmatrix} \partial_{[CO_2]} r & \partial_T r \end{bmatrix} \tag{111}$$

with

$$\begin{aligned} \partial_{[CO_2]} r &= \frac{k_r \, e^{-\frac{E}{RT}}}{k_C[CO_2] + 1} - \frac{k_C k_r [CO_2] e^{-\frac{E}{RT}}}{\left(k_C[CO_2] + 1\right)^2} \\ \partial_T r &= \frac{k_r E [CO_2] e^{-\frac{E}{RT}}}{RT^2 \left(k_C[CO_2] + 1\right)} \end{aligned} \tag{112}$$

Considering the domain of operation of the state variables

$$\mathfrak{D} = \left\{ \left([CO_2], T\right) : 0 \leq [CO_2] \leq 1.2, \ 275 \leq T \leq 660 \right\}$$

we obtain that

$$\begin{aligned} 0 < \partial_{[CO_2]} r([CO_2], T) \leq 12.18 \\ 0 < \partial_T r([CO_2], T) \leq 136. \end{aligned} \tag{113}$$

Then one choice for the local lower and upper bound matrices of the Jacobian matrix in (86) are respectively

$$\Gamma_1 = 0 \ \text{ and } \ \Gamma_2 = \begin{bmatrix} 12.18 \, I & 136 \, I \end{bmatrix}. \tag{114}$$

Online temperature measurement plays an important role in industrial processes monitoring since temperature sensors are usually inexpensive, durable, and easily installable compared to sensors for other process variables. Thus, in this case study we assume the scenario in which we only have temperature sensors to be placed along the process length aiming the online state estimation of both variables *Co* and T.

Considering that the online measurement vector is given by one pointwise measurement

$$y(t) = T(\zeta_1, t) \tag{115}$$

which sets $w_1(z) = \delta(z - \zeta_1), \ c_1 = [0, 1]^T$.

Sensor placement simulation

The local optimality criterion posed in Algorithm is used to determine the location of the unique available temperature sensor. Thus, Figure 9 shows the feasibility region of the LMIs conditions in (89) and (96) with respect to the sensor position ζ_1 and the lower bound of the decay rate γ considering $\theta = 1.5 \times 10^4$ and $\chi = 1.5 \times 10^6$ as parameters of design which allow the numerical implementability of the state observer.

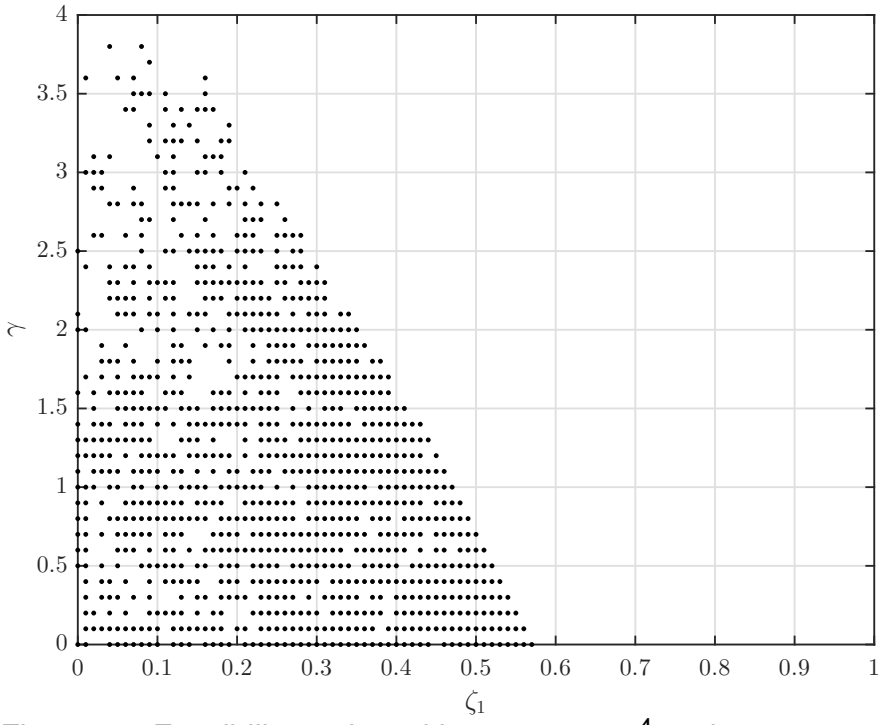

Figure 9 – Feasibility region with $\theta = 1.5 \times 10^4$ and $\chi = 1.5 \times 10^6$.

Figure 9 indicates that there is no feasibility of the state observer design for $\zeta_1 > 0.575$. Furthermore, $\zeta_1 = 0.04$ provides the local maximization of γ, yielding $\gamma_{max} = 3.8$

Optimal initial conditions

Considering the initial profiles for $[CO_2]_0(z)$ and $T_0(z)$ given by the blue lines in Figures 10 and 11, respectively, which were generated as positive polynomials satisfying the boundary conditions. We solve the SDP problem 102 considering $\zeta_1 = 0.04$ to obtain the optimal initial conditions of the state observer.

Observer tests

The observer and system responses are generated via numerical simulation with initial profiles $[CO_2]_0(z)$, $T_0(z)$, $[\hat{CO}_2]_0(z)$ and $\hat{T}_0(z)$. Figures 12 and 13 show the evolution of the actual profiles $[CO_2]$ and T (in red lines) with their respective estimated profiles $[\hat{CO}_2]$ and $\hat{T}$ (in blue lines) considering the proposed observer in four different time instants.

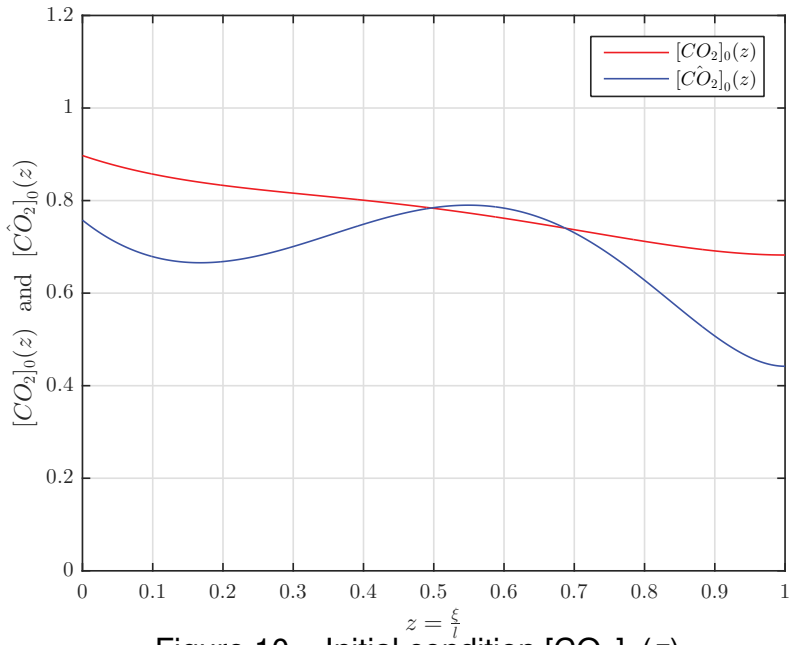

Figure 10 – Initial condition $[CO_2]_0(z)$.

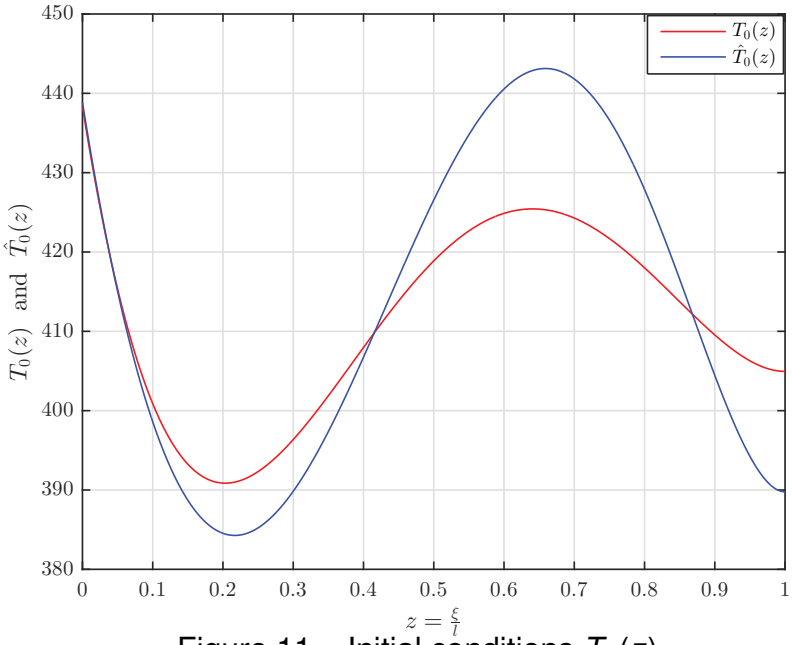

Figure 11 – Initial conditions $T_0(z)$.

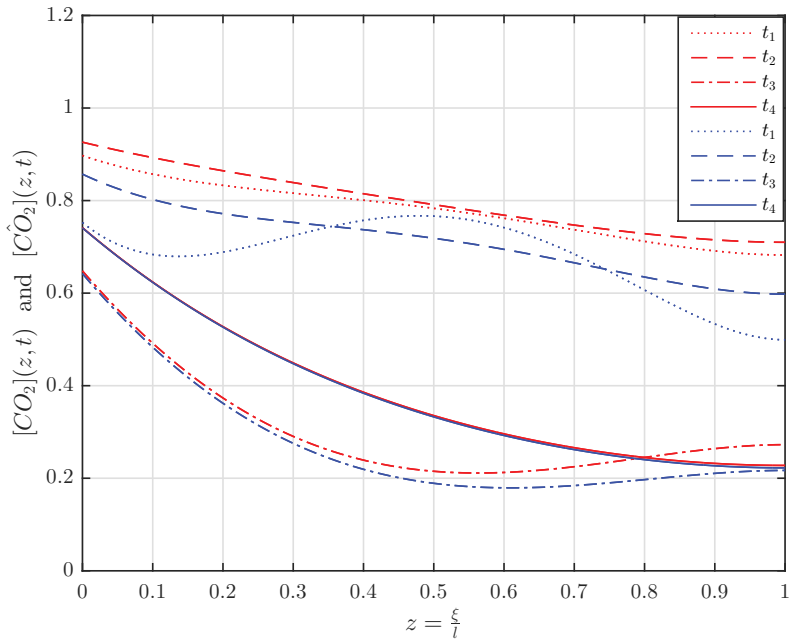

Figure 12 – Time evolution of the spatial profile of $[CO_2](z,t)$ and $[\hat{CO}_2](z,t)$ at time instants $t_1 = 0,\ t_2 = 0.1,\ t_3 = 0.53,\ t_4 = 1.8$.

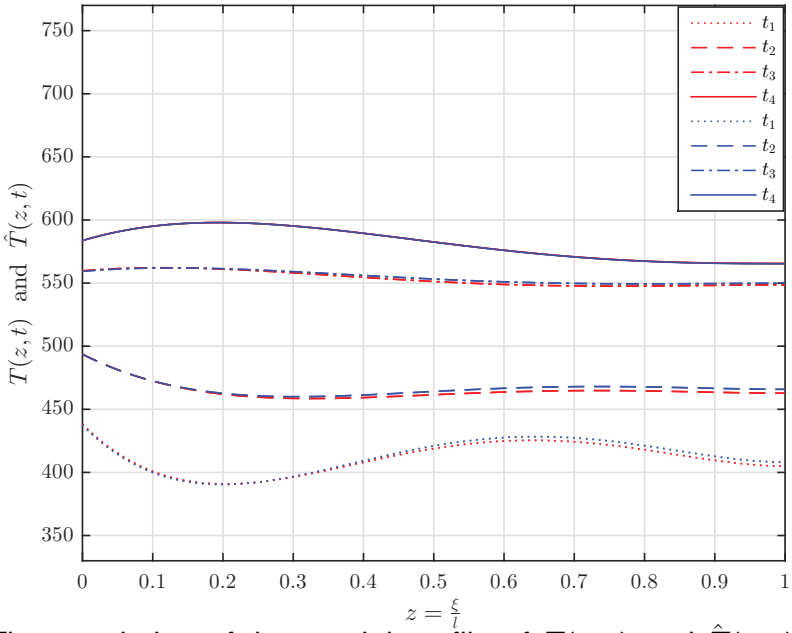

Figure 13 – Time evolution of the spatial profile of $T(z,t)$ and $\hat{T}(z,t)$ at time instants $t_1 = 0,\ t_2 = 0.1,\ t_3 = 0.53,\ t_4 = 1.8$.

As depicted in the above figures. The temperature estimation profile converges faster than that of the concentration, it is substantiated through the optimal selection of the initial estimation profiles, Thus that corresponding to the temperature already provides a good approximation regarding the actual initial condition.

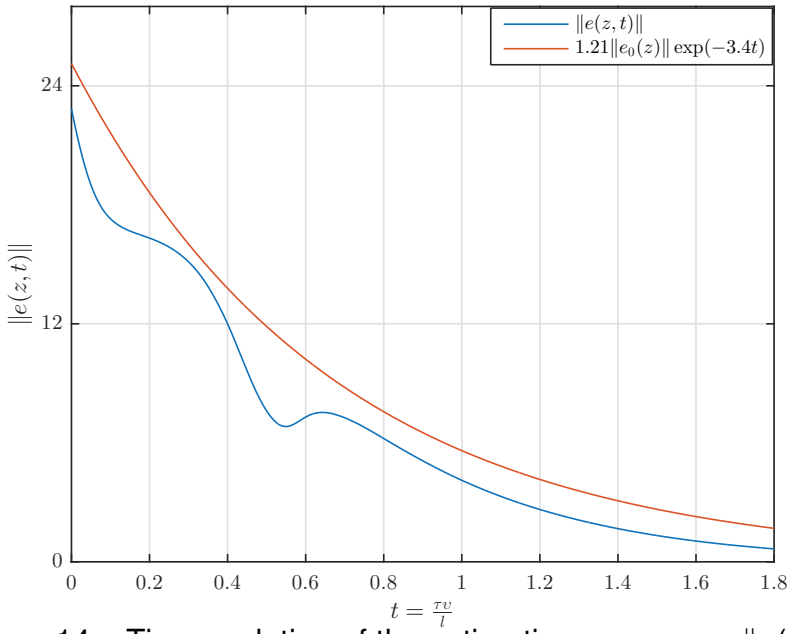

Figure 14 – Time evolution of the estimation error norm $\|e(z, t)\|$.

Finally, Figure 14 shows the evolution of the estimation error norm in the case of one temperature sensors placed in the local optimal locations $\zeta_1 = 0.04$. Since the initial estimation profiles are already a good approximation of the actual variables states, the estimation error norm converges quickly, and hence, provides very satisfactory estimates.

3.5 CONCLUDING REMARKS

In this chapter, we have explored the early lumping approach to the observer design for transport-reaction systems. In particular, the collocation method has been applied to derive a reduced-order finite dimensional approximate model from the semi-linear partial differential equations governing transport-reaction systems. The approximation procedure firstly results in a computation study aiming at obtaining a satisfactory model approximation through the conventional analysis of selecting the appropriate location of the collocation points to guarantee accuracy and robustness. Then, an LMI based conditon was proposed for designing an extended Luenberger observer considering a sector condition to describe the estimation error nonlinearity. In addition, a sensor placement algorithm (embedded into the observer design) was also proposed to optimally allocate the measurement sensors in order to improve the estimation error decay rate. The proposed results were illustrated and numerically tested with a representative tubular reactor case example. It has been clearly noted that the proposed observer has provided accurate estimation of the states.

From an implementation point of view, the proposed method in this chapter provides a procedure to deal with local bounded nonlinearities embedded into the dynam-

ics, sensor placement and optimization of the observer initial condition. More precise convex optimization methodology still needs to be explored to improve the proposed method. Moreover, although the systems considered in this chapter are unidimensional with constant parameters, multidimensional and spatial variant parameters systems can be tackled in the same vein.

4 ON THE MODAL-BASED OBSERVER DESIGN

In this chapter, we are interested in the modal-based observer design problem for the transport-reaction systems of interest. It is known that the observer design problem for linear distributed parameter systems satisfying the spectrum decomposition with bounded observation operators may be solved by the spectral decomposition of the infinite dimensional Hilbert state space (CURTAIN; ZWART, 2020). In view of this preliminary result the purpose of the present study is to extend the modal analysis to transport-reaction systems described by coupled 1-D semi-linear parabolic PDEs systems with multiple in-domain measurements and state dependent nonlinearities.

Thus, we aim to deal with complex local Lipschitz nonlinearities yielding the exponential convergence (local or non-local) of the estimation error. Two synthesis conditions are obtain which are based on:

- the exponential stability of the mild solution of the error dynamics considering the local Lipschitz property assumption of the reaction rate function.
- the characterization of the error dynamics as a Lure-type system which has intrinsic properties of local dissipativity.

The choice of a modal injection gain for the proposed observer led us to transform the synthesis of a distributed observer into a stabilization problem of a finite dimensional system.

4.1 OBSERVER DESIGN

Defining the Luenberger-type state observer for the system described by (1)-(2)

$$\partial_t \hat{x}(z,t) = D\partial_z^2 \hat{x}(z,t) - \mathcal{V}\partial_z \hat{x}(z,t) - \mathrm{K}x(z,t) + B\,u_d(t) + G\,r(\hat{x}(z,t)) + L_D(z)\left(\hat{y}(t) - y(t)\right) \quad (116)$$

for $(z,t) \in (0,1)\times(0,\infty)$, subject to

$$M_{\alpha_0}\hat{x}_z(0,t) + M_{\beta_0}\hat{x}(0,t) = u_0(t) \quad (117)$$

$$M_{\alpha_1}\hat{x}_z(1,t) + M_{\beta_1}\hat{x}(1,t) = u_1(t) \quad (118)$$

and the initial condition

$$\hat{x}_0(z) = \hat{x}(z,0) \quad (119)$$

for $z \in [0,1]$. Here $L_D(z) : [0,1] \to \mathbb{R}^{n_x \times n_y}$ is the output injection gain to be designed. The dynamics of the state estimation error $e(z,t) = x(z,t) - \hat{x}(z,t)$, satisfies

$$\partial_t e(z,t) = D\partial_z^2 e(z,t) - \mathcal{V}\partial_z e(z,t) - \mathrm{K}e(z,t) + G\left[r\left(x(z,t)\right) - r\left(\hat{x}(z,t)\right)\right] + L_D(z)\left(\hat{y}(t) - y(t)\right) \quad (120)$$

subject to

$$M_{\alpha_0} e_z(0,t) + M_{\beta_0} e(0,t) = 0 \quad (121)$$

$$M_{\alpha_1} e_z(1,t) + M_{\beta_1} e(1,t) = 0 \quad (122)$$

and the initial condition

$$e_0(z) = e(z,0). \quad (123)$$

We design the output injection gain in order to ensure the stability of the dynamics of the estimation error described by (120)-(123).

4.1.1 Abstract formulation

The error dynamics described by (120)-(123) can be rewritten as an abstract first order ordinary differential equation in the Hilbert space $\mathcal{H} = \mathbf{L}_2^{n_x}(0,1)$ according to

$$\partial_t e(z,t) = (\mathcal{A} + L_D(z)\mathcal{C})e(z,t) + G\left[r(x(z,t)) - r(\hat{x}(z,t))\right], \quad e(z,0) = e_0(z) \in \mathcal{H} \quad (124)$$

where the operators $\mathcal{A} : D(\mathcal{A}) \to \mathcal{H}$, $\mathcal{C} : D(\mathcal{C}) \to \mathbb{R}^{n_y}$ are defined as

$$\mathcal{A}e(z,t) = D\partial_z^2 e(z,t) - \mathcal{V}\partial_z e(z,t) - \mathrm{K}e(z,t)$$

$$\mathcal{D}(\mathcal{A}) = \{e(z,t) \in \mathcal{H} : \ e(z,t),\ \partial_z e(z,t) \text{ are absolutely continuous,} \quad (125)$$

$$\partial_z^2 e(z,t) \in \mathcal{H} \text{ and}$$

$$M_{\alpha_0}\partial_z e(0,t) + M_{\beta_0} e(0,t) = 0,$$

$$M_{\alpha_1}\partial_z e(1,t) + M_{\beta_1} e(1,t) = 0\Big\}. \quad (126)$$

$$\mathcal{C}e(z,t) = \begin{bmatrix} \langle c_1(\cdot), \mathbf{c}_1^T e(\cdot,t)\rangle \\ \vdots \\ \langle c_{n_y}(\cdot), \mathbf{c}_{n_y}^T e(\cdot,t)\rangle \end{bmatrix}. \quad (127)$$

4.2 SPECTRAL DECOMPOSITION OF THE $\mathcal{A}$ OPERATOR

In view of the abstract formulation of the error dynamics system, the state operator $\mathcal{A}$ is defined as:

$$\mathcal{A} = diag(\mathcal{A}_i), \quad \mathcal{A}_i e_i(z,t) = d_i\partial_z^2 e_i(z,t) - \upsilon_i\partial_z e_i(z,t) - \kappa_i e_i(z,t), \quad i = 1,...,n_x \quad (128)$$

and

$$D(\mathcal{A}_i) = \{e_i(z,t) \in \mathbf{L}_2(0,1) : \ e_i(z,t),\ \partial_z e_i(z,t) \ \text{are absolutely continuous}, \tag{129}$$

$$\partial_z^2 e_i(z,t) \in \mathbf{L}_2(0,1) \ \text{and}$$

$$\alpha_{0,i}\partial_z e_i(0,t) + \beta_{0,i} e_i(0,t) = 0,$$

$$\alpha_{1,i}\partial_z e_i(1,t) + \beta_{1,i} e_i(1,t) = 0\big\}\,. \tag{130}$$

Each $\mathcal{A}_i$ is the negative part of a Sturm-Liouville operator, since it has the form in (34) with ρ_i, p_i and q_i given by

$$\rho_i(z) = e^{-\frac{\upsilon_i}{d_i}z} > 0, \quad p_i(z) = d_i\rho_i(z) > 0, \quad q_i(z) = -\kappa_i, \quad i = 1, ..., n_x. \tag{131}$$

By the analysis in (WINKIN et al., 2000), the spectrum of $\mathcal{A}_i$ consists only of isolated eigenvalues with finite multiplicities. More specifically, the spectrum $\sigma(\mathcal{A}_i)$ of $\mathcal{A}_i$ is calculated through the eigenvalue problem

$$\mathcal{A}_i\varphi_i = \mu\varphi_i, \quad i = 1, ..., n_x. \tag{132}$$

Thus, $\sigma(\mathcal{A}_i) = \{\mu_{i,n} : n \in \mathbb{N}\}$ is a simple set of real numbers with

$$\mu_{i,n} = -\frac{w_{i,n}^2 + \upsilon_i^2}{4d_i} - \kappa_i, \quad i = 1, ..., n_x \ \text{and} \ \ n \in \mathbb{N}. \tag{133}$$

where $\{w_{i,n} : n \in \mathbb{N}\}$ is the set of all the solutions to the resolvent equation:

$$tan\left(\frac{w_i}{2\,d_i}\right) = \frac{2\,d_i\,w_i(\alpha_{0,i}\,\beta_{1,i} - \alpha_{1,i}\beta_{0,i})}{4\,{d_i}^2\,\beta_{0,i}\,\beta_{1,i} + 2\,d_i\,\upsilon_i(\alpha_{0,i}\,\beta_{1,i} + \alpha_{1,i}\,\beta_{0,i}) + \alpha_{0,i}\,\alpha_{1,i}\,(\upsilon_i^2 + w_i^2)} \tag{134}$$

for $w_i > 0$ such that $0 < w_{i,n} < w_{i,n+1}, \ \ n \in \mathbb{N}$. The corresponding eigenvectors $\varphi_{i,n}$ are given by

$$\varphi_{i,n}(z) = p_{i,n}\,e^{\frac{\upsilon_i}{2d_i}z}\left(cos(\frac{w_{i,n}}{2d_i}z) - \left(\frac{2d_i}{w_i}\frac{\beta_{0,i}}{\alpha_{0,i}} + \frac{\upsilon_i}{w_i}\right)sin(\frac{w_{i,n}}{2d_i}z)\right), \ \ i = 1, ..., n_x \ \text{and} \ \ n \in \mathbb{N} \tag{135}$$

where $p_{i,n}$'s are nonzero constants. The adjoint operator $\mathcal{A}_i^*$ is given by

$$\mathcal{A}_i^* e_i(z,t) = d_i\partial_z^2 e_i(z,t) + \upsilon_i\partial_z e_i(z,t) - \kappa_i e_i(z,t), \ \ i = 1, ..., n_x \tag{136}$$

on its domain

$$\mathcal{D}(\mathcal{A}_i^*) = \{e_i(z,t) \in \mathbf{L}_2(0,1) : e_i(z,t),\ \partial_z e_i(z,t) \text{ are absolutely continuous,}$$
$$\partial_z^2 e_i(z,t) \in \mathbf{L}_2(0,1) \text{ and}$$
$$d_i \partial_z e_i(0,t) + (d_i \frac{\beta_{0,i}}{\alpha_{0,i}} + \upsilon_i) e_i(0,t) = 0,$$
$$(d_i \frac{\beta_{1,i}}{\alpha_{1,i}} + d_i) \partial_z e_i(1,t) + \upsilon_i e_i(1,t) = 0 \Big\}. \tag{137}$$

and its corresponding eigenfunctions are given by

$$\Psi_{i,n}(z) = q_{i,n}\, e^{-\frac{\upsilon_i}{2d_i} z} \left(cos(\frac{w_{i,n}}{2d_i} z) - \left(\frac{2d_i}{w_i} \frac{\beta_{0,i}}{\alpha_{0,i}} + \frac{\upsilon_i}{w_i} \right) sin(\frac{w_{i,n}}{2d_i} z) \right),\ i = 1, ..., n_x \text{ and } n \in \mathbb{N} \tag{138}$$

where the $p_{i,n}$, $q_{i,n}$ are nonzero constants which are chosen such that the sequences $\varphi_{i,n}$ and $\Psi_{i,m}$ are biorthonormal, that is,

$$\langle \varphi_{i,n}, \Psi_{i,m} \rangle = \delta_{nm},\ n, m \in \mathbb{N}. \tag{139}$$

Due to the diagonal structure of the operator $\mathcal{A}$, the corresponding eigenvalue-eigenfunction sets are given by the union of the solutions of the diagonal eigenvalue-eigenfunction problems, i.e.,

$$\sigma(\mathcal{A}) = \bigcup_{i=1,...,n_x} \sigma(\mathcal{A}_i) = \left\{ \mu_{1,n},\ \mu_{2,n}, ..., \mu_{n_x,n}, ... \right\}_{n \in \mathbb{N}} \tag{140}$$

and the corresponding set of eigenvectors related to $\mathcal{A}$ and $\mathcal{A}^*$ are given by

$$\left\{ \begin{bmatrix} \varphi_{1,n} \\ 0 \\ \vdots \\ 0 \end{bmatrix}, \begin{bmatrix} 0 \\ \varphi_{2,n} \\ \vdots \\ 0 \end{bmatrix}, \cdots, \begin{bmatrix} 0 \\ \vdots \\ 0 \\ \varphi_{n_x,n} \end{bmatrix}, \cdots \right\}_{n \in \mathbb{N}},$$
$$\left\{ \begin{bmatrix} \Psi_{1,n} \\ 0 \\ \vdots \\ 0 \end{bmatrix}, \begin{bmatrix} 0 \\ \Psi_{2,n} \\ \vdots \\ 0 \end{bmatrix}, \cdots, \begin{bmatrix} 0 \\ \vdots \\ 0 \\ \Psi_{n_x,n} \end{bmatrix}, \cdots \right\}_{n \in \mathbb{N}}. \tag{141}$$

Considering the decreasing rearrangement of the elements of $\sigma(\mathcal{A})$, thus

$$\sigma(\mathcal{A}) = \{\lambda_n : n \in \mathbb{N}\}, \quad \lambda_n > \lambda_{n+1}\ \forall n \in \mathbb{N} \tag{142}$$

thereby, the elements of the sets in (141) are also rearranged correspondingly:

$$\{\phi_n : \ n \in \mathbb{N}\}$$
$$\{\psi_n : \ n \in \mathbb{N}\}. \tag{143}$$

Thus, both sequences of eigenfunctions above form a Riesz basis on $\mathbf{L}_2^{n_x}(0,1)$ and every $e \in \mathbf{L}_2^{n_x}(0,1)$ can be represented uniquely by

$$e = \sum_{n=1}^{\infty} \lambda_n \langle e, \psi_n \rangle \phi_n. \tag{144}$$

Moreover, the linear operator $\mathcal{A}$ is a Riesz-spectral operator and can be represented as

$$\mathcal{A}e = \sum_{n=1}^{\infty} \lambda_n \langle e, \psi_n \rangle \phi_n. \tag{145}$$

Furthermore, $\mathcal{A}$ is the infinitesimal generator of a C_0-semigroup $\mathcal{S}(t)$ given by

$$\mathcal{S}(t)e = \sum_{n=1}^{\infty} \mathrm{e}^{\lambda_n t} \langle e, \psi_n \rangle \phi_n. \tag{146}$$

The growth bound of the semigroup is given by $\omega_0 = \sup_{n\in\mathbb{N}} \lambda_n$ and hence

$$\|\mathcal{S}(t)\| \leq \mathrm{e}^{\omega_0 t}. \tag{147}$$

The Riesz-spectral characterization of the operator $\mathcal{A}$ states that its eigenspectrum can be partitioned into a finite-dimensional part consisting of N slow eigenvalues and a stable infinite-dimensional complement containing the remaining fast eigenvalues as follows

$$\sigma(\mathcal{A}) = \sigma(\mathcal{A}_s) \cup \sigma(\mathcal{A}_f) \tag{148}$$

with $\sigma(\mathcal{A}_s) = \{\lambda_1, \ ..., \ \lambda_N\}$ and $\sigma(\mathcal{A}_f) = \{\lambda_{N+1}, \ ...\}$.

Such eigenspectrum partition of the riesz-spectral operator $\mathcal{A}$ with only finitely many eigenvalues in $\sigma(\mathcal{A}_s)$ is known in the specialized literature as the *spectrum decomposition assumption* at λ_L^* (CURTAIN; ZWART, 2020), i.e, $\sigma(\mathcal{A}_s)$ is bounded and separated from $\sigma(\mathcal{A}_f)$ in such a way that a rectifiable, simple, closed curve, Λ, can be drawn so as to enclose an open set containing $\sigma(\mathcal{A}_s)$ in its interior and $\sigma(\mathcal{A}_f)$ in its exterior.

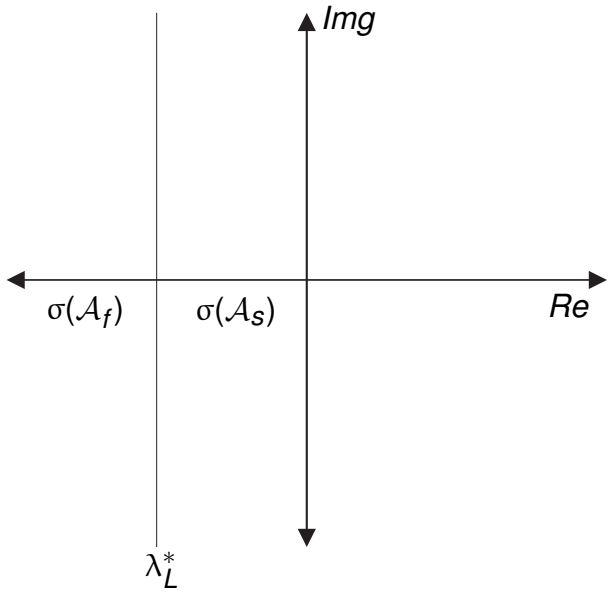

Figure 15 – Spectrum decomposition of $\mathcal{A}$.

The decomposition of the spectrum induces a corresponding decomposition of the state space $\mathcal{H}$ and of the operators $\mathcal{A}$ and $\mathcal{C}$. Summarizing, the spectral projection P_Λ defined by

$$\begin{aligned} P_\Lambda e &= \frac{1}{2\pi j}\int_\Lambda (\lambda I - \mathcal{A})^{-1} e \, d\lambda \\ &= \sum_{n=1}^{N} \langle e, \psi_n \rangle \phi_n \end{aligned} \tag{149}$$

where Λ is traversed once in the positive direction (counterclockwise), induces the following decomposition:

$$\mathcal{H} = \mathcal{H}_s \oplus \mathcal{H}_f \tag{150}$$

with $\mathcal{H}_s = P_\Lambda \mathcal{H}$ and $\mathcal{H}_f = (I - P_\Lambda)\mathcal{H}$. In view of this decomposition, it is convenient to use the notation

$$\mathcal{A} = \begin{bmatrix} \mathcal{A}_s & 0 \\ 0 & \mathcal{A}_f \end{bmatrix}, \quad \mathcal{C} = \begin{bmatrix} \mathcal{C}_s & \mathcal{C}_f \end{bmatrix} \tag{151}$$

where

$$\begin{aligned} \mathcal{A}_s &= \mathcal{A}P_\Lambda = \sum_{n=1}^{N} \lambda_n \langle \cdot, \psi_n \rangle \phi_n, & \mathcal{C}_s &= \mathcal{C}P_\Lambda = \sum_{n=1}^{N} \langle \cdot, \psi_n \rangle \mathcal{C}\phi_n, \\ \mathcal{A}_f &= \mathcal{A}(\mathcal{I} - P_\Lambda) = \sum_{N+1}^{\infty} \lambda_n \langle \cdot, \psi_n \rangle \phi_n, & \mathcal{C}_f &= \mathcal{C}(\mathcal{I} - P_\Lambda) = \sum_{N+1}^{\infty} \langle \cdot, \psi_n \rangle \mathcal{C}\phi_n. \end{aligned} \tag{152}$$

4.3 SPECTRAL ASSIGNMENT OF $L_D(z)$

In the frame of modal decomposition for state estimation of systems described by parabolic PDEs, see e.g. (CURTAIN; ZWART, 2020; SCHAUM, Alexander et al., 2018; KAMRAN, 2016), we consider in this chapter a finite-dimensional modal output injection gain for the Luenberger-type state observer proposed in (116)-(118) given by

$$L_D(z) = \begin{bmatrix} \phi_1(z) & \cdots & \phi_N(z) \end{bmatrix} L \tag{153}$$

with $L \in \mathbb{R}^{N \times n_y}$. According to the spectral representation in (145), we have that

$$\begin{aligned} \mathcal{A}e &= \sum_{n=1}^{\infty} \lambda_n \langle e, \psi_n \rangle \phi_n \\ &= \begin{bmatrix} \phi_1 & \cdots & \phi_N & \phi_{N+1} & \cdots \end{bmatrix} \begin{bmatrix} A_s & 0 \\ 0 & A_f \end{bmatrix} \begin{bmatrix} \langle e, \psi_1 \rangle \\ \vdots \\ \langle e, \psi_N \rangle \\ \langle e, \psi_{N+1} \rangle \\ \vdots \end{bmatrix} \end{aligned} \tag{154}$$

such that

$$A_s = \text{diag}(\lambda_1, ..., \lambda_N), \quad A_f = \text{diag}(\lambda_{N+1}, ...). \tag{155}$$

From the Fourier series expansion in (144), it turns out that

$$\begin{aligned} \mathcal{C}e &= \sum_{n=1}^{\infty} \langle e, \psi_n \rangle \mathcal{C}\phi_n \\ &= \begin{bmatrix} C_s & C_f \end{bmatrix} \begin{bmatrix} \langle e, \psi_1 \rangle \\ \vdots \\ \langle e, \psi_N \rangle \\ \langle e, \psi_{N+1} \rangle \\ \vdots \end{bmatrix} \end{aligned} \tag{156}$$

with

$$C_s = \begin{bmatrix} \langle c_1, \mathbf{c}_1^T \phi_1 \rangle & \cdots & \langle c_1, \mathbf{c}_1^T \phi_N \rangle \\ \vdots & \vdots & \vdots \\ \langle c_{n_y}, \mathbf{c}_{n_y}^T \phi_1 \rangle & \cdots & \langle c_{n_y}, \mathbf{c}_{n_y}^T \phi_N \rangle \end{bmatrix}, \quad C_f = \begin{bmatrix} \langle c_1, \mathbf{c}_1^T \phi_{N+1} \rangle & \cdots \\ \vdots & \vdots \\ \langle c_{n_y}, \mathbf{c}_{n_y}^T \phi_{N+1} \rangle & \cdots \end{bmatrix} \tag{157}$$

Thus, it holds that

$$(\mathcal{A} + L_D(z)\mathcal{C})\, e = \begin{bmatrix} \phi_1 & \cdots & \phi_N & \phi_{N+1} & \cdots \end{bmatrix} \begin{bmatrix} A_s + LC_s & LC_f \\ 0 & A_f \end{bmatrix} \begin{bmatrix} \langle e, \psi_1 \rangle \\ \vdots \\ \langle e, \psi_N \rangle \\ \langle e, \psi_{N+1} \rangle \\ \vdots \end{bmatrix}. \quad (158)$$

Accordingly, if the pair (A_s, C_s) is detectable, the slow eigenvalues $\{\lambda_1, \cdots, \lambda_N\}$ can be rearranged so that the dominant eigenvalue λ_L^* becomes

$$\lambda_L^* = \max\{\lambda_{N+1}, \lambda_{max}(A_s + LC_s)\} \quad (159)$$

and then if $\lambda_L^* < \infty$, $\mathcal{A} + L_D(z)\mathcal{C}$ generates a C_0-semigroup denoted by $S_{\mathcal{A}L}(t)$ which satisfies

$$\|S_{\mathcal{A}L}(t)\| \leq Me^{\lambda_L^* t}, \quad t \geq 0. \quad (160)$$

Thus, if the dimension N of the observer measurement injection is such that the pair (A_s, C_s) is observable, then the gain matrix L can be chosen so that the dominant eigenvalue λ_L^* satisfy conditions to ensure the local exponential stability of the error dynamics (120)-(123).

4.4 LIPSCHITZ CONDITION BASED OBSERVER DESIGN

It is well-known (see e.g. Theorem 6.1.4 in (PAZY, 2012)) that under the assumption that $(\mathcal{A} + L_D(z)\mathcal{C})$ generates a C_0-semigroup $S_{\mathcal{A}L}(t)$, (124) admits an unique mild solution satisfying the integral equation

$$e(z,t) = \mathcal{S}_{\mathcal{A}L}(t)e_0(z) + \int_0^t \mathcal{S}_{\mathcal{A}L}(t-s)G\left[r(x(z,s)) - r(\hat{x}(z,s))\right] ds. \quad (161)$$

Similar to the proof of Gronwalls generalized lemma (VIDYASAGAR, 2002), it follows that

$$\begin{aligned} \|e(\cdot,t)\| &\leq \|\mathcal{S}_{\mathcal{A}L}(t)\|\|e_0(\cdot)\| + \int_0^t \|\mathcal{S}_{\mathcal{A}L}(t-s)\|\|G\|\|r(x(\cdot,s)) - r(\hat{x}(\cdot,s))\| ds \\ &\leq Me^{\lambda_L^* t}\left(\|e_0(\cdot)\| + \int_0^t e^{-\lambda_L^* s}\|G\|\|r(x(\cdot,s)) - r(\hat{x}(\cdot,s))\| ds\right) \\ &\leq Me^{\lambda_L^* t}\left(\|e_0(\cdot)\| + \int_0^t e^{-\lambda_L^* s}\|G\|\, l^r\, \|e(\cdot,s)\| ds\right) \end{aligned} \quad (162)$$

where norms are taken in appropriate spaces, and l^r denotes the local Lipschitz constant of the function $r(\cdot)$ over a subset of $\mathcal{H} = \mathbf{L}_2^{n_x}(0,1)$. Define

$$\eta(t) = e^{\lambda_L^* t}\left(\|e_0(\cdot)\| + \int_0^t e^{-\lambda_L^* s}\|G\|\ l^r\|e(\cdot,s)\|ds\right) \tag{163}$$

so that it follows that

$$\begin{aligned}\dot{\eta}(t) &= \lambda_L^*\eta(t) + \|G\|\ l^r\eta(t)\\ &= (\lambda_L^* + \|G\|l^r)\eta(t).\end{aligned} \tag{164}$$

This implies that for $\lambda_L^* < -\|G\|l^r$ the local convergence of $\|e(\cdot,t)\|$ is ensured. Furthermore, this condition implies the system detectability as stated subsequently.

Theorem 4.1. *When a matrix valued function $L_D : [0,1] \to \mathbb{R}^{n_x \times n_y}$ can be chosen so that $\mathcal{A} + L_D(z)\mathcal{C}$ generates a C_0-semigroup $\mathcal{S}_{\mathcal{A}L}(t)$ such that*

$$\|\mathcal{S}_{\mathcal{A}L}(t)\| \leq Me^{\lambda_L^* t},\ t \geq 0 \tag{165}$$

where $M \geq 1$, then if $\lambda_L^* < -\|G\|l^r$ the system described by (1)-(2) is detectable.

Proof. Under the assumption that $\lambda_L^* < -\|G\|l^r$ is met, from (164) and (162), we obtain that $\lim_{t\to\infty}\|e(\cdot,t)\| = 0$. This, in turn, implies the detectability of the system described by (1)-(2). □

Corollary 4.1. *Consider the estimation error system in* (124). *If $L_D(z) : [0,1] \to \mathbb{R}^{n_x \times n_y}$ is selected such that $\mathcal{A} + L_D(z)\mathcal{C}$ generates a C_0-semigroup $S_{\mathcal{A}L}(t)$ with growth bound λ_L^*, such that*

$$\lambda_L^* \leq -\gamma - \|G\|l^r, \tag{166}$$

then the estimation error exponentially converges to zero with decay rate γ according to

$$\|e(\cdot,t)\| \leq M\|e_0(\cdot)\|e^{-\gamma t}. \tag{167}$$

Observer design techniques based on Lipschitz conditions may guarantee stability only for small values of Lipschitz constants which directly translates into small stability regions. All available results on Lipschitz systems, however, provide only sufficient conditions for stability and the actual observer might still work with larger Lipschitz constants, even though the tool used in the analysis and design are unable to provide theoretical evidence. The implication is that there is a significant degree of conservativeness in the Lipschitz formulation. We can approach Lipschitz restrictions in a different way and avoid high output injection gains in the observer design by representing the

error dynamics as Lure system (WANG, Y. et al., 2014) and using the theory of dissipativity (ROCHA-CÓZATL; MORENO, 2011) for the stability analysis as presented in the following section.

4.5 DISSIPATIVE OBSERVER DESIGN

The error dynamics in (124) can be represented as a Lure-type dynamic-static system interconnection (POPOV, 1962; KHALIL, 2002) shown in Figure 16.

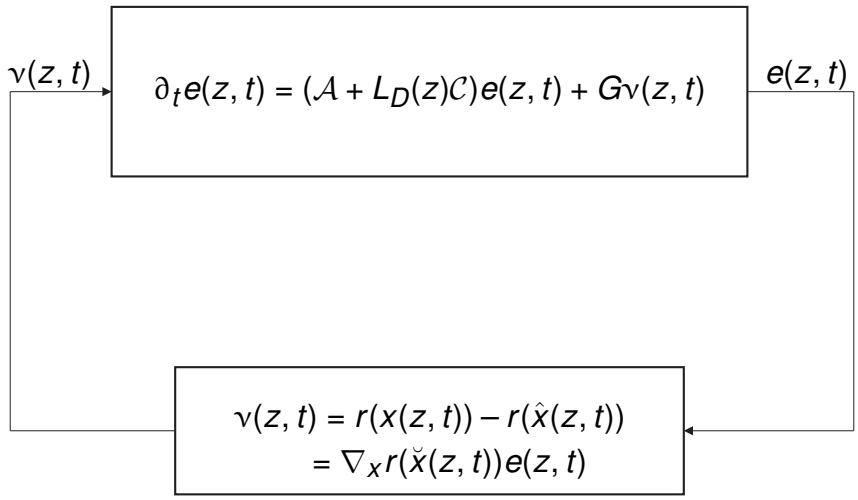

Figure 16 – Lure-System representation of the observer error system.

Based on the assumption that $r(\cdot)$ is locally Lipschitz , the function denoted as $\nu(z,t) = r(x(z,t)) - r(\hat{x}(z,t))$ and the the estimation error $e(z,t) = x(z,t) - \hat{x}(z,t)$ satisfy different algebraic conditions (AÇIKMEŞE; CORLESS, 2011; ARCAK; KOKOTOVIĆ, 2001). In this thesis, we use a sector condition based on the boundedness of the Jacobian matrix of the nonlinear function $r(\cdot)$.

4.5.1 Sector condition for $e(z,t)$ and $\nu(z,t)$

Suppose that the two matrices $\Gamma_1,\ \Gamma_2 \in \mathbb{R}^{n_r \times n_x}$ are constant matrices whose entries are the local lower and upper bounds, respectively, of the Jacobian matrix entries of $r(\cdot)$ defined as

$$\Gamma(x) = \nabla_x r(x) \tag{168}$$

then, the Differential Mean Value Theorem gives

$$\begin{aligned} \nu(z,t) &= r(x(z,t)) - r(\hat{x}(z,t)) \\ &= \nabla_x r\left(\breve{x}(z,t)\right) e(z,t) \end{aligned} \tag{169}$$

where $\breve{x}(z,t) \in Co(x(z,t), \hat{x}(z,t))$ and the following inequality holds

$$\Gamma_1 \; e(z,t) \leq \nu(z,t) \leq \Gamma_2 \; e(z,t). \tag{170}$$

Hence, the following sector condition is straightforward to obtain

$$(\nu(z,t) - \Gamma_1 e(z,t))^T (\Gamma_2 e(z,t) - \nu(z,t)) \geq 0 \tag{171}$$

which can be rewritten in the following quadratic form

$$\left\langle \begin{bmatrix} e(\cdot,t) \\ \nu(\cdot,t) \end{bmatrix}, \underbrace{\begin{bmatrix} \frac{\Gamma_1^T\Gamma_2 + \Gamma_2^T\Gamma_1}{2} & -\frac{\Gamma_1^T + \Gamma_2^T}{2} \\ -\frac{\Gamma_1 + \Gamma_2}{2} & I \end{bmatrix}}_{M} \begin{bmatrix} e(\cdot,t) \\ \nu(\cdot,t) \end{bmatrix} \right\rangle \leq 0 \tag{172}$$

In the light of Lyapunov theory for DPSs, the squared error potential energy dissipation is analyzed aiming at the achievement of local convergence conditions for the estimation error $e(z,t)$. For this aim, the dissipation components corresponding to the linear dynamical transport and the nonlinear kinetic subsystem are identified in the quadratic sector condition (172) (SCHAUM, Alexander et al., 2018).

4.5.2 Some dissipativity concepts

In a system-theoretic framework, the concept of dissipativity is strictly related to the concept of a power supply w, which represents a measure of energy change in a system in terms of its inputs and outputs. Consider the system decribed in Figure 16, $w(e(z,t), \nu(z,t))$ is a function of inputs $\nu(z,t)$ and outputs $e(z,t)$. The concept of dissipativity, represents a generalization of the concept of passivity, in the sense that it applies to non-quadratic systems. For reasons of applicability, supply rates given by quadratic forms in inputs and outputs are considered, i.e.

$$w(e(z,t), \nu(z,t)) = \left\langle \begin{bmatrix} e(\cdot,t) \\ \nu(\cdot,t) \end{bmatrix}, \begin{bmatrix} Q(\cdot) & S(\cdot) \\ S^T(\cdot) & R(\cdot) \end{bmatrix} \begin{bmatrix} e(\cdot,t) \\ \nu(\cdot,t) \end{bmatrix} \right\rangle \tag{173}$$

with real matrix-valued functions $Q(z) : [0,1] \to \mathbb{S}^{n_x}$, $R(z) : [0,1] \to \mathbb{S}^{n_r}$, $S(z) : [0,1] \to \mathbb{R}^{n_x \times n_r}$. Dissipativity of the system (124) with respect to the supply rate w given by (173) can therefore be identified with the fulfillment of an inequality characterizing the change in the stored energy $E(e(z,t))$, defined as a positive functional in $\mathcal{H} = \mathbf{L}_2^{n_x}(0,1)$, in terms of the supplied power $w(e(z,t), \nu(z,t))$. The following definition is essential in the sequel

Definition 4.1. *The system defined in* (124) *is called* (Q,S,R)*-state strictly dissipative with dissipation rate* 2γ*, if the positive definite functional* $E(e(z,t))$ *defined in* (175)*,*

called the storage functional such that

$$\dot{E}(e(z,t)) \leq w(e(z,t),\nu(z,t)) - 2\gamma\|e(z,t)\| \tag{174}$$

Consider the quadratic storage functional

$$E(e(z,t)) = \left\langle e(z,t), e(z,t)\right\rangle \tag{175}$$

then,

$$\begin{aligned}\dot{E}(t) &= \left\langle \partial_t e(\cdot,t), e(\cdot,t)\right\rangle + \left\langle e(\cdot,t), \partial_t e(\cdot,t)\right\rangle \\ &= \left\langle (\mathcal{A}+L_D(z)\mathcal{C})e(\cdot,t) + G\nu(\cdot,t), e(\cdot,t)\right\rangle + \left\langle e(\cdot,t), (\mathcal{A}+L_D(z)\mathcal{C})e(\cdot,t) + G\nu(\cdot,t)\right\rangle \\ &= \langle (\mathcal{A}+L_D(z)\mathcal{C})e(\cdot,t), e(\cdot,t)\rangle + \langle e(\cdot,t), (\mathcal{A}+L_D(z)\mathcal{C})e(\cdot,t)\rangle + 2\langle e(\cdot,t), G\nu(\cdot,t)\rangle.\end{aligned} \tag{176}$$

Substituting (176) and (173) into (174) yields

$$\begin{aligned}&\langle (\mathcal{A}+L_D(z)\mathcal{C})e(\cdot,t), e(\cdot,t)\rangle + \langle e(\cdot,t), (\mathcal{A}+L_D(z)\mathcal{C})e(\cdot,t)\rangle + 2\langle e(\cdot,t), G\nu(\cdot,t)\rangle \leq \\ &\quad \langle e(\cdot,t), Qe(\cdot,t)\rangle + 2\langle e(\cdot,t), S\nu(\cdot,t)\rangle + \langle \nu(\cdot,t), R\nu(\cdot,t)\rangle - 2\gamma\langle e(\cdot,t), e(\cdot,t)\rangle\end{aligned} \tag{177}$$

which can be rewritten as

$$\begin{aligned}&\langle (\mathcal{A}+L_D(z)\mathcal{C})e(\cdot,t), e(\cdot,t)\rangle + \langle e(\cdot,t), (\mathcal{A}+L_D(z)\mathcal{C})e(\cdot,t)\rangle + 2\gamma\langle e(\cdot,t), e(\cdot,t)\rangle \\ &\quad - \langle e(\cdot,t), Qe(\cdot,t)\rangle + 2\langle e(\cdot,t), (G-S)\nu(\cdot,t)\rangle - \langle \nu(\cdot,t), R\nu(\cdot,t)\rangle \leq 0\end{aligned} \tag{178}$$

Based on the considerations above, the following result is a direct application of the infinite-dimensional set-up presented in (SCHAUM, Alexander et al., 2018) to the class of systems of interest.

Theorem 4.2. *Consider the Lure-type interconnection shown in Figure 16. If* $L_D(z) : [0,1] \to \mathbb{R}^{n_x \times n_y}$ *is chosen such that the system* (124) *is* $(\Gamma_1^T\Gamma_2, \frac{\Gamma_1^T+\Gamma_2^T}{2}, -I)$*-state strictly dissipative with dissipation rate* $2\gamma > 0$*, then the estimation error exponentially converges to zero with rate* γ*.*

Proof. Consider the storage functional $E(t) = \langle e(\cdot,t), e(\cdot,t)\rangle$ and its time derivative

$$\begin{aligned}\dot{E}(t) &= \langle \partial_t e(\cdot,t), e(\cdot,t)\rangle + \langle e(\cdot,t), \partial_t e(\cdot,t)\rangle \\ &= \langle (\mathcal{A}+L_D(z)\mathcal{C})e(\cdot,t) + G\nu(\cdot,t), e(\cdot,t)\rangle + \langle e(\cdot,t), (\mathcal{A}+L_D(z)\mathcal{C})e(\cdot,t) + G\nu(\cdot,t)\rangle \\ &= \langle (\mathcal{A}+L_D(z)\mathcal{C})e(\cdot,t), e(\cdot,t)\rangle + \langle e(\cdot,t), (\mathcal{A}+L_D(z)\mathcal{C})e(\cdot,t)\rangle + 2\langle e(\cdot,t), G\nu(\cdot,t)\rangle.\end{aligned} \tag{179}$$

By the assumption that $\Sigma(\mathcal{A}+L_D(z)\mathcal{C},G,I)$ is $(\Gamma_1^T\Gamma_2,-\frac{\Gamma_1^T+\Gamma_2^T}{2},I)$-state strictly dissipative with dissipation rate $2\gamma>0$ it follows by virtue of the dissipation inequality (174) that

$$\begin{aligned}\dot{E}(t) &\leq \Big\langle e(\cdot,t),\Gamma_1^T\Gamma_2 e(\cdot,t)\Big\rangle + 2\left\langle e(\cdot,t),-\frac{\Gamma_1^T+\Gamma_2^T}{2}\nu(\cdot,t)\right\rangle \\ &\qquad + \big\langle \nu(\cdot,t),\nu(\cdot,t)\big\rangle - 2\gamma\langle e,e\rangle \\ &\leq \left\langle \begin{bmatrix} e(\cdot,t)\\ \nu(\cdot,t)\end{bmatrix}, \begin{bmatrix} \frac{\Gamma_1^T\Gamma_2+\Gamma_2^T\Gamma_1}{2} & -\frac{\Gamma_1^T+\Gamma_2^T}{2}\\ -\frac{\Gamma_1+\Gamma_2}{2} & I\end{bmatrix}\begin{bmatrix} e(\cdot,t)\\ \nu(\cdot,t)\end{bmatrix}\right\rangle - 2\gamma\langle e(\cdot,t),e(\cdot,t)\rangle.\end{aligned} \tag{180}$$

Taking (172) into account, it follows that

$$\dot{E}(t)\leq -2\gamma\langle e(\cdot,t),e(\cdot,t)\rangle = -2\gamma E(t) \tag{181}$$

and hence,

$$\|e(\cdot,t)\|\leq \|e_0(\cdot)\|\mathrm{e}^{-\gamma t}. \tag{182}$$

□

Theorem 4.3. *Consider the estimation error system in* (124)*. If* $L_D(z):[0,1]\to\mathbb{R}^{n_x\times n_y}$ *is selected such that*

$$\lambda_L^*<\frac{1}{2}\lambda_{\min}\left(-2\gamma I+\Gamma_1^T\Gamma_2-\left(G+\frac{\Gamma_1^T+\Gamma_2^T}{2}\right)\left(G^T+\frac{\Gamma_1+\Gamma_2}{2}\right)\right) \tag{183}$$

then the estimation error exponentially converges to zero with decay rate γ *according to*

$$\|e(\cdot,t)\|\leq \|e_0(\cdot)\|\mathrm{e}^{-\gamma t}. \tag{184}$$

Proof. Consider λ_L^* defined in (159), then

$$\langle(\mathcal{A}+L_D(z)\mathcal{C})e(\cdot,t),e(\cdot,t)\rangle+\langle e(\cdot,t),(\mathcal{A}+L_D(z)\mathcal{C})e(\cdot,t)\rangle\leq 2\lambda_L^*\langle e(\cdot,t),e(\cdot,t)\rangle. \tag{185}$$

By the assumption that $\Sigma(\mathcal{A}+L_D(z)\mathcal{C},G,I)$ is $(\Gamma_1^T\Gamma_2,-\frac{\Gamma_1^T+\Gamma_2^T}{2},I)$-state strictly dissipative with dissipation rate $2\gamma>0$ it follows by virtue of the dissipation inequality (178) that

$$\begin{aligned}&\Big\langle(\mathcal{A}+L_D(z)\mathcal{C})e(\cdot,t),e(\cdot,t)\Big\rangle+\Big\langle e(\cdot,t),(\mathcal{A}+L_D(z)\mathcal{C})e(\cdot,t)\Big\rangle+2\gamma\Big\langle e(\cdot,t),e(\cdot,t)\Big\rangle\\ &-\Big\langle e(\cdot,t),\Gamma_1^T\Gamma_2 e(\cdot,t)\Big\rangle+2\left\langle e(\cdot,t),\left(G+\frac{\Gamma_1^T+\Gamma_2^T}{2}\right)\nu(\cdot,t)\right\rangle-\big\langle\nu(\cdot,t),\nu(\cdot,t)\big\rangle\leq 0.\end{aligned} \tag{186}$$

Substituting (185) into inequality (186) it follows that

$$\left\langle \begin{bmatrix} e(\cdot,t) \\ \nu(\cdot,t) \end{bmatrix}, \begin{bmatrix} 2(\lambda_L^* + \gamma)I + \Gamma_1^T\Gamma_2 & G + \frac{\Gamma_1^T + \Gamma_2^T}{2} \\ G + \frac{\Gamma_1 + \Gamma_2}{2} & -I \end{bmatrix} \begin{bmatrix} e(\cdot,t) \\ \nu(\cdot,t) \end{bmatrix} \right\rangle. \tag{187}$$

This is satisfied if the LMI

$$\begin{bmatrix} 2(\lambda_L^* + \gamma)I + \Gamma_1^T\Gamma_2 & G + \frac{\Gamma_1^T + \Gamma_2^T}{2} \\ G + \frac{\Gamma_1 + \Gamma_2}{2} & I \end{bmatrix} \leq 0 \tag{188}$$

holds true. Taking the Schur complement this property is ensured if

$$2\lambda_L^* I \leq \left(-2\gamma I + \Gamma_1^T\Gamma_2 - (G + \frac{\Gamma_1^T + \Gamma_2^T}{2})(G^T + \frac{\Gamma_1 + \Gamma_2}{2}) \right) \tag{189}$$

this in turn is fulfilled, if the smallest value over of the minimum eigenvalue of the right-side of (189) is larger than $2\lambda_L^*$, i.e. if (183) is satisfied.

□

4.6 CATALYTIC CRACKING REACTOR

As a case study, a tubular catalytic cracking reactor is considered here. Indeed, catalytic cracking is one of the most important conversion processes in petroleum refineries. It is widely used to convert high-boiling, high-molecular weight hydrocarbon fractions of petroleum crude oils into more valuable gasoline, olefinic gases and other products (WEEKMAN JR, 1969). Here, let us consider the chemical process of a tubular catalytic cracking reactor in which the following reactions occur

$$\begin{aligned} &A \overset{k_A}{\rightarrow} B \overset{k_B}{\rightarrow} C, \\ &A \overset{k_C}{\rightarrow} C \end{aligned} \tag{190}$$

where A represents gas oil, B gasoline and C other products (e.g butanes, coke, etc.). If x_A and x_B represent the weight fractions of reactants A and B, then the rate equations are given by (WEEKMAN JR, 1969)

$$\begin{aligned} r_A &= -(k_A + k_C)x_A^2 = -k_{AC}x_A^2, \\ r_B &= k_A x_A^2 - k_B x_B \end{aligned} \tag{191}$$

with k_A, k_B and k_C are the kinetic constants of the reactions, respectively. If we consider an isothermal process and assume axial dispersion, then by using the mass bal-

ances within the reactor, the dynamics of the system can be described by the following parabolic PDE system

$$\begin{aligned} \partial_t x_A(z,t) &= d\partial_z^2 x_A(z,t) - \upsilon\partial_z x_A(z,t) + r_A(x_A) \\ \partial_t x_B(z,t) &= d\partial_z^2 x_B(z,t) - \upsilon\partial_z x_B(z,t) + r_B(x_A, x_B) \end{aligned} \tag{192}$$

along with with the boundary conditions

$$\begin{aligned} d\partial_z x_A(0,t) &= \upsilon(x_A(0,t) - u_A(t)) \\ d\partial_z x_B(0,t) &= \upsilon(x_B(0,t) - u_B(t)) \\ \partial_z x_A(l,t) &= 0 \\ \partial_z x_B(l,t) &= 0. \end{aligned} \tag{193}$$

In the above equations, x_A, x_B, d, υ, $x_{A,in}$ and $x_{B,in}$ denote the weight fractions of reactant A and B, the axial dispersion coefficient, the superficial velocity, the inlet weight fraction of component A and the inlet weight fraction of component B, respectively. The adopted numerical values for the process parameters are taken from Table 2.

Table 2 – Parameter values

Parameter	**Value**	**Definition**
d	0.5 m^2h^{-1}	Mass dispersion coefficient
υ	2 mh^{-1}	Flow velocity
l	1 m	Reactor length
k_A	18.1 (h weight fraction)$^{-1}$	Kinetic constant
k_B	1.7 h^{-1}	Kinetic constant
k_C	4.8 (h weight fraction)$^{-1}$	Kinetic constant
$x_{A,in}$	0.7 weight fraction	Inlet weight fraction of A
$x_{B,in}$	0 weight fraction	Inlet weight fraction of B

The system modeled by (192)-(193) takes the form of (1)-(2) by considering

$$\begin{aligned} x(z,t) &= \begin{bmatrix} x_A(z,t) & x_B(z,t) \end{bmatrix}^T, \; u_d = 0, \\ u_0(t) &= \begin{bmatrix} x_{A,in} & x_{B,in} \end{bmatrix}^T, \; u_1(t) = 0, \\ D &= d\ l, \; \mathcal{V} = \upsilon, \; \mathrm{K} = 0, \\ B &= 0, \quad G = \begin{bmatrix} -k_{AC} & 0 \\ k_A & -k_B \end{bmatrix}, \\ M_{\alpha_0} &= \frac{d}{\upsilon} I, \; M_{\beta_0} = -I, \; M_{\alpha_1} = I, \; M_{\beta_1} = 0 \end{aligned} \tag{194}$$

with rate function defined as

$$r(x) = \begin{bmatrix} x_A^2 \\ x_B \end{bmatrix} \tag{195}$$

and hence its corresponding Jacobian is given by

$$\nabla_x r(x) = \begin{bmatrix} 2x_A & 0 \\ 0 & 1 \end{bmatrix}. \tag{196}$$

Considering the domain of operation of the state variables

$$\mathfrak{D} = \left\{ (x_A, x_B) \in \mathbb{R}^2 : 0 \leq x_A \leq 0.4341,\ 0 \leq x_B \leq 0.7 \right\}$$

we obtain that the local lower and upper bound matrices of the Jacobian matrix are respectively

$$\Gamma_1 = \begin{bmatrix} 0 & 0 \\ 0 & 1 \end{bmatrix} \qquad \Gamma_2 = \begin{bmatrix} 0.8682 & 0 \\ 0 & 1 \end{bmatrix}. \tag{197}$$

Moreover, a possible local Lipschitz constant l^r for the reaction function may be derived using the Jacobian matrix as follows

$$\begin{aligned} \sup_{x \in \mathfrak{D}} \|\nabla_x r(x)\| &\leq l^r \\ \max(2x_A, 1) &\leq l^r \\ 1 &\leq l^r. \end{aligned} \tag{198}$$

According to Section 4.2, we set the eigenvalue problem for operator $\mathcal{A}$ defined in the abstract formulation of the error dynamics (124), that is

$$\begin{aligned} &\mathcal{A} = \operatorname{diag}(\mathcal{A}_i),\ i = 1, 2, \\ &\mathcal{A}_i = \frac{1}{Pe}\partial_z^2 - \partial_z,\ i = 1, 2, \\ &\mathcal{D}(\mathcal{A}_i) = \{ e_i(z,t) \in \mathbf{L}_2(0,1) : e_i(z,t),\ \partial_z e_i(z,t) \text{ are absolutely continuous,} \\ &\qquad \partial_z^2 e_i(z,t) \in \mathbf{L}_2(0,1) \text{ and} \\ &\qquad \frac{1}{Pe}\partial_z e_i(0,t) - e_i(0,t) = 0, \\ &\qquad \partial_z e_i(1,t) = 0 \},\ i = 1, 2. \end{aligned}$$

Since $\mathcal{A}_1 = \mathcal{A}_2$, the spectrum of $\mathcal{A}$ is then defined by

$$\sigma(\mathcal{A}) = \bigcup_{i=1,2} \sigma(\mathcal{A}_i) = \{ \lambda_n : n \in \mathbb{N} \} \tag{199}$$

with

$$\lambda_n = -\frac{w_n^2 + \upsilon^2}{4d}, \quad n \in \mathbb{N} \tag{200}$$

where $\{w_n : n \in \mathbb{N}\}$ is the set of all the solutions to the resolvent equation:

$$tan\left(\frac{w}{2d}\right) = \frac{2w\upsilon}{w^2 - \upsilon^2} \tag{201}$$

for $w > 0$ such that $0 < w_n < w_{n+1}, \ \forall n \in \mathbb{N}$. The corresponding set of eigenvalues-eigenvectors pairs related to $\mathcal{A}$ and $\mathcal{A}^*$ are given by

$$\begin{gathered}\left\{(\lambda_n, \begin{bmatrix}\varphi_n \\ 0\end{bmatrix}), (\lambda_n, \begin{bmatrix}0 \\ \varphi_n\end{bmatrix})\right\}_{n\in\mathbb{N}}, \\ \left\{(\lambda_n, \begin{bmatrix}\Psi_n \\ 0\end{bmatrix}), (\lambda_n, \begin{bmatrix}0 \\ \Psi_n\end{bmatrix})\right\}_{n\in\mathbb{N}}\end{gathered} \tag{202}$$

where

$$\begin{aligned}\varphi_n(z) &= p_n\, e^{\frac{\upsilon}{2d}z}\left(cos\left(\frac{w_n}{2d}z\right) + \left(\frac{\upsilon}{w_n}\right) sin\left(\frac{w_n}{2d}z\right)\right) \\ \Psi_n(z) &= q_n\, e^{\frac{\upsilon}{2d}(1-z)}\left(cos\left(\frac{w_n}{2d}(1-z)\right) + \left(\frac{\upsilon}{w_n}\right) sin\left(\frac{w_n}{2d}(1-z)\right)\right), \quad n \in \mathbb{N},\end{aligned} \tag{203}$$

and the normalization constants $p_n, \ q_n, \ n \in \mathbb{N}$ are chosen so that $\langle \varphi_n, \Psi_m \rangle = \delta_{nm}$.

For the purpose of determining the appropriate number of modes N in the implementation of the output injection gain $L_D(z)$ in (153) that ensures a lower bound γ for the decay rate of the estimation error norm, we first applied the criteria given in (166) and (183) with $\gamma = 4.5$ corresponding to the Lipchitz constant and sector condition based observer design respectively. Thus, Figures 17 and 18 depict the selection of an appropriate γ_L^* and hence of the number of modes N to be used in the implementation of $L_D(z)$ through the spectrum decomposition of operator $\mathcal{A}$.

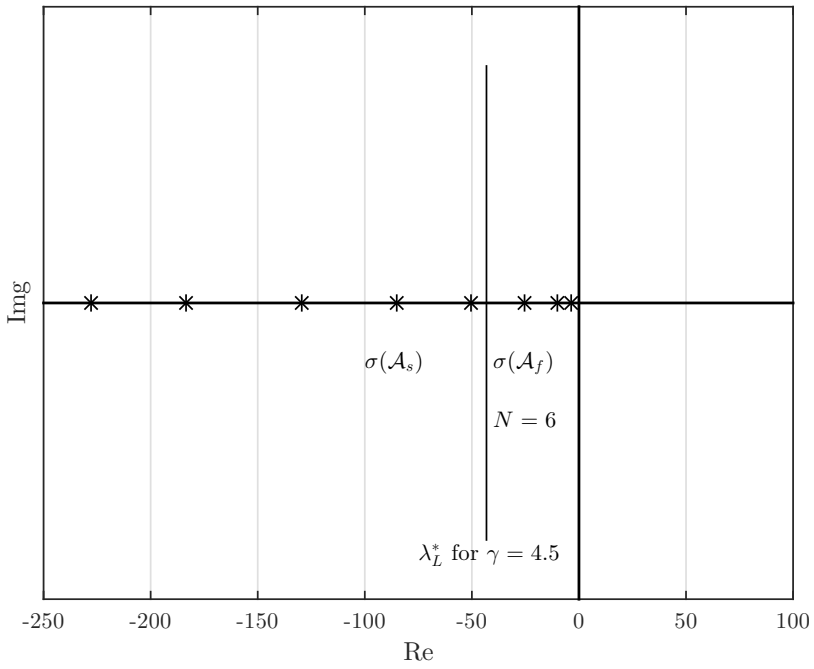

Figure 17 – Spectrum $\sigma(\mathcal{A})$ decomposition regarding γ = 4.5 considering (166).

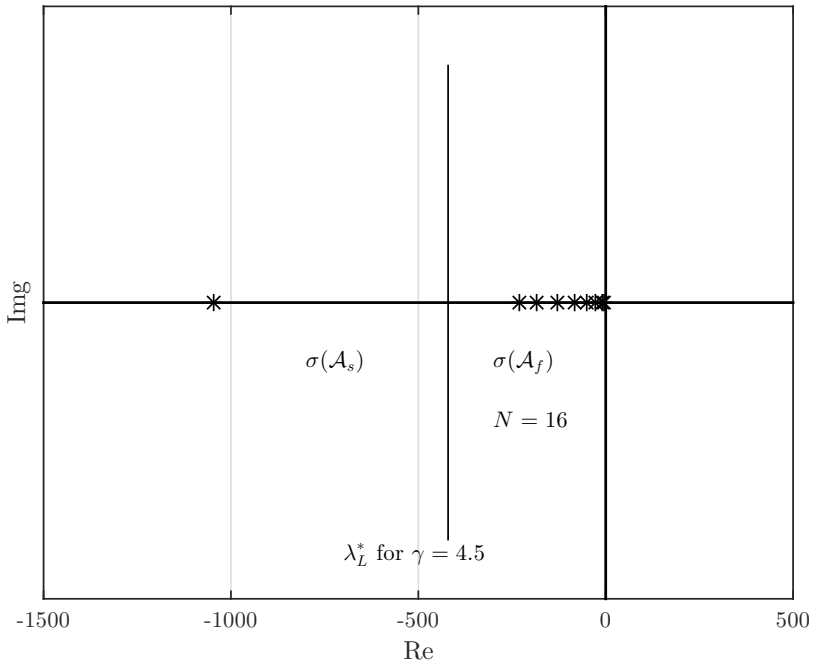

Figure 18 – Spectrum $\sigma(\mathcal{A})$ decomposition regarding γ = 4.5 considering (183).

Considering that the online measurement vector is given by one piecewise measurement

$$y(t) = \int_{\zeta_1-\varepsilon_1}^{\zeta_1+\varepsilon_1} x_A(z,t)dz \tag{204}$$

setting $\varepsilon_1 = 0.01$, $\mathbf{c}_1^T = [0\ 1]$, and $\zeta_1 = 0.3$ in (5) and (7). Thus, the output injection gain $L_D(z)$ is implemented according to (153) with $N = 6$.

4.6.1 Observer tests

The observer and system responses are generated via numerical simulation with initial profiles that were generated as positive polynomials satisfying the boundary conditions, upper bounds selected by the physical conditioning of the process and matching the initial measurements. Figures 19 and 20 show the evolution of the actual profiles x_A and x_B (in red lines) with their respective estimated profiles $\hat{x}_A$ and $\hat{x}_B$ (in blue lines) considering the proposed observer in four different time instants.

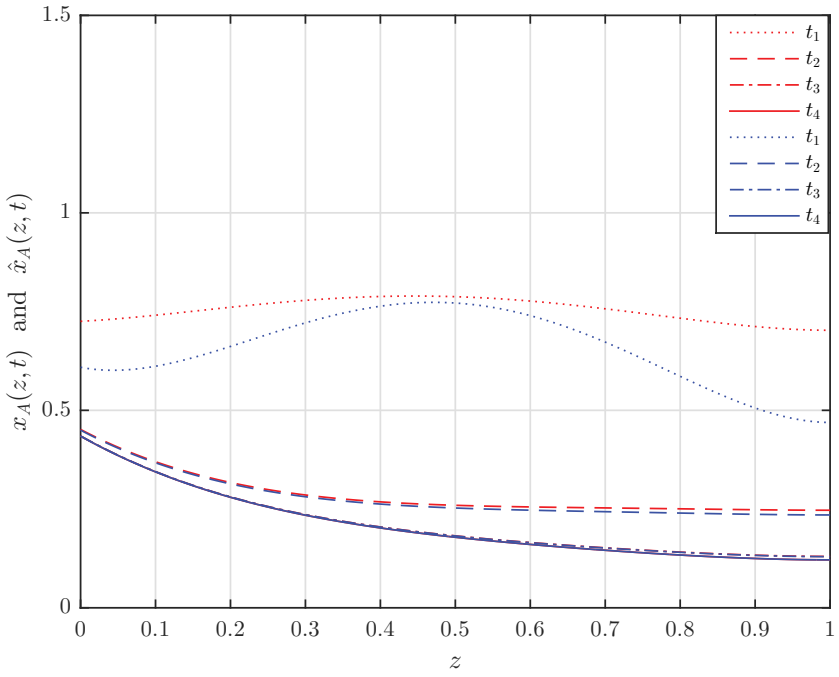

Figure 19 – Time evolution of the spatial profile of $x_A(z,t)$ and $\hat{x}_A(z,t)$ at time instants $t_1 = 0,\ t_2 = 0.12,\ t_3 = 0.36,\ t_4 = 0.6$.

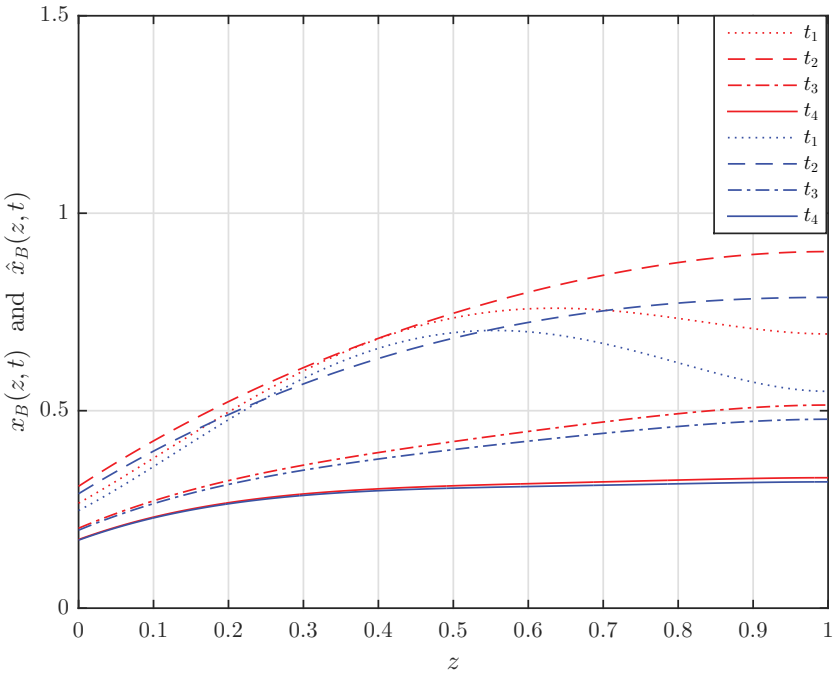

Figure 20 – Time evolution of the spatial profile of $x_B(z,t)$ and $\hat{x}_B(z,t)$ at time instants $t_1 = 0,\ t_2 = 0.12,\ t_3 = 0.36,\ t_4 = 0.6$.

Figure 21 shows the evolution of the estimation error norm in the case of one temperature sensors placed in the local optimal location $\zeta_1 = 0.5$. Since the initial estimation profiles are already a good approximation of the actual variables states, the estimation error norm converges quickly, and hence, provides very satisfactory estimates.

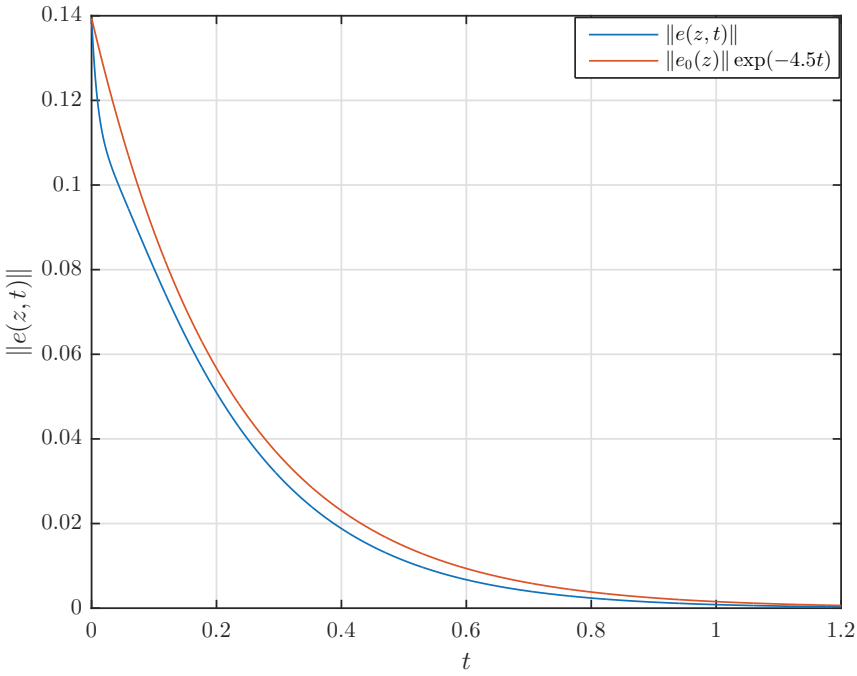

Figure 21 – Time evolution of the estimation error norm $\|e(z, t)\|$.

4.7 CONCLUDING REMARKS

In this chapter, we have explored the late lumping approach to the observer design for transport-reaction systems. In particular, the Lipschitz condition assumption related to the reaction rate function has been considered to derive sufficient conditions for the local exponential stability of the state estimation error dynamics. The choice of a modal injection gain for the observer allow us to analyse the stability conditions in terms of the slow eigenvalues of the error dynamics state operator which turns the observer design into a stabilization problem of a finite dimensional system.

The proposed results were illustrated and numerically tested with a representative tubular reactor case example. It has been clearly noted that the proposed observer has provided accurate estimation of the states. From an implementation point of view, the proposed method in this chapter provides a procedure to deal with local bounded nonlinearities embedded into the dynamics. More precise convex optimization methodology still needs to be explored to improve the proposed method. Moreover, although the systems considered in this chapter are unidimensional with constant parameters, multidimensional and spatial variant parameters systems can be tackled in the same vein.

5 LYAPUNOV-BASED OBSERVER SYNTHESIS

This chapter is devoted to the Lyapunov-based design method for the state observer synthesis of the class of transport-reaction systems of interest. We accomplish this task by constructing Lyapunov functions parametrized by sum-of-squares polynomials. In addition, the output injection matrix gain is parametrized by polynomials with prescribed degree. In particular, we reduce the stability analysis of the nonlinear dynamics of the state estimation error by using local algebraic sector conditions to represent the error dynamics as a Lure system. It should be noticed that the proposed approach concerns a large class of semilinear PDE systems within which the polynomial parametrization of the observer synthesis and a guaranteed prescribed decay rate of convergence are obtained through the solution of an appropriately formulated SOS program. We also discuss an extension of the proposed class of observers that is applicable to the distributed state observation problem for uncertain systems. A case study related to a nonisothermal tubular reactor is presented to demonstrate the observer performance as well as the advantages of the proposed formulation.

5.1 OBSERVER DESIGN

Defining the Luenberger-type state observer for (1)-(2)

$$\partial_t \hat{x}(z,t) = D\partial_z^2 \hat{x}(z,t) - \mathcal{V}\partial_z \hat{x}(z,t) - \mathrm{K}\hat{x}(z,t) + G\, r(\hat{x}(z,t)) + L_D(z)\left(\hat{y}(t) - y(t)\right) \quad (205)$$

for $(z,t) \in (0,1) \times (0,\infty)$, subject to

$$M_{\alpha_0}\hat{x}_z(0,t) + M_{\beta_0}\hat{x}(0,t) = u_0(t) \quad (206)$$

$$M_{\alpha_1}\hat{x}_z(1,t) + M_{\beta_1}\hat{x}(1,t) = u_1(t) \quad (207)$$

and the initial condition

$$\hat{x}_0(z) = \hat{x}(z,0) \quad (208)$$

for $z \in [0,1]$. Here the gain $L_D(z) : [0,1] \to \mathbb{R}^{n_x \times n_y}$ is the output injection gain to be designed. The dynamics of the state estimation error $e(z,t) = x(z,t) - \hat{x}(z,t)$, satisfies

$$\partial_t e(z,t) = D\partial_z^2 e(z,t) - \mathcal{V}\partial_z e(z,t) - \mathrm{K}e(z,t) + G\left[r\left(x(z,t)\right) - r\left(\hat{x}(z,t)\right)\right] + L_D(z)\left(\hat{y}(t) - y(t)\right) \quad (209)$$

subject to

$$M_{\alpha_0} e_z(0,t) + M_{\beta_0} e(0,t) = 0 \quad (210)$$

$$M_{\alpha_1} e_z(1,t) + M_{\beta_1} e(1,t) = 0 \quad (211)$$

and the initial condition

$$e_0(z) = e(z,0). \tag{212}$$

We design the output injection gain using the Lyapunov methodology in order to obtain sufficient conditions for the stability of the dynamics of the estimation error described by (209)-(212).

As asserted in Section 4.5, the function denoted as $\nu(z,t) = r(x(z,t)) - r(\hat{x}(z,t))$ and the the estimation error $e(z,t) = x(z,t) - \hat{x}(z,t)$ satisfy a sector condition based on the boundedness of the Jacobian matrix of the nonlinear function $r(\cdot)$.

5.1.1 Sector Condition for $e(z,t)$ and $\nu(z,t)$

Suppose that the two matrices $\Gamma_1,\ \Gamma_2 \in \mathbb{R}^{n_r \times n_x}$ are constant matrices whose entries are the local lower and upper bounds, respectively, of the Jacobian matrix entries of $r(\cdot)$ defined as

$$\Gamma(x(z,t)) = \nabla_x r(x(z,t)) \tag{213}$$

then, the Differential Mean Value Theorem gives

$$\begin{aligned} \nu(z,t) &= r(x(z,t)) - r(\hat{x}(z,t)) \\ &= \nabla_x r\left(\breve{x}(z,t)\right) e(z,t) \end{aligned} \tag{214}$$

where $\breve{x}(z,t) \in Co(x(z,t), \hat{x}(z,t))$ and the following inequality holds

$$\Gamma_1\ e(z,t) \leq \nu(z,t) \leq \Gamma_2\ e(z,t). \tag{215}$$

Hence, the following sector condition is straightforward to obtain

$$\left(\nu(z,t) - \Gamma_1 e(z,t)\right)^T \left(\Gamma_2 e(z,t) - \nu(z,t)\right) \geq 0 \tag{216}$$

which can be rewritten in the following quadratic form

$$\left\langle \begin{bmatrix} e(z,t) \\ \nu(z,t) \end{bmatrix}, \underbrace{\begin{bmatrix} \frac{\Gamma_1^T\Gamma_2 + \Gamma_2^T\Gamma_1}{2} & -\frac{\Gamma_1^T + \Gamma_2^T}{2} \\ -\frac{\Gamma_1 + \Gamma_2}{2} & I \end{bmatrix}}_{M} \begin{bmatrix} e(z,t) \\ \nu(z,t) \end{bmatrix} \right\rangle \leq 0 \tag{217}$$

5.1.2 Abstract formulation

The error dynamics described by (209)-(212) can be rewritten as an abstract first order ordinary differential equation in the Hilbert space $\mathcal{H} = \mathbf{L}_2^{n_x}(0,1)$ according to

$$\partial_t e(z,t) = (\mathcal{A} + L_D(z)\mathcal{C})e(z,t) + G\nu(z,t), \quad e(z,0) = e_0(z) \in \mathcal{H} \tag{218}$$

where the operators $\mathcal{A} : D(\mathcal{A}) \to \mathcal{H}$, $\mathcal{C} : D(\mathcal{C}) \to \mathbb{R}^{n_y}$ are defined as

$$\begin{aligned}
\mathcal{A}e(z,t) &= D\partial_z^2 e(z,t) - \mathcal{V}\partial_z e(z,t) - \mathrm{K}e(z,t) \\
D(\mathcal{A}) &= \{e(z,t) \in \mathcal{H} : e(z,t),\ \partial_z e(z,t) \text{ are absolutely continuous,} \\
&\qquad \partial_z^2 e(z,t) \in H \text{ and} \\
&\qquad M_{\alpha_0}\partial_z e(0,t) + M_{\beta_0} e(0,t) = 0, \\
&\qquad M_{\alpha_1}\partial_z e(1,t) + M_{\beta_1} e(1,t) = 0\big\}.
\end{aligned} \tag{219, 220}$$

$$\mathcal{C}e(z,t) = \begin{bmatrix} \langle c_1(\cdot), \mathrm{c}_1^T e(\cdot,t)\rangle \\ \vdots \\ \langle c_{n_y}(\cdot), \mathrm{c}_{n_y}^T e(\cdot,t)\rangle \end{bmatrix}. \tag{221}$$

The error dynamics in (218) can be represented as a Lure system shown in Figure 22 where the sector condition for the estimation error $e(t)$ and the deviation function $\nu(t)$ are expressed through the semidefinite constraint (217) that can be embedded into the stability analysis by applying the S-Procedure (BOYD, S. et al., 1994).

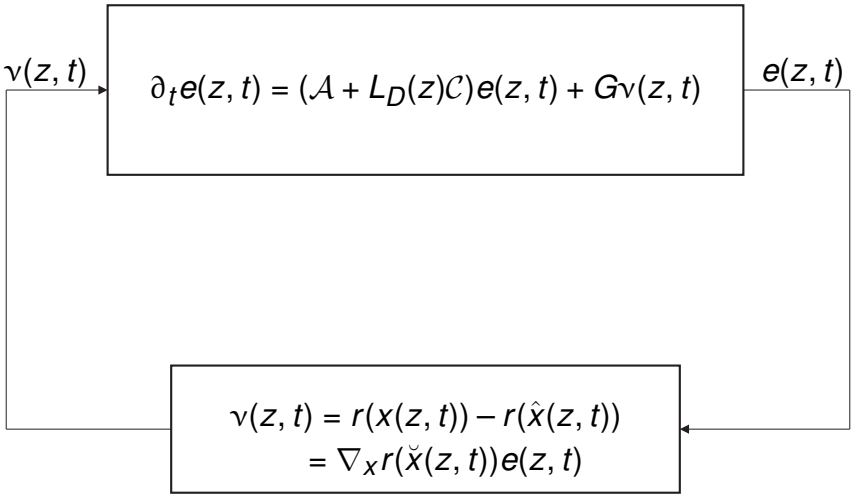

Figure 22 – Lure-System representation of the observer error system.

5.1.3 Lyapunov convergence assessment

In this work, the design problem will be addressed within a weighted Lyapunov framework, with the weight function as a degree of freedom (SCHAUM, Alexander et al., 2014). The analysis of the corresponding dissipation mechanism leads to LMI convergence conditions, which depends on the spatial coordinate, the observer gains, and the Lyapunov weight function. To this end, let us set the positive-definite weighted candidate Lyapunov functional $V : \mathbf{L}_2^{n_x}(0,1) \to \mathbb{R}$ as

$$V(t) = \langle e(\cdot,t), \mathcal{P}e(\cdot,t)\rangle \tag{222}$$

where $\mathcal{P} : \mathbf{L}_2^{n_x}(0,1) \to \mathbf{L}_2^{n_x}(0,1)$ is a strictly positive operator defined by the polynomial matrix $W(z)$ as

$$(\mathcal{P}e)(z) = W(z)e(z). \tag{223}$$

for all $z \in (0,1)$. The following Lemma shows how two positive semi-definite matrices $Q,\ R > 0$ and some constant $\epsilon > 0$ can be used to define the polynomial matrix $W(z)$ such that the operator $\mathcal{P}$ is positive and therefore the functional V is a Lyapunov candidate for the observation error dynamics (209)-(212).

Lemma 5.1. *(MEYER; PEET, Matthew M, 2016) Given any positive semi-definite matrices $Q,\ R \in \mathbb{S}^{n(m+1)}$, and*

$$Z(z) = Z_m(z) \otimes I_n \tag{224}$$

where $z \in (0,1)$, Z_m is a vector of monomials with degree m or less and $\otimes$ is the Kronecker product. Let for all $z \in [0,1]$

$$g(z) = z(1-z). \tag{225}$$

If for some $\epsilon > 0$

$$W(z) = Z(z)^T(Q + g(z)R)Z(z) + \epsilon I_n, \tag{226}$$

then the functional $V : \mathbf{L}_2^{n_x}(0,1) \to \mathbb{R}^+$, defined as

$$V(e(\cdot,t)) = \langle e(\cdot,t), \mathcal{P}e(\cdot,t)\rangle = \int_0^1 e(z,t)^T W(z)e(z,t)dz, \tag{227}$$

is a strictly positive functional over $\mathbf{L}_2^{n_x}(0,1)$, whenever $e(\cdot,t) \not\equiv 0$, and satisfies

$$V(e(\cdot,t)) = \langle e(\cdot,t), \mathcal{P}e(\cdot,t)\rangle \geq \epsilon\|e(\cdot,t)\|^2, \quad \forall e(\cdot,t) \in \mathbf{L}_2^{n_x}(0,1). \tag{228}$$

Proof. Substituting (226) into (227), we obtain

$$V(e(\cdot,t)) = \int_0^1 e(z,t)^T \underbrace{\Big(Z(z)^T(Q + g(z)R)Z(z)\Big)}_{\dagger} e(z,t)dz + \epsilon\int_0^1 e(z,t)^T e(z,t)dz. \tag{229}$$

Since $Q,\ R > 0$ and $g(z) > 0,\ \forall z \in [0,1]$, $\dagger$ describes a SOS matrix polynomial (PAPACHRISTODOULOU et al., 2013), hence

$$\begin{aligned} V(e(\cdot,t)) &\geq \epsilon\int_0^1 e(z,t)^T e(z,t)dz \\ &\geq \epsilon\|e(\cdot,t)\|^2, \quad \forall e(\cdot,t) \in \mathbf{L}_2^{n_x}(0,1). \end{aligned} \tag{230}$$

□

5.1.3.1 Dissipation inequality

We wish to prove that with the chosen observer gain $L_D(z)$, the dissipation inequality

$$\dot{V}(t) + 2\gamma V(t) \leq 0, \quad \gamma > 0, \tag{231}$$

is satisfied along the trajectories of the estimation error dynamics (218) which proves the exponential stability of the estimation error dynamics, since it can be easily shown that

$$\|e(\cdot, t)\| \leq M_e \, \mathrm{e}^{-\gamma t}, \quad M_e = \sqrt{\frac{V(e_0(z))}{\epsilon}}. \tag{232}$$

The substitution of (222) into (231) yields

$$\dot{V}(t) + 2\gamma V(t) = \langle \partial_t e(\cdot, t), \mathcal{P} e(\cdot, t) \rangle + \langle e(\cdot, t), \mathcal{P} \partial_t e(\cdot, t) \rangle + 2\gamma \langle e(\cdot, t), \mathcal{P} e(\cdot, t) \rangle. \tag{233}$$

Using the self-adjointness of $\mathcal{P}$, (233) becomes

$$\dot{V}(t) + 2\gamma V(t) = 2\langle e(\cdot, t), P \partial_t e(\cdot, t) \rangle + 2\gamma \langle e(\cdot, t), \mathcal{P} e(\cdot, t) \rangle \tag{234}$$

and along the error dynamics (218), it becomes

$$\begin{aligned} \dot{V}(t) + 2\gamma V(t) = 2\langle e(\cdot, t), \mathcal{P}\mathcal{A} e(\cdot, t) \rangle + 2\langle e(\cdot, t), \mathcal{P} G \nu(z, t) \rangle + 2\langle e(\cdot, t), \mathcal{P} L_D(z) \mathcal{C} e(\cdot, t) \rangle \\ + 2\gamma \langle e(\cdot, t), \mathcal{P} e(\cdot, t) \rangle. \end{aligned} \tag{235}$$

The next step is the exploitation of (235) to express (231) in terms of LMIs that can be approached by a semidefinite programming problem (SDP).

5.2 OBSERVER DESIGN – MAIN RESULT

In this section, a LMI formulation of the distributed observation problems is developed. The local exponential stability of the estimation error system (209)-(212) is ensured for two cases of in domain distributed measurement: pointwise measurement and piecewise measurement.

5.2.1 Pointwise measurements at ζ_j, $j = 1, ..., n_y$

In this case, as shown in Figure 23, we divide the spatial domain $[0, 1]$ into n_y subintervals $[\tilde{z}_j, \tilde{z}_{j+1}]$, $j = 1, ..., n_y$ according to the position of the measurement sensors. From Figure 23, we get that $0 = \tilde{z}_1 < ... < \tilde{z}_{n_y+1} = 1$ and

$$\zeta_j \in [\tilde{z}_j, \tilde{z}_{j+1}], \text{ for } j = 1, ..., n_y. \tag{236}$$

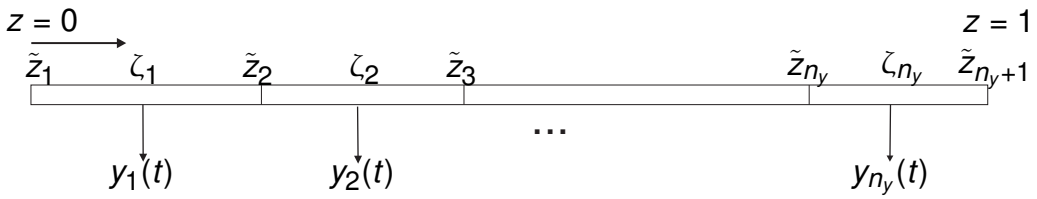

Figure 23 – Distributed pointwise measurements.

Theorem 5.1. *The error dynamics in* (209)-(212) *($c_j(z),\ j = 1, ..., n_y$ defined as in* (6)*) is asymptotically stable with a decay rate γ if there exist*

- $m \in \mathbb{N},\ \epsilon,\ \tau > 0$,
- *either positive semidefinite matrices $Q,\ R \in \mathbb{S}^{n(m+1)}$ (for the equi-diffusivity and equi-advectivity case, i.e., $D = dI_{n_x}$ and $\mathcal{V} = \upsilon I_{n_x}$) or diagonal matrices $Q,\ R \in \mathbb{R}^{n(m+1)}$ such that the polynomial matrix $W : [0,1] \to \mathbb{R}^{n_x \times n_x}$ satisfy* (226)*,*
- *polynomials $l_j : [0,1] \to \mathbb{R}^{n_x},\ j = 1, ..., n_y$ defining the observer gain according to*

$$L_D(z) = \begin{bmatrix} 1_{[\tilde{z}_1,\tilde{z}_2]} l_1(z) & \cdots & 1_{[\tilde{z}_{n_y},\tilde{z}_{n_y+1}]} l_{n_y}(z) \end{bmatrix} \tag{237}$$

such that the following matrix inequalities hold:

$$\begin{aligned} 2\tilde{D}(1)M_{\alpha_1}^{-1}M_{\beta_1} + \partial_z\tilde{D}(1) + \tilde{\mathcal{V}}(1) \geq 0 \\ 2\tilde{D}(0)M_{\alpha_0}^{-1}M_{\beta_0} + \partial_z\tilde{D}(0) + \tilde{\mathcal{V}}(0) \leq 0 \end{aligned} \tag{238}$$

$$P_j(z) - \tau \begin{bmatrix} M & 0_{n_x n_y} \\ 0_{n_x n_y \times (n_x+n_r)} & 0_{n_x n_y} \end{bmatrix} \leq 0, \tag{239}$$

for $j = 1, ..., n_y$ and $z \in [0,1]$ where

$$P_j(z) = \begin{bmatrix} \partial_z^2\tilde{D}(z) + \partial_z\tilde{V}(z) - \tilde{K}(z) - \frac{\pi^2\epsilon D_{\min}}{2p_j^2} I_{n_x} + 4\gamma W(z) & \tilde{G}(z) & \frac{\pi^2\epsilon}{2p_j^2} I_{n_x} + \tilde{l}_j(z)\mathbf{c}_j^T \\ * & 0_{n_r} & 0_{n_r \times n_x} \\ * & * & -\frac{\pi^2\epsilon D_{\min}}{2p_j^2} I_{n_x} \end{bmatrix} \tag{240}$$

with

$$\begin{aligned} \tilde{D}(z) = W(z)D,\ \tilde{\mathcal{V}}(z) = W(z)\mathcal{V},\ \tilde{K}(z) = \mathrm{H_e}\{W(z)K\},\ \tilde{G}(z) = W(z)G, \\ \tilde{l}_j(z) = W(z)l_j(z),\ p_j^2 = \max\{(\zeta_j - \tilde{z}_j)^2, (\tilde{z}_{j+1} - \zeta_j)^2\},\ j = 1, ..., n_y, \\ D_{\min} = \min_{i=1,...,n_x} d_i. \end{aligned} \tag{241}$$

Proof. Consider the linear dissipation expression of the Lyapunov function given in (235)

$$\begin{aligned}\dot{V}(t)+2\gamma V(t)=2\langle e(\cdot,t),\mathcal{P}\mathcal{A}e(\cdot,t)\rangle+2\langle e(\cdot,t),\mathcal{P}G\nu(\cdot,t)\rangle+2\langle e(\cdot,t),\mathcal{P}L_D(z)\mathcal{C}e(\cdot,t)\rangle\\+2\gamma\langle e(\cdot,t),\mathcal{P}e(\cdot,t)\rangle.\end{aligned}\tag{242}$$

Taking the definition of $L_D(z)$ in (237), then the substitution of (209) and (223) into (242) yields

$$\begin{aligned}\dot{V}(t)+2\gamma V(t)=2\int_0^1 e^T(z,t)W(z)\left(D\partial_z^2e(z,t)-\mathcal{V}\partial_z e(z,t)-(K-\gamma I_{n_x})e(z,t)\right)dz\\+2\int_0^1 e^T(z,t)W(z)G\nu(z,t)dz+2\sum_{j=1}^{n_y}\int_{\tilde{z}_j}^{\tilde{z}_{j+1}} e^T(z,t)W(z)l_j(z)\mathbf{c}_j^Te(\zeta_j,t)dz.\end{aligned}\tag{243}$$

Regarding the definitions of $\tilde{D}(z)$, $\tilde{\mathcal{V}}(z)$, $\tilde{K}(z)$, $\tilde{G}(z)$ and $\tilde{l}_j(z)$ in (241), we must first notice that under the constrain existence definitions of Q and R, $\tilde{D}$, $\tilde{\mathcal{V}}:[0,1]\to\mathbb{S}^{n_x}$. Then, for the application of integration by parts into (243), we take into consideration the formulas in (355) and (357) presented in Appendix D, thus (243) becomes

$$\begin{aligned}\dot{V}(t)+2\gamma V(t)=&-e^T(1,t)\left[2\tilde{D}(1)M_{\alpha_1}^{-1}M_{\beta_1}+\partial_z\tilde{D}(1)+\tilde{\mathcal{V}}(1)\right]e(1,t)\\&+e^T(0,t)\left[2\tilde{D}(0)M_{\alpha_0}^{-1}M_{\beta_0}+\partial_z\tilde{D}(0)+\tilde{\mathcal{V}}(0)\right]e(0,t)\\&-2\int_0^1\partial_z e^T(z,t)\tilde{D}(z)\partial_z e(z,t)dz+2\int_0^1 e^T(z,t)\tilde{G}(z)\nu(z,t)dz\\&+\int_0^1 e^T(z,t)\left[\partial_z^2\tilde{D}(z)+\partial_z\tilde{V}(z)-\tilde{K}(z)+2\gamma W(z)\right]e(z,t)dz\\&+2\sum_{j=1}^{n_y}\int_{\tilde{z}_j}^{\tilde{z}_{j+1}} e^T(z,t)\tilde{l}_j(z)\mathbf{c}_j^Te(\zeta_j,t)dz.\end{aligned}\tag{244}$$

Notice by virtue of Wirtinger's inequality that the following hold

$$\begin{aligned}-\int_{\tilde{z}_j}^{\zeta_j}\partial_z e^T(z,t)\tilde{D}(z)\partial_z e(z,t)dz\leq\\\frac{-\pi^2\epsilon D_{\min}}{4(\zeta_j-\tilde{z}_j)^2}\int_{\tilde{z}_j}^{\zeta_j}\left(e(z,t)-e(\zeta_j,t)\right)^T\left(e(z,t)-e(\zeta_j,t)\right)dz\end{aligned}\tag{245}$$

and

$$
\begin{aligned}
-\int_{z_j}^{\tilde{z}_{j+1}} \partial_z e^T(z,t)\tilde{D}(z)\partial_z e(z,t)dz \leq \\
\frac{-\pi^2\epsilon D_{\min}}{4(\tilde{z}_{j+1}-z_j)^2}\int_{z_j}^{\tilde{z}_{j+1}} \Big(e(z,t)-e(\zeta_j,t)\Big)^T \Big(e(z,t)-e(\zeta_j,t)\Big)\,dz.
\end{aligned} \tag{246}
$$

where $D_{\min} = \min_{i=1,...,n_x} d_i$.

Next, summing up (245) and (246) yields

$$
\begin{aligned}
-\int_{\tilde{z}_j}^{\tilde{z}_{j+1}} \partial_z e^T(z,t)\tilde{D}(z)\partial_z e(z,t)dz \leq \\
-\frac{\pi^2\epsilon D_{\min}}{4p_j^2}\int_{\tilde{z}_j}^{\tilde{z}_{j+1}} e^T(z,t)e(z,t)dz + \frac{\pi^2\epsilon D_{\min}}{2p_j^2}\int_{\tilde{z}_j}^{\tilde{z}_{j+1}} e^T(z,t)e(\zeta_j,t)dz \\
-\frac{\pi^2\epsilon D_{\min}}{4p_j^2}\int_{\tilde{z}_j}^{\tilde{z}_{j+1}} e^T(\zeta_j,t)e(\zeta_j,t)dz
\end{aligned} \tag{247}
$$

where $p_j^2 = \max\{(\zeta_j-\tilde{z}_j)^2, (\tilde{z}_{j+1}-\zeta_j)^2\},\ j = 1, ..., n_y$.

Hence, substituting (247) into (244) leads to

$$
\begin{aligned}
&\dot{V}(t) + 2\gamma V(t) \leq \\
&\quad -e^T(1,t)\left[2\tilde{D}(1)M_{\alpha_1}^{-1}M_{\beta_1} + \partial_z\tilde{D}(1) + \tilde{\mathcal{V}}(1)\right]e(1,t) \\
&\quad + e^T(0,t)\left[2\tilde{D}(0)M_{\alpha_0}^{-1}M_{\beta_0} + \partial_z\tilde{D}(0) + \tilde{\mathcal{V}}(0)\right]e(0,t) \\
&+\sum_{j=1}^{n_y}\int_{\tilde{z}_j}^{\tilde{z}_{j+1}} e^T(z,t)\left[\partial_{zz}\tilde{D}(z) + \partial_z\tilde{V}(z) - \tilde{K}(z) - \frac{\pi^2\epsilon D_{\min}}{2p_j^2}I_{n_x} + 2\gamma W(z)\right]e(z,t)dz \\
&\quad + 2\sum_{j=1}^{n_y}\int_{\tilde{z}_j}^{\tilde{z}_{j+1}} e^T(z,t)\tilde{G}(z)\nu(z,t)dz - \sum_{j=1}^{n_y}\frac{\pi^2\epsilon D_{\min}}{2p_j^2}\int_{\tilde{z}_j}^{\tilde{z}_{j+1}} e^T(\zeta_j,t)e(\zeta_j,t)dz \\
&\quad + \sum_{j=1}^{n_y}\frac{\pi^2\epsilon D_{\min}}{p_j^2}\int_{\tilde{z}_j}^{\tilde{z}_{j+1}} e^T(z,t)e(\zeta_j,t)dz \\
&\quad + 2\sum_{j=1}^{n_y}\int_{\tilde{z}_j}^{\tilde{z}_{j+1}} e^T(z,t)\tilde{l}_j(z)\mathbf{c}_j^T e(\zeta_j,t)dz.
\end{aligned} \tag{248}
$$

We can rewrite (248) as

$$\begin{aligned}\dot{V}(t)+2\gamma V(t) \leq & -e^T(1,t)\left[2\tilde{D}(1)M_{\alpha_1}^{-1}M_{\beta_1}+\partial_z\tilde{D}(1)+\tilde{\mathcal{V}}(1)\right]e(1,t)\\ & +e^T(0,t)\left[2\tilde{D}(0)M_{\alpha_0}^{-1}M_{\beta_0}+\partial_z\tilde{D}(0)+\tilde{\mathcal{V}}(0)\right]e(0,t)\\ & +\sum_{j=1}^{n_y}\int_{\tilde{z}_j}^{\tilde{z}_{j+1}}\mathbf{e}^T(z,t)P_j(z)\,\mathbf{e}(z,t)dz\end{aligned} \tag{249}$$

where $\mathbf{e}_j(z,t)=[e(z,t)\ \ \nu(z,t)\ \ e(\zeta_j,t)]^T$. Therefore, in order to ensure the negativity of the right side of (249), it suffices that

$$\begin{aligned}2\tilde{D}(1)M_{\alpha_1}^{-1}M_{\beta_1}+\partial_z\tilde{D}(1)+\tilde{\mathcal{V}}(1)\geq 0\\ 2\tilde{D}(0)M_{\alpha_0}^{-1}M_{\beta_0}+\partial_z\tilde{D}(0)+\tilde{\mathcal{V}}(0)\leq 0\end{aligned} \tag{250}$$

and

$$P_j(z)\leq 0,\ j=1,...,n_y. \tag{251}$$

Applying the *S*-procedure to (251) and (88), we obtain

$$P_j(z)-\tau\begin{bmatrix}M & 0\\ 0 & 0\end{bmatrix}\leq 0,\ j=1,...,n_y. \tag{252}$$

Then, (250) and (252) imply that

$$V(t)\leq e^{-2\gamma t}V(0) \tag{253}$$

and from Section 5.1.3.1, it follows that

$$\|e(z,t)\|\leq M_e e^{-\gamma t}\|e_0(z)\|. \tag{254}$$

□

5.2.2 Piecewise measurements on $[\zeta_j-\varepsilon_j,\zeta_j+\varepsilon_j],\ j=1,...,n_y$

In this case, as shown in Figure 24, we divide the spatial domain $[0,1]$ into n_y subintervals $[\tilde{z}_j,\tilde{z}_{j+1}],\ j=1,...,n_y$ according to the position of the measurement sensors. From Figure 24, we get that $0=\tilde{z}_1<...<\tilde{z}_{n_y+1}=1$ and

$$[\zeta_j-\varepsilon_j,\zeta_j+\varepsilon_j]\subset[z_j,z_{j+1}],\ \text{for } j=1,...,n_y. \tag{255}$$

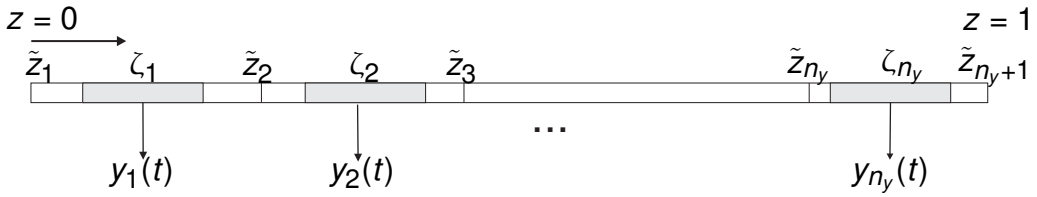

Figure 24 – Distributed piecewise measurements.

Theorem 5.2. *The error dynamics in* (209)-(212) *($c_j(z)$, $j = 1, ..., n_y$ defined as* (7)*) is asymptotically stable with a decay rate γ if conditions in Theorem 5.1 are satisfied and whenever p_j, $j = 1, ..., n_y$ is redefined as*

$$p_j^2 = \max\{(\zeta_j + \varepsilon_j - \tilde{z}_j)^2, (\tilde{z}_{j+1} - \zeta_j + \varepsilon_j)^2\},\ j = 1, ..., n_y. \tag{256}$$

Proof. We proceed in the same way as in the proof of Theorem 5.1, the linear dissipation expression of the Lyapunov function given in (235) along (209) is expressed as

$$\begin{aligned}\dot{V}(t) + 2\gamma V(t) = 2\int_0^1 e^T(z,t)W(z)\left(D\partial_z^2 e(z,t) - \mathcal{V}\partial_z e(z,t) - (K - \gamma I_{n_x})e(z,t)\right)dz \\ + 2\int_0^1 e^T(z,t)W(z)G\nu(z,t)dz \\ + 2\sum_{j=1}^{n_y}\int_{\tilde{z}_j}^{\tilde{z}_{j+1}} e^T(z,t)W(z)l_j(z)\mathrm{c}_j^T\left(\frac{1}{2\varepsilon_j}\int_{\zeta_j-\varepsilon_j}^{\zeta_j+\varepsilon_j} e(z,t)dz\right)dz.\end{aligned} \tag{257}$$

Applying the first mean value theorem for integration, for each $j = 1, ..., n_y$ and any $t \geq 0$, there exists a scalar $\bar{\zeta}_j^t \in [\zeta_j - \epsilon_j, \zeta_j + \epsilon_j]$ such that

$$\frac{1}{2\epsilon_j}\int_{\zeta_j-\varepsilon_j}^{\zeta_j+\varepsilon_j} e(z,t)dz = e(\bar{\zeta}_j^t, t) \tag{258}$$

Regarding the definitions of $\tilde{D}(z)$, $\tilde{\mathcal{V}}(z)$, $\tilde{K}(z)$, $\tilde{G}(z)$ and $\tilde{l}_j(z)$ in (241) and applying the integration by parts into (257), we obtain (244) where $e(\zeta_j, t)$ is now substituted by $e(\tilde{\zeta}_j^t, t)$. By the application of Wirtinger's inequality lemma, the following hold

$$\begin{aligned}-\int_{\tilde{z}_j}^{\tilde{\zeta}_j^t}\partial_z e^T(z,t)\tilde{D}(z)\partial_z e(z,t)dz \leq \\ \frac{-\pi^2\epsilon D_{\min}}{4(\tilde{\zeta}_j^t - \tilde{z}_j)^2}\int_{\tilde{z}_j}^{\tilde{\zeta}_j^t}\left(e(z,t) - e(\tilde{\zeta}_j^t, t)\right)^T\left(e(z,t) - e(\tilde{\zeta}_j^t, t)\right)dz\end{aligned} \tag{259}$$

and

$$
\begin{aligned}
-\int_{\tilde{\zeta}_j^t}^{\tilde{z}_{j+1}} \partial_z e^T(z,t)\tilde{D}(z)\partial_z e(z,t)dz \leq \\
\frac{-\pi^2 \epsilon D_{\min}}{4(\tilde{z}_{j+1}-\tilde{\zeta}_j^t)^2}\int_{\tilde{\zeta}_j^t}^{\tilde{z}_{j+1}} \left(e(z,t)-e(\tilde{\zeta}_j^t,t)\right)^T \left(e(z,t)-e(\tilde{\zeta}_j^t,t)\right) dz.
\end{aligned} \tag{260}
$$

where $D_{\min} = \min_{i=1,...,n_x} d_i$.

As $\tilde{\zeta}_j^t \in [\zeta_j - \varepsilon_j, \zeta_j + \varepsilon_j] \subset [z_j, z_{j+1}]$, $j = 1, ..., n_y$ and $t \geq 0$, we get

$$
\tilde{\zeta}_j^t - \tilde{z}_j \leq \zeta_j + \varepsilon_j - \tilde{z}_j \quad \text{and} \quad \tilde{z}_{j+1} - \tilde{\zeta}_j^t \leq \tilde{z}_{j+1} - \zeta_j + \varepsilon_j \tag{261}
$$

Next, summing up (259) and (260) yields

$$
\begin{aligned}
-\int_{\tilde{z}_j}^{\tilde{z}_{j+1}} \partial_z e^T(z,t)\tilde{D}(z)\partial_z e(z,t)dz \leq \\
-\frac{\pi^2 \epsilon D_{\min}}{4p_j^2}\int_{\tilde{z}_j}^{\tilde{z}_{j+1}} e^T(z,t)e(z,t)dz + \frac{\pi^2 \epsilon D_{\min}}{2p_j^2}\int_{\tilde{z}_j}^{\tilde{z}_{j+1}} e^T(z,t)e(\tilde{\zeta}_j^t,t)dz \\
-\frac{\pi^2 \epsilon D_{\min}}{4p_j^2}\int_{\tilde{z}_j}^{\tilde{z}_{j+1}} e^T(\tilde{\zeta}_j^t,t)e(\tilde{\zeta}_j^t,t)dz
\end{aligned} \tag{262}
$$

where $p_j^2 = \max\{(\zeta_j + \varepsilon_j - \tilde{z}_j)^2, (\tilde{z}_{j+1} - \zeta_j + \varepsilon_j)^2\}$, $j = 1, ..., n_y$.

Hence, taking (262) into consideration, (248)-(249) is true (regarding the substitution of $e(\zeta_j, t)$ by $e(\tilde{\zeta}_j^t, t)$). Finally (250) and (252) ensures that

$$
\|e(z,t)\|_2 < M_e e^{-\gamma t}\|e_0(z)\|. \tag{263}
$$

□

5.3 GLUCONIC ACID PRODUCTION

In order to illustrate the methodology developed in previous sections, we consider a tubular reactor for gluconic acid production whose biological features has been largely studied in (MIRÓN et al., 2002).

The process takes place in a tubular reactor fed with glucose and oxygen. The consumption of glucose (G) by the microorganisms (X) to produce gluconic acid (GA) motivates the following simplified mechanism

$$
\begin{aligned}
G + X &\rightarrow X \\
G + \frac{1}{2}O_2 &\rightarrow GA.
\end{aligned} \tag{264}
$$

The evolution of the concentration spatial profiles are described by the dynamic PDE model

$$\begin{aligned}
\partial_t[X](z,t) &= d\partial_z^2[X](z,t) - \upsilon[X](z,t) + r_X([X](z,t),[G](z,t)) \\
\partial_t[GA](z,t) &= d\partial_z^2[GA](z,t) - \upsilon[GA](z,t) + r_{GA}([GA](z,t),[G](z,t)) \\
\partial_t[G](z,t) &= d\partial_z^2[G](z,t) - \upsilon[G](z,t) - r_X([X](z,t),[G](z,t)) - r_{GA}([GA](z,t),[G](z,t)) \\
\partial_t[O_2](z,t) &= d\partial_z^2[O_2](z,t) - \upsilon[O_2](z,t) + kla([O_2^*] - [O_2]) - 0.5 r_{GA}([GA](z,t),[G](z,t))
\end{aligned} \tag{265}$$

for $(z,t) \in (0,1) \times (0,\infty)$ and subject to

$$\begin{aligned}
d\partial_z[X](0,t) &= \upsilon([X](0,t) - [X]_{in}(t)) \\
d\partial_z[GA](0,t) &= \upsilon([GA](0,t) - [GA]_{in}(t)) \\
d\partial_z[G](0,t) &= \upsilon([G](0,t) - [G]_{in}(t)) \\
d\partial_z[O_2](0,t) &= \upsilon([O_2](0,t) - [O_2]_{in}(t)) \\
\partial_z[X](1,t) &= 0 \\
\partial_z[GA](1,t) &= 0 \\
\partial_z[G](1,t) &= 0 \\
\partial_z[O_2](1,t) &= 0
\end{aligned} \tag{266}$$

where the biomass and gluconic acid reaction rates correspond with

$$r_X([X](z,t),[G](z,t)) = \mu^X[X](z,t)\frac{k_1^X - [X](z,t)}{k_1^X}, \quad \mu^X = \frac{\mu_{max}^X[G](z,t)}{k_2^X + [G](z,t)} \tag{267}$$

$$r_{GA}([GA](z,t),[G](z,t)) = \mu^{GA}[GA](z,t)\frac{k_1^{GA} - [GA](z,t)}{k_1^{GA}}, \quad \mu^{GA} = \frac{\mu_{max}^{GA}[G](z,t)}{k_2^{GA} + [G](z,t)} \tag{268}$$

The system parameters definition and its respective numerical values are listed in Table 3.

The system modeled by (265)-(266) take the form of (1)-(2) by considering

Table 3 – Parameter values

Parameter	**Value**	**Definition**
d	0.01 m^2h^{-1}	Mass dispersion coefficient
υ	0.01 mh^{-1}	Flow velocity
kla	600 h^{-1}	Mass exchange parameter
O_2^*	7.5e^{-3}g l^{-1}	Saturation of dissolved oxygen
$[G]_{in}$	115 gl^{-1}	Glucose stream
$[O_2]_{in}$	7.5e^{-3} gl^{-1}	Dissolved oxygen stream
μ_{max}^X	0.219 h^{-1}	Constant
k_1^X	2.53 gl^{-1}	Constant
k_2^X	5 gl^{-1}	Constant
μ_{max}^{GA}	0.312 h^{-1}	Constant
k_1^{GA}	109 gl^{-1}	Constant
k_2^{GA}	6 gl^{-1}	Constant

.

$$
\begin{aligned}
x(z,t) &= \begin{bmatrix}[X](z,t) & [GA](z,t) & [G](z,t) & [O_2](z,t)\end{bmatrix}^T,\\
u_d &= \begin{bmatrix}0 & 0 & 0 & [O_2]^*\end{bmatrix}^T,\\
u_0(t) &= \begin{bmatrix}0 & 0 & [G]_{in} & [O_2]_{in}\end{bmatrix}^T,\ u_1(t) = 0,\\
D &= d\ I,\ \mathcal{V} = \upsilon I,\ \mathrm{K} = diag(0,-kla),\\
B &= diag(0,kla),\quad G = \begin{bmatrix}1 & 0\\ 0 & 1\\ -1 & -1\\ 0 & -0.5\end{bmatrix},\\
M_{\alpha_0} &= d\ I,\ M_{\beta_0} = -\upsilon\ I,\ M_{\alpha_1} = I,\ M_{\beta_1} = 0.
\end{aligned}
\tag{269}
$$

and rate function defined as

$$
r(x) = \begin{bmatrix} r_X([X],[G]) \\ r_{GA}([GA],[G]) \end{bmatrix} \tag{270}
$$

and hence its Jacobian matrix is given by

$$
\nabla_x r(x) = \begin{bmatrix} \partial_{[X]} r_X & 0 & \partial_{[G]} r_X & 0 \\ 0 & \partial_{[GA]} r_{GA} & \partial_{[G]} r_{GA} & 0 \end{bmatrix} \tag{271}
$$

with

$$\begin{aligned}
\partial_{[X]} r_X &= \frac{\mu^X_{\max}\,[G]\,(k_1^X - [X])}{k_1^X\,(k_2^X + [G])} - \frac{\mu^X_{\max}\,[X]\,[G]}{k_1^X (k_2^X + [G])} \\
\partial_{[G]} r_X &= \frac{\mu^X_{\max}\,[X]\,(k_1^X - [X])}{k_1^X\,(k_2^X + [G])} - \frac{\mu^X_{\max}\,[X]\,[G]\,(k_1^X - [X])}{k_1^X (k_2^X + [G])^2} \\
\partial_{[GA]} r_{GA} &= \frac{\mu^X_{max}[G]\,(k_1^{GA} - [GA])}{k_1^{GA}(k_2^{GA} + [G])} - \frac{mu^{GA}_{max}[GA][G]}{k_1^{GA}\,(k_2^{GA} + [G])} \\
\partial_{[G]} r_{GA} &= \frac{\mu^{GA}_{max}\,[GA]\,(k_1^{GA} - [GA])}{k_1^{GA}\,(k_2^{GA} + [G])} - \frac{\mu^{GA}_{max}[GA][G](k_1^{GA} - [GA])}{k_1^{GA}(k_2^{GA} + [G])^2}
\end{aligned} \tag{272}$$

Considering the domain of operation of the state variables

$$\begin{aligned}
\mathfrak{D} = \{([X],[GA],[G],[O_2]) : 0 \le [X] \le 3,\ 0 \le [GA] \le 120,\ 0 \le [G] \le 60, \\
0 \le [O_2] \le 0.0075\}
\end{aligned}$$

we obtain that

$$\begin{aligned}
&-3.813 < \partial_{[X]} r_X \le 0 && -59.7 < \partial_{[G]} r_X \le 0 \\
&-0.340 < \partial_{[GA]} r_{GA} \le 0.2836 && -0.63 < \partial_{[G]} r_{GA} \le 1.417.
\end{aligned} \tag{273}$$

Then one choice for the local lower and upper bound matrices of the Jacobian matrix are respectively

$$\Gamma_1 = \begin{bmatrix} -3.813 & 0 & -59.7 & 0 \\ 0 & -0.340 & -0.63 & 0 \end{bmatrix} \qquad \Gamma_2 = \begin{bmatrix} 0 & 0 & 0 & 0 \\ 0 & 0.2836 & 1.417 & 0 \end{bmatrix}. \tag{274}$$

It is also assumed that the measured output is given by four piecewise measurements of the Glucose and Oxygen concentrations

$$y(t) = \begin{bmatrix} \int_{\zeta_1-\varepsilon_1}^{\zeta_1+\varepsilon_1} [G](z,t)dz \\ \int_{\zeta_2-\varepsilon_2}^{\zeta_2+\varepsilon_2} [G](z,t)dz \\ \int_{\zeta_3-\varepsilon_3}^{\zeta_3+\varepsilon_3} [O_2](z,t)dz \\ \int_{\zeta_4-\varepsilon_4}^{\zeta_4+\varepsilon_4} [O_2](z,t)dz \end{bmatrix} \tag{275}$$

which sets $\epsilon_j = 0.01,\ j = 1,...,4,\ \mathbf{c}_1^T = \mathbf{c}_2^T = [0\ 0\ 1\ 0],\ \mathbf{c}_3^T = \mathbf{c}_4^T = [0\ 0\ 0\ 1]$ and $\zeta_1 = 0.3,\ \zeta_2 = 0.7,\ \zeta_3 = 0.5,\ \zeta_4 = 0.8$ in (5) and (7).

Thus, the output injection gain $L_D(z)$ is calculated by solving the LMIs conditions in Theorem 5.2 and considering $\tilde{z}_1 = 0,\ \tilde{z}_2 = 0.45,\ \tilde{z}_3 = 0$ and decay rate $\gamma = 5.25$ yielding

5.3.1 Observer tests

The observer and system responses are generated via numerical simulation with initial profiles that were generated as positive polynomials satisfying the boundary conditions, upper bounds selected by the physical conditioning of the process and matching the initial measurements. Figures 25, 26, 27 and 28 show the evolution of the actual profiles (in red lines) with their respective estimated profiles (in blue lines) considering the proposed observer in four different time instants.

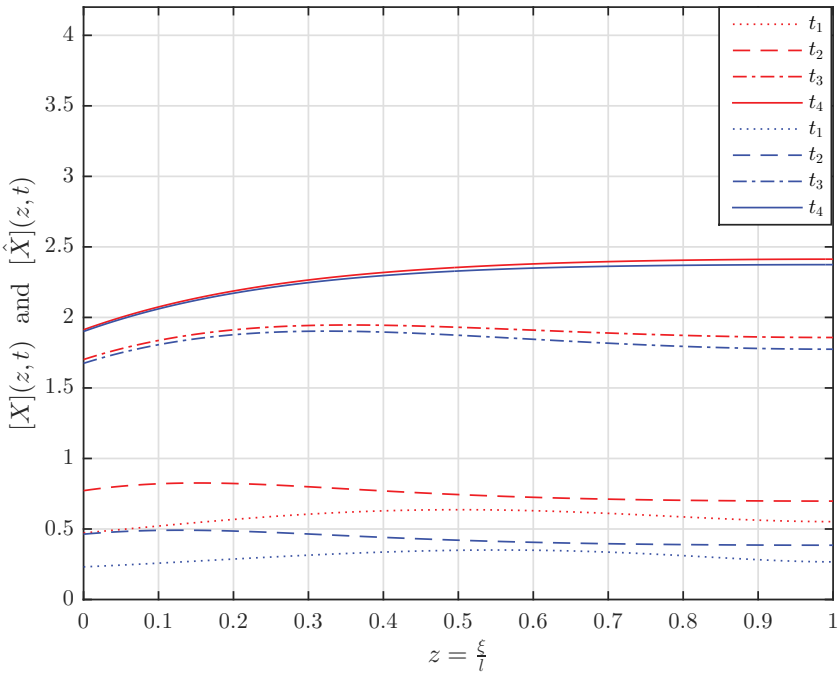

Figure 25 – Time evolution of the spatial profile of $[X](z, t)$ and $[\hat{X}](z, t)$ at time instants $t_1 = 0,\ t_2 = 4,\ t_3 = 10,\ t_4 = 20$.

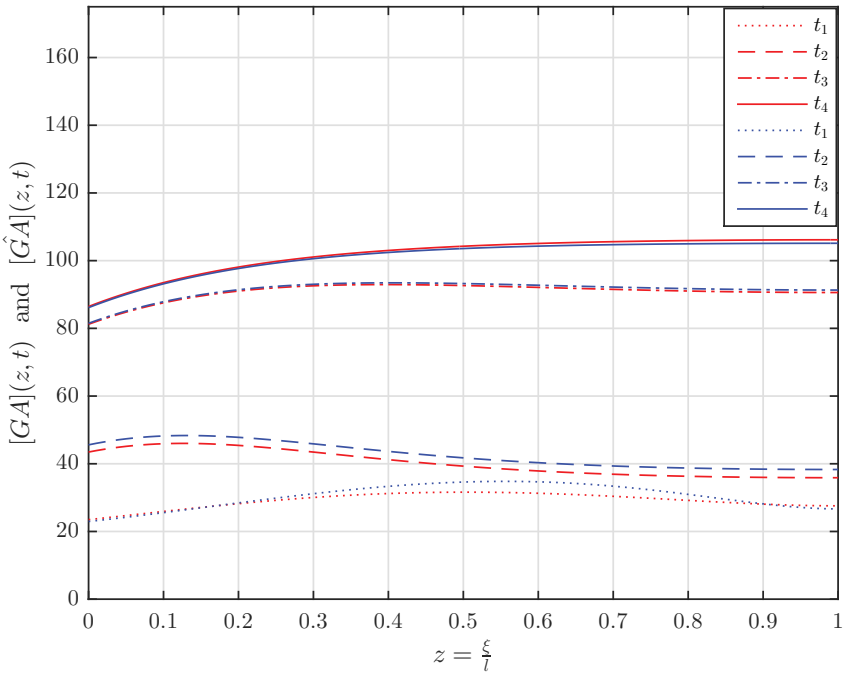

Figure 26 – Time evolution of the spatial profile of $[GA](z,t)$ and $[\hat{GA}](z,t)$ at time instants $t_1 = 0,\ t_2 = 4,\ t_3 = 10,\ t_4 = 20$.

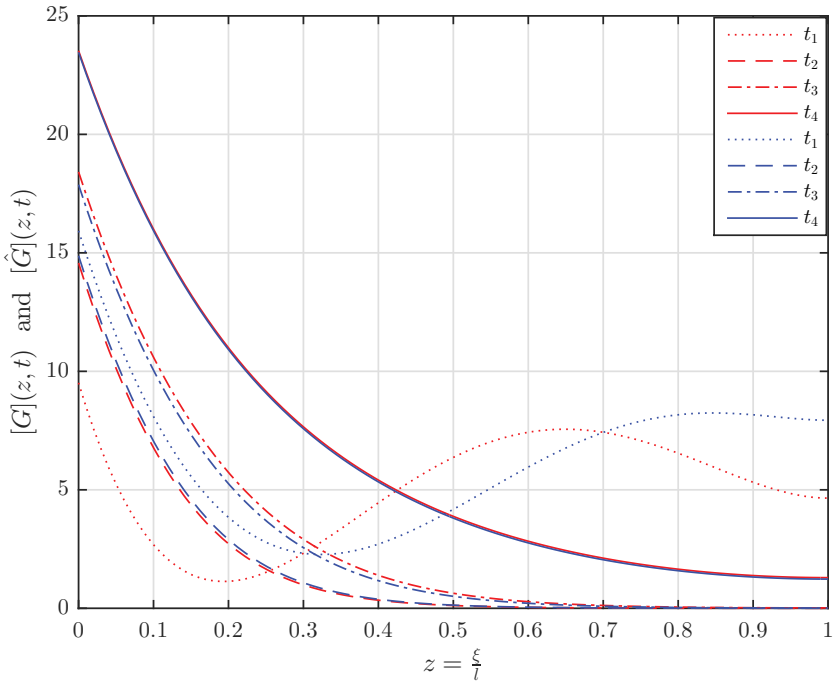

Figure 27 – Time evolution of the spatial profile of $[G](z,t)$ and $[\hat{G}](z,t)$ at time instants $t_1 = 0,\ t_2 = 4,\ t_3 = 10,\ t_4 = 20$.

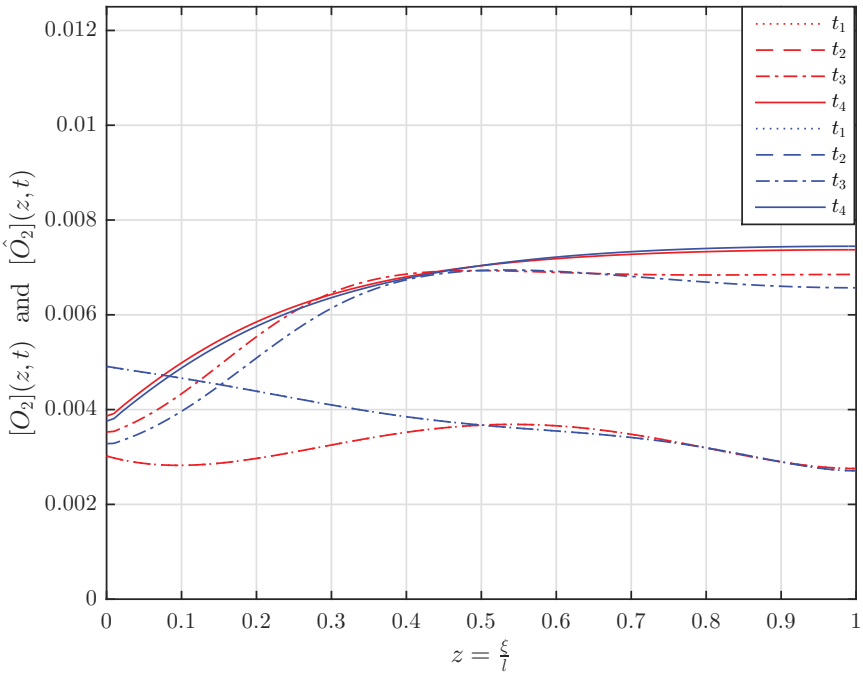

Figure 28 – Time evolution of the spatial profiles of $[O_2](z,t)$ and $[\hat{O}_2](z,t)$ at time instants $t_1 = 0,\ t_2 = 4,\ t_3 = 10,\ t_4 = 20$.

Figure 29 shows the evolution of the estimation error norm. Since the initial estimation profiles are already a good approximation of the actual variables states, the estimation error norm converges quickly, and hence, provides very satisfactory estimates.

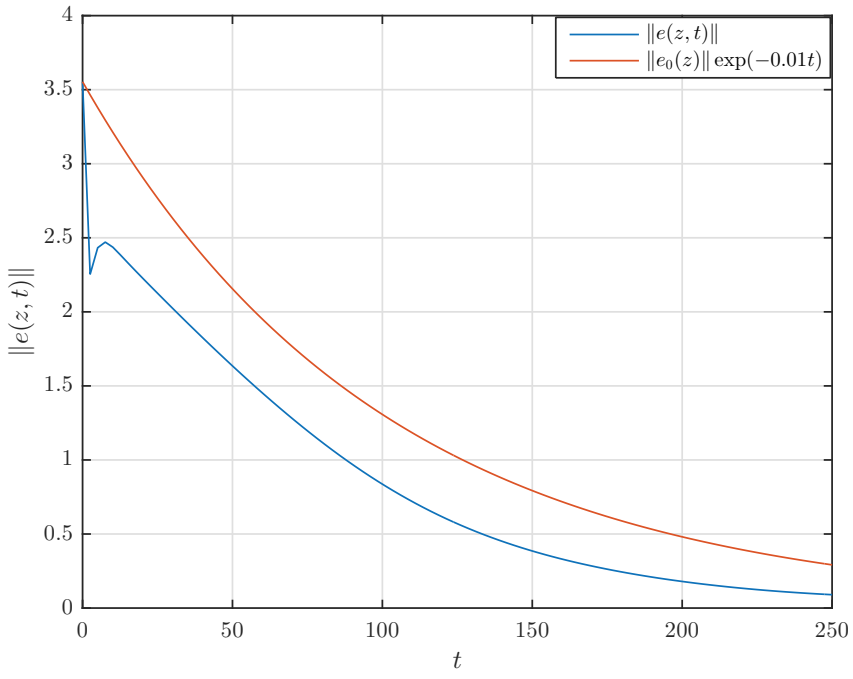

Figure 29 – Time evolution of the estimation error norm $\|e(z,t)\|$.

5.4 CONCLUDING REMARKS

In this chapter, we proposed a late lumping approach to the observer design of transport-reaction systems described by a set of coupled semilinear parabolic PDEs. In particular, the Lyapunov method has been applied to derive a set of LMI based conditions for designing a nonlinear Luenberger observer in which the observer error dynamics can be modeled as a Lure type system with multivariable sector conditions from the bound Jacobian matrices. The proposed methodology sets a non-conservative approach through a polynomial parametrization of the decision variables and is verified by means of the wide-range of feasibility of the set of LMIs. Polynomial parametrization of the Lyapunov functional and the observer gain is not constraining since, according to Weierstrass approximation theorem, any continuous function on a bounded interval can be approximated by a polynomial. The drawback is that the degree of the corresponding approximating polynomials may not be known a priori.

The methodology presented here employed the integration by parts as a crucial step on the stability analysis of PDEs as well as local checks, which is provided by embedding results on bounded domains as the Wirtinger's inequality and the S-procedure for local stability analysis based on sector condition are also important to derive less conservative LMIs. Our scope was to make these steps computationally tractable by formulating a semidefinite programming problem (SDP). It is clear that the results presented in sections (5.2.1) and (5.2.2) can also be directly extended to optimization problems with constraints in a convex optimization framework as for instance the H_∞-optimal observer synthesis.

6 MONITORING OF COVID-19 SPREAD

Lately, the study of social networks and the epidemiological analysis of diseases have attracted considerable attention, and extensive research has been carried out in these areas due to their prominent role in human life (SANATKAR et al., 2015). Social networks provide practical methodologies to simulate diseases epidemic by developing mathematical models to predict and monitor critical features of outbreaks (including the size and variation of its response).

The 2019 novel coronavirus, termed as COVID-19 or SARSCoV-2 by the World Health Organization (WHO), affects the respiratory system similar to the influenza virus, with some common symptoms such as cough, fever, exhaustion, and breathlessness. The rapid spread of COVID-19 all over the world has become a matter of grave concern and has hugely altered the lifestyle and social behavior of humans from the beginning of 2020. Indeed, it poses considerable economic, environmental, and political challenges for the entire human population. Consequently, considerable research effort has been made to investigate precise mathematical models for the outbreak of this newborn virus and rapid estimation of its future transmission and mortality rates.

In this chapter, employing a new generalized epidemiological SEIR model of COVID-19 spread (MAMMERI, 2020), a model based state estimator design is developed for the COVID-19 epidemic spread in a host population. The presence of modeling uncertainties and incomplete measurement feedback is tackled through the Lyapunov based approach in order to identify susceptible, exposed and infected populations since it represents a serious measurement limitation on these groups in the real situation. In this framework, the global numbers of symptomatic and deceased people with bounded inaccuracies in statistical data are taken into account as the only available feedback signals. The appropriate choice of the observer gains resulting from a SDP problem solution let us to estimate the other compartmental variables. Numerical experiments are presented to illustrate the method efficiency.

6.1 COVID-19 OUTBREAK

In late 2019, a disease outbreak emerged in a city of Wuhan, China. The culprit was a certain strain called Coronavirus Disease 2019 or COVID-19 in brief. This virus has been identified to cause fever, cough, hortness of breath, muscle ache, confusion, headache, sore throat, rhinorrhoea, chest pain, diarrhea, and nausea and vomiting (CHEN, N. et al., 2020). COVID-19 belongs to the Coronaviridae family. A family of coronaviruses that cause diseases in humans and animals, ranging from the common cold to more severe diseases. Although only seven coronaviruses are known to cause disease in humans, three of these, COVID-19 included, can cause a much severe infection, and sometimes fatal to humans. The other two to complete the list were the

severe acute respiratory syndrome (SARS) identified in 2002 in China, and the Middle East respiratory syndrome (MERS) originated decade after in Saudi Arabia.

Like MERS and SARS, COVID-19 is a zoonotic virus and believed to be originated from bats transmitted to humans (ZHOU, P. et al., 2020). In comparison with SARS, MERS, the COVID-19 appears to be less deadly. However, the World Health Organization (WHO) reported that it has already infected and killed more people than its predecessors combined. Also, COVID-19 spreads much faster than SARS and MERS. It only took over a month before it surpassed the number of cases recorded by the SARS outbreak in 2012. According to WHO, it only took 67 days from the beginning of the outbreak in China last December 2019 for the virus to infect the first 100000 people worldwide. As of the 25th of March 2020, a cumulative total of 372757 confirmed cases, while 16231 deaths have been recorded for COVID-19 by World Health Organization.

For the time being and in spite of the massive vaccination, COVID-19 infection is still on the rise in many countries. Governments struggle to accelerate the vaccination campaigns to combat the disease whereas research institutions try to find out the effectiveness of the vaccines regarding the new variants of the virus circulating in many countries.

Several mathematical models have been proposed from various epidemiological groups. These models help governments as an early warning device about the size of the outbreak, how quickly it will spread, and how effective control measures may be. However, due to the limited emerging understanding of the new virus and its transmission mechanisms, the results are largely inconsistent across studies.

6.2 SPATIOTEMPORAL MODEL OF COVID-19 INFECTION SPREAD

We consider the mathematical model based on the SIR model (ARCEDE et al., 2020) and developed in (MAMMERI, 2020) where it is assumed that a host population of individuals is divided into compartments corresponding to disease status, modeling the movement in space and time of the subpopulation in each compartment. Specifically, these compartments are the densities of Susceptible population (S), Exposed population (E), Symptomatic Infected population (I_s), Asymptomatic Infected population (I_a), Under treatment population (U) and Removed population (R) and the deceased population D_e. Note that D_e refers only to deaths due to COVID-19. We denote the living host population as $N = S + E + I_a + I_s + U + R$. Due to the names of the compartments used, this model may be called a susceptible-exposed-infected-recovered (SEIR) model. We therefore formulate the problem in terms of the state vector $x = [S, E, Ia, I_s, U, R]^T$ containing the different compartments. This model assumes that

- the spatial mobility is governed by diffusion coefficients according to the mobility

restriccions of the host population;

- only susceptible, exposed and asymptomatic individuals are moving;
- there is a latency period between exposure and the development of symptoms;
- the probability of contagion increases with population size.

Description of the infection flow

Susceptible class contains individuals who do not have the temporary immunity to the virus, then might become infected if exposed. Exposed class contains individuals who have been infected but do not have symptoms. The period that starts when the person becomes infected, until the person becomes symptomatic or asymptomatic is the latent period $\frac{1}{\delta_I}$ = 5 days. Under treatment class contains individuals who are currently infected and can not transmit the infection because of adequate isolation. Recovered class contains individuals who returned to a normal state of health after having been infected during the latent period $\frac{1}{\gamma_r}$ = 7 days. The number of deaths depends only on the death rate as the number of recovered depends only on the recovery rate. Finally, the cumulative number of infected depends only on the exposed and the incubation period. The diffusion parameters are included in the model to spread the disease spatially. Figure 30 depicts the infection flow according to the explanation above.

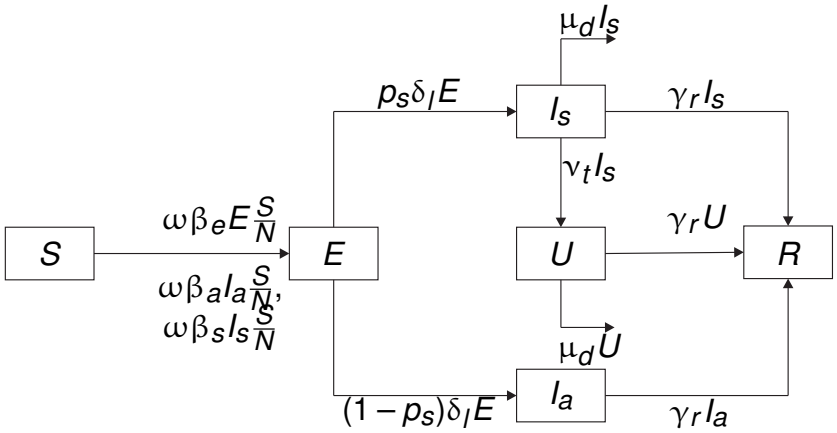

Figure 30 – Compartmental representation of the SEI_aI_sUR-model.

The dynamics is governed by a system of three partial differential equations (PDE) and three ordinary differential equations (ODE) as follows

$$
\begin{aligned}
\partial_t S(\mathrm{z},t) &= d(t)\Delta_z S(\mathrm{z},t) - w(t)\left(\beta_e E(\mathrm{z},t) + \beta_s I_s(\mathrm{z},t) + \beta_a I_a(\mathrm{z},t)\right)\frac{S}{N}(\mathrm{z},t)\\
\partial_t E(\mathrm{z},t) &= d(t)\Delta_z E(\mathrm{z},t) + w(t)\left(\beta_e E(\mathrm{z},t) + \beta_s I_s(\mathrm{z},t) + \beta_a I_a(\mathrm{z},t)\right)\frac{S}{N}(\mathrm{z},t) - \delta_I E(\mathrm{z},t)\\
\partial_t I_a(\mathrm{z},t) &= d(t)\Delta_z I_a(\mathrm{z},t) + (1-p_s)\delta_I E(\mathrm{z},t) - \gamma_r I_a(\mathrm{z},t)\\
\partial_t I_s(\mathrm{z},t) &= p_s\delta_I E(\mathrm{z},t) - (\gamma_r + \mu_d + \nu_t)\, I_s(\mathrm{z},t)\\
\partial_t U(\mathrm{z},t) &= \nu_t I_s(\mathrm{z},t) - (\gamma_r + \mu_d)\, U(\mathrm{z},t)\\
\partial_t R(\mathrm{z},t) &= \gamma_r\left(I_a(\mathrm{z},t) + I_s(\mathrm{z},t) + U(\mathrm{z},t)\right)
\end{aligned}
\tag{276}
$$

for $(\mathrm{z},t) \in \Omega \subset \mathbb{R}^2 \times (0,\infty)$ as spatial and time domains, respectively, where Δ_z is the Laplacian operator defined as

$$\Delta_z(\cdot) = \sum_{i=1}^{2} \partial^2_{z_i}(\cdot).$$

In this chapter, we address our analysis in a rectangular spatial domain defined by $\Omega = (0, l_1) \times (0, l_2) \subset \mathbb{R}^2$. The total living population is $N = S + E + I_a + I_s + U + R$ and the deaths are $D_e = \mu_d(I_s + U)$. No new recruit is added and If we assume that the region of interest is isolated, we prescribe the following homogeneous Neumann boundary conditions,

$$
\begin{aligned}
\nabla_z S \cdot \mathbf{n}\Big|_{\partial\Omega} &= 0 \qquad & \nabla_z E \cdot \mathbf{n}\Big|_{\partial\Omega} &= 0\\
\nabla_z I_a \cdot \mathbf{n}\Big|_{\partial\Omega} &= 0 \qquad & \nabla_z I_s \cdot \mathbf{n}\Big|_{\partial\Omega} &= 0\\
\nabla_z U \cdot \mathbf{n}\Big|_{\partial\Omega} &= 0 \qquad & \nabla_z R \cdot \mathbf{n}\Big|_{\partial\Omega} &= 0
\end{aligned}
\tag{277}
$$

where $\mathbf{n}$ is the outward normal vector to $\partial\Omega$ and ∇_z is the Gradient vector operator. This selection of boundary conditions represents the situation where the spatial region under consideration is closed to any in- or out- flow of populations, so that the epidemic spread is only due to local infections, which was the case during lock-down conditions in the first and second wave of the pandemic. If the population is traveling in or out of the considered spatial region, then the boundary conditions need to be formulated in another way using more general boundary conditions or mixed boundary conditions. However the computational procedure proposed in the following is not suited to these conditions, and the approach should be revisited. Specifically, when other kinds of boundary conditions are considered, the additional terms in the integration by parts procedure within the Lyapunov analysis may yield terms that cannot be expressed in an affine way and hence could not be approached using SDP tools directly.

The system parameters definition are listed in Table 4.

Table 4 – Parameter definition.

Parameter	**Definition**
$w\beta_e$	Transmission rate from S to E from contact with E
$w\beta_s$	Transmission rate from S to E from contact with I_s
$w\beta_a$	Transmission rate from S to E from contact with I_a
δ_I	Latency rate
p_s	Probability of being symptomatic
$1-p_s$	Probability of being asymptomatic
γ_r	Recovery rates
μ_d	Death rate
ν_t	Under treatment rate

Latency period and infection period have been estimated as 5 days and 7 days respectively (LAUER et al., 2020), and thus $\delta_I = \frac{1}{5}$, $\gamma_r = \frac{1}{7}$. To account for the lockdown and unlockdown, the average number of contacts is updated as follows (LIU, Z. et al., 2020)

$$w(t) = \begin{cases} w_0, \ t \leq t_{bol} \\ w_0 e^{-\rho(t-t_{bol})}, \ t_{bol} \leq t \leq t_{eol} \\ \frac{(1-\eta)w_0}{1+((1-\eta)e^{-\rho(t_{eol}-t_{bol})}-1)e^{-2\rho(t-t_{eol})}}, \ t \geq t_{eol} \end{cases} \tag{278}$$

while the diffusion coefficient is set up to

$$d(t) = \begin{cases} d_0, \ t \leq t_{bol} \\ d_0 e^{-\rho(t-t_{bol})}, \ t_{bol} \leq t \leq t_{eol} \\ \frac{d_0}{1+(e^{\rho(t_{eol}-t_{bol})}-1)e^{-2\rho(t-t_{eol})}}, \ t \geq t_{eol} \end{cases} \tag{279}$$

Here *bol* denotes beginning of lockdown and *eol* end of lockdown. Unlockdown is assumed to be faster than lockdown. The parameter $0 \leq \eta \leq 1$ is a varying coefficient translating respect for distancing. The value of d_0 is fixed according to the average daily commute related to the host population. Six parameters $\theta = (\rho, \beta_e, \beta_s, \beta_a, p_s, \mu_d)$ remain to be determined. Given, for N days, the observations $I_s(t_i)$ and $D_e(t_i)$, the cost function consists of the nonlinear least square function

$$J(\theta) = \sum_{i=1}^{N} (I_{s,ob}(t_i) - \bar{I}_s(t_i, \theta))^2 + (D_{e,obs}(t_i) - \overline{D}_e(t_i, \theta))^2, \tag{280}$$

with constraints $\theta \geq 0$. Here

$$\bar{I}_s(t_i, \theta) = \int_\Omega I_s(\mathbf{z}, t_i, \theta) d\Omega \tag{281}$$

and

$$\overline{D}_e(t_i, \theta) = \int_\Omega D_e(\mathbf{z}, t_i, \theta) d\Omega \tag{282}$$

denote the output of the mathematical model at time t_i computed with the parameters θ. The optimization problem may be solved using Approximate Bayesian Computation combined with a quasi-Newton method (MAMMERI, 2020).

6.2.1 Basic reproduction numbers

The basic viral reproduction number $\mathcal{R}_0$ of the infection is the expected number of cases directly generated by one case in a population where all individuals are susceptible to infection. The most important uses of $\mathcal{R}_0$ are determining if an emerging infectious disease can spread in a population and determining what proportion of the population should be immunized through vaccination to eradicate a disease. In (MAMMERI, 2020), a condition on parameters which defines the basic reproduction number related to the model described by (276)-(277) such that the disease has an exponential initial growth is given.

Theorem 6.1. *Let* $\left(S_0, E_0, I_{a,0}, I_{s,0}, 0, 0\right)$ *be a nonnegative initial datum. If the basic reproduction number*

$$\mathcal{R}_0 = w_0 \left(\frac{\beta_e}{\sigma} + \frac{(1-p)\beta_a}{\gamma_r} + \frac{p\beta_s}{\gamma_r + \mu_d + \nu_t} \right) \frac{S_0}{N_0} > 1, \tag{283}$$

then (E, I_a, I_s) *exponentially grows*

The term $\frac{\beta_e}{\sigma_l}$ represents the transmission rate by exposed during the average latency period $\frac{1}{\sigma_l}$. The term $\frac{(1-p)\beta_a}{\gamma_r}$ is the transmission rate by asymptomatic during the average infection period $\frac{1}{\gamma_r}$, and the last one is the part of symptomatic.

Proof. See (MAMMERI, 2020) for details. □

To reflect the spatio-temporal dynamics of the disease, we consider the effective reproduction number

$$\mathcal{R}_{eff}(\mathbf{z}, t) = w(t) \left(\frac{\beta_e}{\sigma} + \frac{(1-p)\beta_a}{\gamma_r} + \frac{p\beta_s}{\gamma_r + \mu_d + \nu_t} \right) \frac{S(\mathbf{z}, t)}{N(\mathbf{z}, t)}, \tag{284}$$

and its mean with respect to the domain Ω

$$\overline{\mathcal{R}}_{eff}(t) = \frac{1}{A(\Omega_z)} \int_\Omega \mathcal{R}_{eff}(\mathbf{z}, t) d\Omega. \tag{285}$$

Property 6.1. *The density population of any host population, at any time t, would remain constant based on the epidemiological dynamics (8):*

$$S(\mathbf{z}, t) + E(\mathbf{z}, t) + I_a(\mathbf{z}, t) + I_s(\mathbf{z}, t) + U(\mathbf{z}, t) + R(\mathbf{z}, t) = N(\mathbf{z}, t). \tag{286}$$

Also, it is worth mentioning that all compartmental variables have positive values (populations). Thus, it can be concluded that all of these variables remain bounded during the outbreak management time due to the boundedness of the total density population $N(\mathbf{z}, t)$*.*

6.3 STATE OBSERVER DESIGN

In this section, we describe the corresponding developments to estimate the compartmental states of the COVID-19 spread dynamics described by (276)-(277). The reason why a state estimation is required is two-fold: (a) it is impossible to accurately measure the numbers of susceptible, exposed, and infected people; and (b) other state measurements are typically noisy, so it might not be convenient to use them in real-time control design as that proposed in (RAJAEI et al., 2021). In order to simplify the mathematical analysis arising from the choice of a Lyapunov weighted functional, we address the state estimation problem in a rectangular spatial domain defined by $\Omega = (0, l_1) \times (0, l_2) \subset \mathbb{R}^2$.

6.3.1 Instrumental tools

It is also assumed that the measured output is given by the total symptomatic and death individuals which corresponds to the data usually provided by health authorities. Thus, we consider

$$y(t) = \begin{bmatrix} \bar{I}_s(t) \\ \overline{D}_e(t) \end{bmatrix} = \begin{bmatrix} \int_\Omega I_s(\mathbf{z}, t) d\Omega \\ \int_\Omega D_e(\mathbf{z}, t) d\Omega \end{bmatrix}. \tag{287}$$

Then, (276)-(277) take the form of

$$\partial_t x(\mathbf{z}, t) = D(t)\Delta_Z x(\mathbf{z}, t) - \mathrm{K} x(\mathbf{z}, t) + G\, r(x(\mathbf{z}, t)) \tag{288}$$

$$\nabla_Z x(\mathbf{z}, t) \cdot \mathbf{n}\Big|_{\partial\Omega} = 0. \tag{289}$$

by considering

$$x(\mathrm{z},t) = \begin{bmatrix} S(\mathrm{z},t) & E(\mathrm{z},t) & I_a(\mathrm{z},t) & I_s(\mathrm{z},t) & U(\mathrm{z},t) & R(\mathrm{z},t) \end{bmatrix}^T$$

$$D(t) = diag(d(t), d(t), d(t), 0, 0, 0)$$

$$\mathrm{K} = \begin{bmatrix} 0 & 0 & 0 & 0 & 0 & 0 \\ 0 & \delta_I & 0 & 0 & 0 & 0 \\ 0 & -(1-p_s)\delta_I & \gamma_r & 0 & 0 & 0 \\ 0 & -p_s\delta_I & 0 & (\gamma_r + \mu_d + \nu_t) & 0 & 0 \\ 0 & 0 & 0 & -\nu_t & \gamma_r + \mu_d & 0 \\ 0 & 0 & -\gamma_r & -\gamma_r & -\gamma_r & 0 \end{bmatrix}$$

$$G = \begin{bmatrix} -1 & 1 & 0 & 0 & 0 & 0 \end{bmatrix}^T \tag{290}$$

and

$$r(x(\mathrm{z},t)) = (w\beta_e E(\mathrm{z},t) + w\beta_s I_s(\mathrm{z},t) + w\beta_a I_a(\mathrm{z},t)) \frac{S}{N}(\mathrm{z},t) \tag{291}$$

with output measurement

$$y(t) = \int_\Omega C_m\, x(\mathrm{z},t) d\Omega \in \mathbb{R}^2 \tag{292}$$

where

$$C_m = \begin{bmatrix} 0 & 0 & 0 & 1 & 0 & 0 \\ 0 & 0 & 0 & \mu_d & \mu_d & 0 \end{bmatrix}. \tag{293}$$

since $D_e = \mu_d(I_s + U)$.

6.3.2 Nonlinear Luenberger-type state observer

Defining the Luenberger-type state observer for

$$\partial_t \hat{x}(\mathrm{z},t) = D(t)\Delta_z \hat{x}(\mathrm{z},t) - \mathrm{K}\ \hat{x}(\mathrm{z},t) + G\ r\left(\hat{x}(\mathrm{z},t)\right) + L_D(\mathrm{z})\left(\hat{y}(t) - y(t)\right) \tag{294}$$

for $(\mathrm{z},t) \in \Omega \times (0,\infty)$, subject to

$$\nabla_z x \cdot \mathbf{n}\Big|_{\partial\Omega} = 0 \tag{295}$$

and the initial condition

$$\hat{x}_0(\mathrm{z}) = \hat{x}(\mathrm{z},0) \tag{296}$$

for $\mathrm{z} \in \Omega$. Here the gain $L_D(\mathrm{z}) : \Omega \to \mathbb{R}^{n_x \times n_y}$ is the output injection gain to be designed. The dynamics of the state estimation error $e(\mathrm{z},t) = x(\mathrm{z},t) - \hat{x}(\mathrm{z},t)$, satisfies

$$\partial_t e(\mathbf{z},t) \;=\; D(t)\Delta_Z e(\mathbf{z},t) - \mathrm{K}e(\mathbf{z},t) \,+\, G\left[r\left(x(\mathbf{z},t)\right) - r\left(\hat{x}(\mathbf{z},t)\right)\right] \,+\, L_D(\mathbf{z})\left(\hat{y}(t) - y(t)\right) \tag{297}$$

subject to

$$\nabla_Z e \cdot \mathbf{n}\Big|_{\partial\Omega} = 0 \tag{298}$$

and the initial condition

$$e_0(\mathbf{z}) = e(\mathbf{z},0). \tag{299}$$

Similarly to the approach in Chapter 5, the function denoted as $\nu(\mathbf{z},t) = r(x(\mathbf{z},t)) - r(\hat{x}(\mathbf{z},t))$ and the estimation error $e(\mathbf{z},t)$ satisfy a sector condition based on the boundedness of the Jacobian matrix of the nonlinear function $r(\cdot)$. Then, the Differential Mean Value Theorem gives

$$\begin{aligned} \nu(\mathbf{z},t) &= r(x(\mathbf{z},t)) - r(\hat{x}(\mathbf{z},t)) \\ &= \nabla_x r\left(\breve{x}(\mathbf{z},t)\right) e(\mathbf{z},t) \end{aligned} \tag{300}$$

where $\breve{x}(\mathbf{z},t) \in Co(x(\mathbf{z},t), \hat{x}(\mathbf{z},t))$ for all $(\mathbf{z},t) = \Omega \times (0,\infty)$. Let $\Gamma_1,\ \Gamma_2 \in \mathbb{R}^{1\times 6}$ be the constant matrices whose entries are the local lower and upper bounds, respectively, of the Jacobian matrix entries of $r(\cdot)$ and hence the following inequality holds

$$\Gamma_1\ e(\mathbf{z},t) \le \nu(\mathbf{z},t) \le \Gamma_2\ e(\mathbf{z},t), \tag{301}$$

which implies the following

$$\left\langle \begin{bmatrix} e(\mathbf{z},t) \\ \nu(\mathbf{z},t) \end{bmatrix}, \underbrace{\begin{bmatrix} \frac{\Gamma_1^T\Gamma_2 + \Gamma_2^T\Gamma_1}{2} & -\frac{\Gamma_1^T + \Gamma_2^T}{2} \\ -\frac{\Gamma_1 + \Gamma_2}{2} & I \end{bmatrix}}_{M} \begin{bmatrix} e(\mathbf{z},t) \\ \nu(\mathbf{z},t) \end{bmatrix} \right\rangle \le 0 \tag{302}$$

From the definition of the rate function in (291), its jacobian is given by

$$\nabla_x r(x) = \begin{bmatrix} w\beta_e\frac{E}{N} + w\beta_s\frac{I_s}{N} + w\beta_a\frac{I_a}{N} - \frac{S}{N}\left(w\beta_e\frac{E}{N} + w\beta_s\frac{I_s}{N} + w\beta_a\frac{I_a}{N}\right) \\ w\beta_e\frac{S}{N} - \frac{S}{N}\left(w\beta_e\frac{E}{N} + w\beta_s\frac{I_s}{N} + w\beta_a\frac{I_a}{N}\right) \\ w\beta_a\frac{S}{N} - \frac{S}{N}\left(w\beta_e\frac{E}{N} + w\beta_s\frac{I_s}{N} + w\beta_a\frac{I_a}{N}\right) \\ w\beta_s\frac{S}{N} - \frac{S}{N}\left(w\beta_e\frac{E}{N} + w\beta_s\frac{I_s}{N} + w\beta_a\frac{I_a}{N}\right) \\ -\frac{S}{N}\left(w\beta_e\frac{E}{N} + w\beta_s\frac{I_s}{N} + w\beta_a\frac{I_a}{N}\right) \\ -\frac{S}{N}\left(w\beta_e\frac{E}{N} + w\beta_s\frac{I_s}{N} + w\beta_a\frac{I_a}{N}\right) \end{bmatrix}^T. \tag{303}$$

From Property 6.1, $\frac{E}{N}$, $\frac{I_s}{N}$, $\frac{I_a}{N}$ and $\frac{S}{N} \in [0,1]$, hence one choice for Γ_1, Γ_2 may be defined as

$$\Gamma_1 = \begin{bmatrix} 0 \\ -w_{\max}\beta_s - w_{\max}\beta_a \\ -w_{\max}\beta_e - w_{\max}\beta_s \\ -w_{\max}\beta_e - w_{\max}\beta_a \\ -w_{\max}\beta_e - w_{\max}\beta_s - w_{\max}\beta_a \\ -w_{\max}\beta_e - w_{\max}\beta_s - w_{\max}\beta_a \end{bmatrix}^T, \quad \Gamma_2 = \begin{bmatrix} w_{\max}\beta_e + w_{\max}\beta_s + w_{\max}\beta_a \\ w_{\max}\beta_e \\ w_{\max}\beta_a \\ w_{\max}\beta_s \\ 0 \\ 0 \end{bmatrix}^T \tag{304}$$

with $w_{\max} = \max_{t\in\mathbb{R}^+} w(t)$.

6.3.3 Abstract formulation

The error dynamics described by (297)-(298) can be rewritten as an abstract first order ordinary differential equation in the Hilbert space $\mathcal{H} = \mathbf{L}_2^6(\Omega)$ according to

$$\partial_t e(\mathbf{z},t) = (\mathcal{A} + L_D(\mathbf{z})\mathcal{C})e(\mathbf{z},t) + G\nu(\mathbf{z},t), \quad e(\mathbf{z},0) = e_0(\mathbf{z}) \in \mathcal{H} \tag{305}$$

where the operators $\mathcal{A} : D(\mathcal{A}) \to \mathcal{H}$, $\mathcal{C} : D(\mathcal{C}) \to \mathbb{R}^2$ are defined as

$$\begin{aligned} \mathcal{A}e(\mathbf{z},t) &= D(t)\Delta e(\mathbf{z},t) - \mathrm{K}e(\mathbf{z},t) \\ D(\mathcal{A}) &= \big\{ e(\mathbf{z},t) \in \mathcal{H} : e(\mathbf{z},t),\ \partial_{z_1} e(\mathbf{z},t),\ \partial_{z_2} e(\mathbf{z},t) \\ &\qquad \text{are absolutely continuous, } \Delta e(\mathbf{z},t) \in \mathcal{H} \\ &\qquad\qquad \text{and } \nabla e(\mathbf{z},t)\cdot\mathbf{n}|_{\partial\Omega} = 0\big\} \end{aligned} \tag{306}$$

$$\mathcal{C}e(\mathbf{z},t) = \begin{bmatrix} \langle 1_\Omega(\cdot), \mathbf{c}_1^T e(\cdot,t)\rangle \\ \langle 1_\Omega(\cdot), \mathbf{c}_2^T e(\cdot,t)\rangle \end{bmatrix}. \tag{307}$$

6.3.4 Lyapunov convergence analysis

The state observer design problem is addressed within a weighted Lyapunov framework, with the weight function as a degree of freedom in a similar fashion to that presented in Chapter 5. The analysis of the corresponding dissipation mechanism leads to a LMI convergence condition, which depends on the spatial coordinates, the observer gains, and the Lyapunov weight function. To this end, let us set the positive-definite weighted candidate Lyapunov functional $V : \mathbf{L}_2^6(\Omega) \to \mathbb{R}$ as

$$V(t) = \langle e(\cdot,t), \mathcal{P}e(\cdot,t)\rangle \tag{308}$$

where $\mathcal{P} : \mathbf{L}_2^6(\Omega) \to \mathbf{L}_2^6(\Omega)$ is a strictly positive operator defined by the polynomial matrix $W(\mathbf{z})$ as

$$(\mathcal{P}e)(\mathbf{z}) = W(\mathbf{z})e(\mathbf{z}). \tag{309}$$

for all $\mathbf{z} \in \Omega$. The following Lemma shows how two positive semi-definite matrices Q, $R > 0$ and some constant $\epsilon > 0$ can be used to define the polynomial matrix $W(\mathbf{z})$ such that the operator $\mathcal{P}$ is positive and therefore the functional V is a Lyapunov candidate for the observation error dynamics (305).

Lemma 6.1. *Given any positive semi-definite matrices Q, R_1, $R_2 \in \mathbb{S}^{3(m+1)(m+2)}$, and*

$$Z(\mathbf{z}) = Z_m(z_1, z_2) \otimes I_6 \tag{310}$$

where $\mathbf{z} \in \Omega = (0, l_1) \times (0, l_2) \subset \mathbb{R}^2$, $Z_m(\mathbf{z})$ is a vector of monomials with degree m or less and $\otimes$ is the Kronecker product. Let for all $z \in \Omega$

$$g_1(z_1) = z_1(l_1 - z_1), \quad g_2(z_2)(l_2 - z_2). \tag{311}$$

If for some $\epsilon > 0$

$$W(\mathbf{z}) = Z(\mathbf{z})^T(Q + g_1(z_1)R_1 + g_2(z_2)R_2)Z(\mathbf{z}) + \epsilon I_n, \tag{312}$$

then the functional $V : \mathbf{L}_2^6(\Omega) \to \mathbb{R}$, defined as

$$V(e(\cdot, t)) = \langle e(\cdot, t), \mathcal{P}e(\cdot, t)\rangle = \int_\Omega e(\mathbf{z}, t)^T W(\mathbf{z})e(\mathbf{z}, t)d\Omega, \tag{313}$$

is a strictly positive functional over $\mathbf{L}_2^6(\Omega)$, whenever $e(\cdot, t) \not\equiv 0$, and satisfies

$$V(e(\cdot, t)) = \langle e(\cdot, t), \mathcal{P}e(\cdot, t)\rangle \geq \epsilon\|e(\cdot, t)\|^2, \ \ \forall e(\cdot, t) \in \mathbf{L}_2^6(\Omega). \tag{314}$$

Theorem 6.2. *The error dynamics in* (305) *is (locally) exponentially stable with decay rate γ if there exist*

- *m, $q \in \mathbb{N}$, and real positive scalars ϵ, τ,*
- *block diagonal positive semidefinite matrices $Q = \text{diag}(Q_1, Q_2)$, $R_1 = \text{diag}(R_{11}, R_{12})$, $R_2 = \text{diag}(R_{21}, R_{22})$ with Q_1, Q_2, R_{11}, R_{12}, $R_{2,1}$, $R_{2,2} \in \mathbb{S}^{\frac{3}{2}(m+1)(m+2)}$ such that the polynomial matrix $W(\mathbf{z}) : \Omega \to \mathbb{R}^{6\times 6}$ satisfy* (312)*,*
- *the polynomial matrix $L_D(\mathbf{z}) : \Omega \to \mathbb{R}^{6\times 3}$*

and the following matrix inequality is feasible:

$$P(\mathbf{z}, t) - \tau \begin{bmatrix} M & 0 \\ 0 & 0 \end{bmatrix} < 0 \tag{315}$$

$\forall z \in \Omega$ *and* $t \in \mathbb{R}^+$ *where*

$$P(\mathbf{z}, t) = \begin{bmatrix} P_{11}(\mathbf{z}, t) & P_{12}(\mathbf{z}) & P_{13}(\mathbf{z}) \\ * & P_{22}(\mathbf{z}) & P_{23}(\mathbf{z}) \\ * & * & P_{33}(\mathbf{z}) \end{bmatrix} \tag{316}$$

with

$$\begin{aligned} P_{11}(\mathbf{z}, t) &= -\Delta W(\mathbf{z}) D(t) - W(\mathbf{z}) K - K^T W(\mathbf{z}) + 2\gamma W(\mathbf{z}) \\ P_{12}(\mathbf{z}) &= W(\mathbf{z}) G \\ P_{13}(\mathbf{z}) &= l_1 l_2 \left(\tilde{L}_D(\mathbf{z}) C_m + C_m^T \tilde{L}_D^T(\mathbf{z}) \right) \\ &\quad + \frac{2\sqrt{l_1^2 + l_2^2}\, d(t) \epsilon}{\pi} I \\ P_{22}(\mathbf{z}) &= 0 \\ P_{23}(\mathbf{z}) &= 0 \\ P_{33}(\mathbf{z}) &= -\frac{2\sqrt{l_1^2 + l_2^2}\, d(t) \epsilon}{\pi} I \end{aligned} \tag{317}$$

with

$$\tilde{L}_D(\mathbf{z}) = W(\mathbf{z}) L_D(\mathbf{z}) \tag{318}$$

Proof. Consider the linear dissipation expression of the Lyapunov function

$$\begin{aligned} \dot{V}(t) + 2\gamma V(t) = 2\langle e(\cdot, t), \mathcal{P}\mathcal{A} e(\cdot, t) \rangle + 2\langle e(\cdot, t), \mathcal{P} G \nu(\cdot, t) \rangle + 2\langle e(\cdot, t), \mathcal{P} L_D(\mathbf{z}) \mathcal{C} e(\cdot, t) \rangle \\ + 2\gamma \langle e(\cdot, t), \mathcal{P} e(\cdot, t) \rangle \end{aligned} \tag{319}$$

then, the substitution of (297) into (319) yields

$$\begin{aligned} &\dot{V}(t) + 2\gamma V(t) = \\ &\quad 2\int_\Omega e^T(\mathbf{z}, t) W(\mathbf{z}) D(t) \Delta e(\mathbf{z}, t) d\Omega - 2\int_\Omega e^T(\mathbf{z}, t) W(\mathbf{z}) \left(K - \gamma I\right) e(\mathbf{z}, t) d\Omega \\ &\qquad + 2\int_\Omega e^T(\mathbf{z}, t) W(\mathbf{z}) G \nu(\mathbf{z}, t) d\Omega \\ &\qquad + 2\int_\Omega e^T(\mathbf{z}, t) W(\mathbf{z}) L_D(\mathbf{z}) C_m \left(\int_\Omega e(\mathbf{z}, t) d\Omega \right) d\Omega. \end{aligned} \tag{320}$$

Applying the first mean value theorem for integration, there exists a scalar $\mathbf{z}_m^t \in \Omega$ such that

$$e(\mathbf{z}_m^t, t) = \frac{1}{l_1 l_2} \int_\Omega e(\mathbf{z}, t) d\Omega, \quad \forall t \in \mathbb{R}^+. \tag{321}$$

Regarding the definition (318) and applying the integration by parts into (320), we obtain

$$\begin{aligned}\dot{V}(t) + 2\gamma V(t) = & \\ & \int_\Omega e^T(\mathbf{z},t)\Delta W(\mathbf{z})D(t)e(\mathbf{z},t)d\Omega \\ & -2\int_\Omega (\mathrm{vec}\nabla e(\mathbf{z},t))^T \left[I_2 \otimes W(\mathbf{z})D(t)\right](\mathrm{vec}\nabla e(\mathbf{z},t))\, d\Omega \\ & -\int_\Omega e^T(\mathbf{z},t)\left(KW(\mathbf{z}) + W(\mathbf{z})K^T - 2\gamma W(\mathbf{z})\right)e(\mathbf{z},t)d\Omega \\ & +2\int_\Omega e^T(\mathbf{z},t)W(\mathbf{z})G\nu(\mathbf{z},t)d\Omega + 2l_1l_2\int_\Omega e^T(\mathbf{z},t)\tilde{L}_D(\mathbf{z})C_m e(\mathbf{z}_m^t,t)d\Omega.\end{aligned} \tag{322}$$

Notice by the virtue of Poincaire inequality that the following holds

$$\begin{aligned}-2\int_\Omega (\mathrm{vec}\nabla e(\mathbf{z},t))^T \left[I_2 \otimes W(\mathbf{z})D(t)\right](\mathrm{vec}\nabla e(\mathbf{z},t))\, d\Omega \leq & \\ -\frac{2\sqrt{l_1^2+l_2^2}d(t)\epsilon}{\pi}\int_\Omega \left(e(\mathbf{z},t)-e(\mathbf{z}_m^t,t)\right)^T\left(e(\mathbf{z},t)-e(\mathbf{z}_m^t,t)\right)d\Omega.\end{aligned} \tag{323}$$

Hence, substituting (323) into (322) leads to

$$\begin{aligned}\dot{V}(t) + 2\gamma V(t) \leq & \\ \int_\Omega e^T(\mathbf{z},t)\left[-\Delta W(\mathbf{z})D(t) - KW(\mathbf{z}) - W(\mathbf{z})K^T + 2\gamma W(\mathbf{z}) - \frac{2\sqrt{l_1^2+l_2^2}d(t)\epsilon}{\pi}I\right]e(\mathbf{z},t)d\Omega & \\ +2\int_\Omega e^T(\mathbf{z},t)W(\mathbf{z})G\nu(\mathbf{z},t)d\Omega & \\ \int_\Omega e^T(\mathbf{z},t)\left(2l_1l_2\tilde{L}_D(\mathbf{z})C_m + \frac{4\sqrt{l_1^2+l_2^2}d(t)\epsilon}{\pi}I\right)e(\mathbf{z}_m^t,t)d\Omega & \\ -\frac{2\sqrt{l_1^2+l_2^2}d(t)\epsilon}{\pi}\int_\Omega e^T(\mathbf{z}_m^t,t)e(\mathbf{z}_m^t,t)d\Omega. &\end{aligned} \tag{324}$$

We can rewrite (324) as

$$\dot{V}(t) + 2\gamma V(t) \leq \int_\Omega \mathbf{e}^T(\mathbf{z},t)P(\mathbf{z},t)\,\mathbf{e}\,(\mathbf{z},t)d\Omega \tag{325}$$

where $\mathbf{e}(\mathbf{z},t) = [e(\mathbf{z},t)\ \ \nu(\mathbf{z},t)\ \ e(\mathbf{z}_m^t,t)]^T$. Therefore, in order to ensure the negativity of the right side of (325), it suffices that

$$P(\mathbf{z},t) < 0,\ \forall z \in \Omega \text{ and } t \in \mathbb{R}^+. \tag{326}$$

Applying the *S*-procedure to (326) and (302), we obtain

$$P(\mathbf{z},t)-\tau\begin{bmatrix}M & 0\\ 0 & 0\end{bmatrix}<0,\quad \forall z\in\Omega \text{ and } t\in\mathbb{R}^{+}. \tag{327}$$

Then (327) implies that

$$V(t)\leq \mathrm{e}^{-2\gamma t}V(0) \tag{328}$$

and from Chapter 5, it follows that

$$\|e(\mathbf{z},t)\|\leq M_e\|e_0(\mathbf{z})\|\mathrm{e}^{-\gamma t}. \tag{329}$$

□

6.4 COVID SPREAD MONITORING

In this section we provide some numerical simulations obtained from the formulation scheme presented in Section 6.3. Firstly, we show the feasibility provided through the solution of the LMIs in (315) for different selections of lower bound decay rates γ. Then, the convergence features of the proposed observer are depicted through the numerical simulation of the observer system. We consider the case study regarding the state estimation of the compartmental variables in a host population defined by the 2D spatial domain $\Omega = (0,100)\times(0,200)$ in which the average commuting defines $d_0 = \frac{25^2}{16}$ and the values corresponding to the model parameters are listed in Table. 6

Table 5 – Parameter values.

Parameter	**Value**	**Definition**
$w_0\beta_e$	0.122920	Transmission rate from S to E from contact with E
$w_0\beta_s$	0.384542	Transmission rate from S to E from contact with I_s
$w_0\beta_a$	0.445237	Transmission rate from S to E from contact with I_a
ρ	0.043198	Lockdown decay
δ_I	$\frac{1}{5}$	Latency rate
p_s	0.503939	Probability of being symptomatic
$1-p_s$	0.496061	Probability of being asymptomatic
γ_r	$\frac{1}{7}$	recovery rates
μ_d	0.010381	Death rate

The population distribution is assumed to be defined by

$$\begin{aligned} S_0(\mathbf{z}) &= 2\times 10^4 \mathrm{e}^{-\frac{(z_1-100)^2+(z_2-125)^2}{500}} + 1.5\times 10^4 \mathrm{e}^{-\frac{(z_1-100)^2+(z_2-55)^2}{500}} \\ &\quad + 8\times 10^3 \mathrm{e}^{-\frac{(z_1-150)^2+(z_2-100)^2}{300}} + 9\times 10^3 \mathrm{e}^{-\frac{(z_1-75)^2+(z_2-175)^2}{300}} \\ E_0(\mathbf{z}) &= 10\mathrm{e}^{-\frac{(z_1-100)^2+(z_2-125)^2}{200}} \\ I_{a0}(\mathbf{z}) &= 0, \quad I_{s0}(\mathbf{z}) = 0, \quad U_0(\mathbf{z}) = 0, \quad R_0(\mathbf{z}) = 0 \end{aligned} \tag{330}$$

which is depicted in Figure 31, yielding a total host population of

$$\overline{N}_0 = \int_\Omega \left(S_0(\mathbf{z}) + E_0(\mathbf{z})\right) d\Omega = 20896065 \text{ persons.} \tag{331}$$

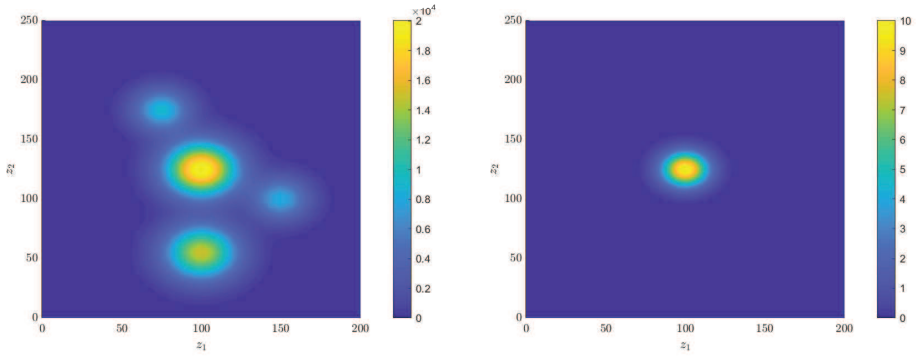

(a) $S_0(\mathbf{z})$ (b) $E_0(\mathbf{z})$

Figure 31 – Initial conditions of the compartmental variables defining the population distribution

Figure 31 depicts the initial simulation scenario in which the population distribution corresponds to four contiguous cities and where that located in the center is the largest and where exposed people to the virus appears initially.

To obtain the output injection gain $L_D(\mathbf{z}) : \Omega \to \mathbb{R}^{6\times 2}$ through the application of the sufficient conditions presented in Theorem 6.2, we solve the LMI in (315) only at the vertices of the polytope defined by the bounded time variant parameter $d(t)$ defined in (279) (OLIVEIRA; PERES, 2005). Thus, its solution for different values of m and q along with bisection search provides $\gamma_{\max}$ for each case according to Table 6.

Table 6 – $\gamma_{\max}$ of the proposed approach for different combinations of m and q.

(m, q)	$\gamma_{\max}$
$(4, 2)$	0.14
$(5, 3)$	0.26
$(7, 4)$	0.35

For $(m, q) = (7, 4)$, the observer and system responses are generated via numerical simulation with system initial conditions in (330) and those corresponding to the observer are set to be zero. The simulation scenario considers $t_{\text{bol}} = 10$ days, $t_{\text{eol}} = 25$ days which specifies the degree of danger of the epidemic through the time variant definitions of $w(t)$ and $d(t)$ in (278) and (279) respectively.

Figure 32 shows some snapshots of the evolution of the actual distribution (on the left) with its respective estimated distribution (on the right) of the I_a asymptomatic compartmental variable considering the proposed observer in three different time instants. As depicted in the corresponding figures, the uniform wave front propagates from the center to the corners (where the disease starts) with the infected asymptomatic individuals rapidly increasing when $t \leq t_{bol}$ which is then attenuated for $t \geq t_{eol}$. This is logical, because $w(t)$ and $d(t)$ specify the degree of danger of the epidemic according to this modeling. It may also be seen that the estimation distributions of the compartmental state variables converge to the actual profiles for $t = 10$ days.

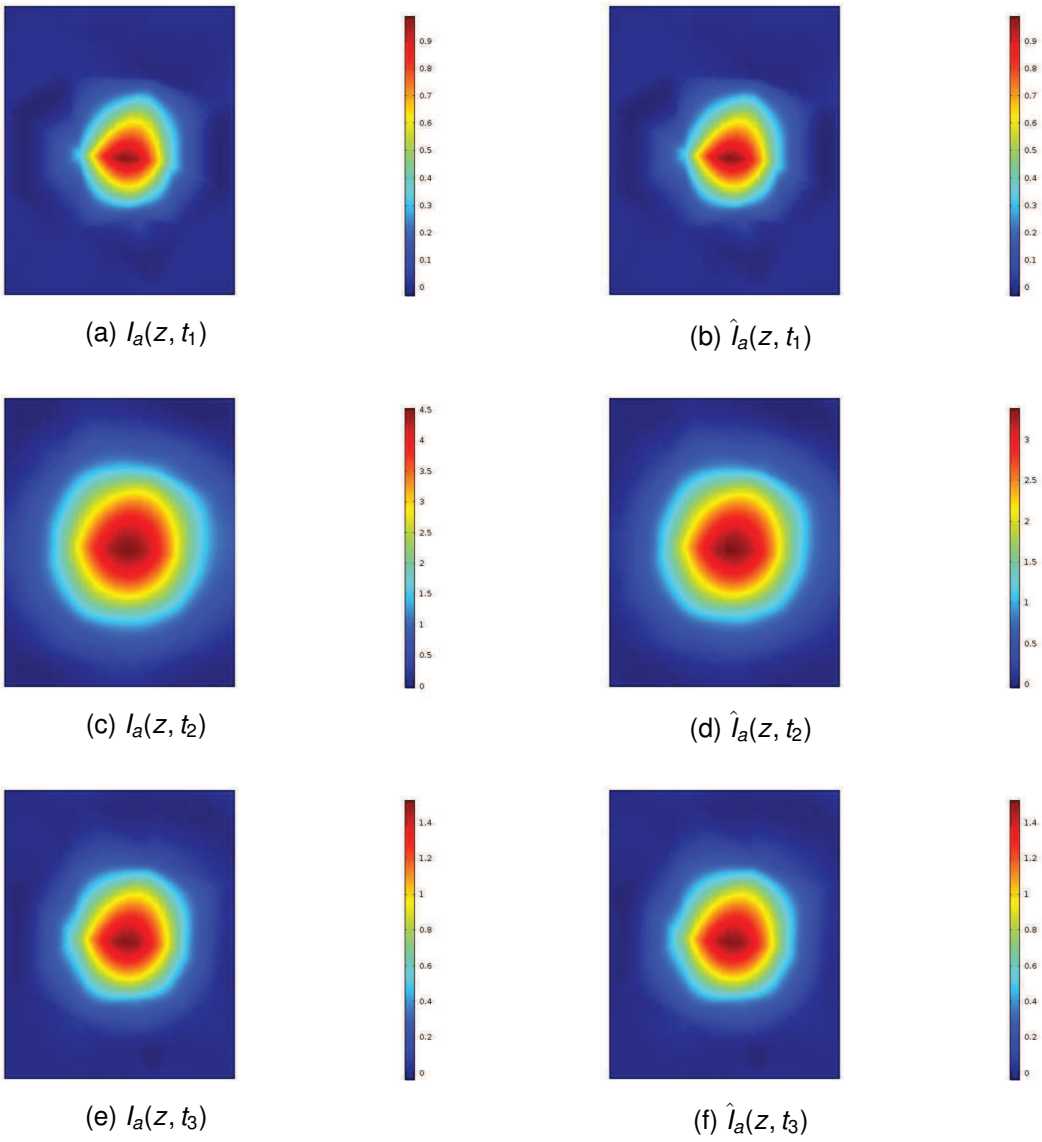

(a) $I_a(z, t_1)$ (b) $\hat{I}_a(z, t_1)$

(c) $I_a(z, t_2)$ (d) $\hat{I}_a(z, t_2)$

(e) $I_a(z, t_3)$ (f) $\hat{I}_a(z, t_3)$

Figure 32 – Spatial distribution of $I_a(\mathrm{z}, t)$ and $\hat{I}_a(\mathrm{z}, t)$ at time instants $t_1 = 10$, $t_2 = 15$, $t_3 = 30$ days.

Figure 33 shows the profile evolution of the absolute values related to all compartmental variables for the host population.

Then, Figure 34 shows the evolution of the estimation error norm. Although the initial estimation profiles were all set to be zero, the estimation error norm converges quickly, and hence, provides very satisfactory estimates. In the same figure, the result corresponding to the inclusion of measurement white noise ($V = 2.7$) in the $\bar{I}_s(t)$ variable is depicted. It should be observed that the procedure outlined here guarantees that the state estimate robustly converges to the true state.

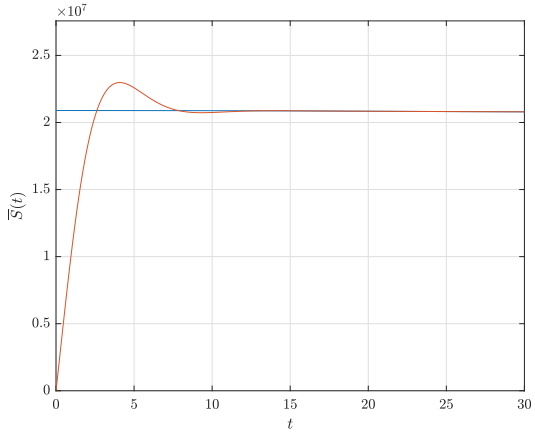

(a) $\overline{S}(t)$ and $\overline{\hat{S}}(t)$

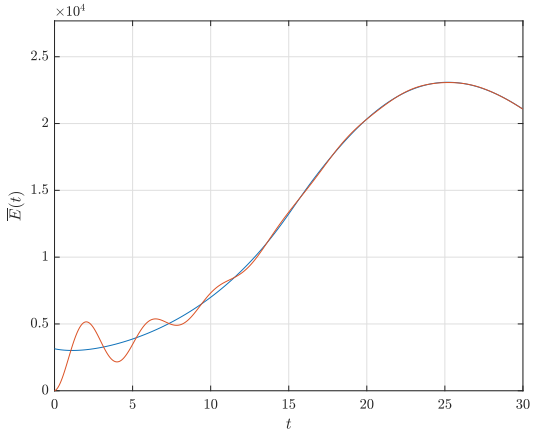

(b) $\overline{E}(t)$ and $\overline{\hat{E}}(t)$

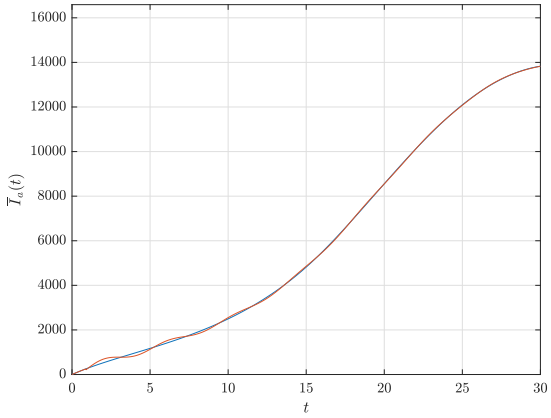

(c) $\overline{I}_a(t)$ and $\overline{\hat{I}}_a(t)$

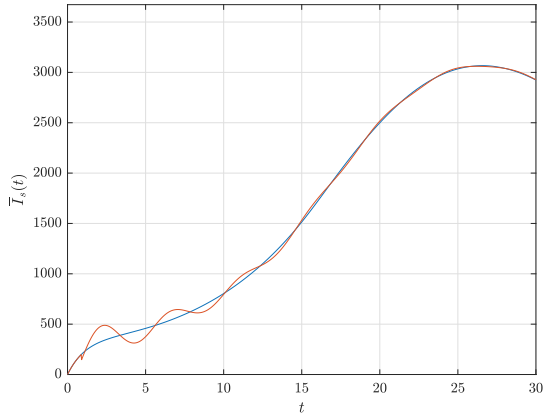

(d) $\overline{I}_s(t)$ and $\overline{\hat{I}}_s(t)$

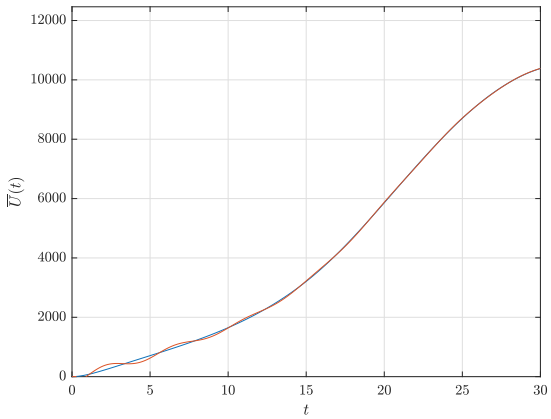

(e) $\overline{U}(t)$ and $\overline{\hat{U}}(t)$

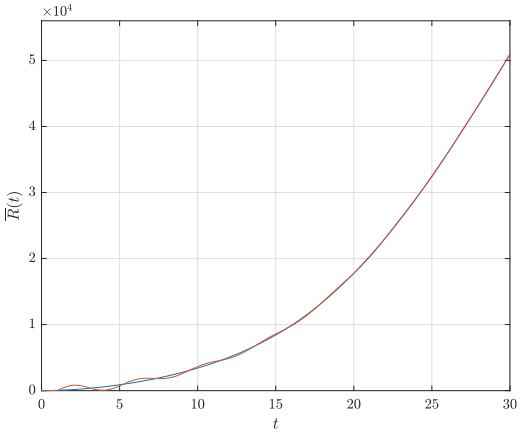

(f) $\overline{R}(t)$ and $\overline{\hat{R}}(t)$

Figure 33 – Time evolution of the global number of variables of the generalized epidemiological SEIR model of COVID-19.

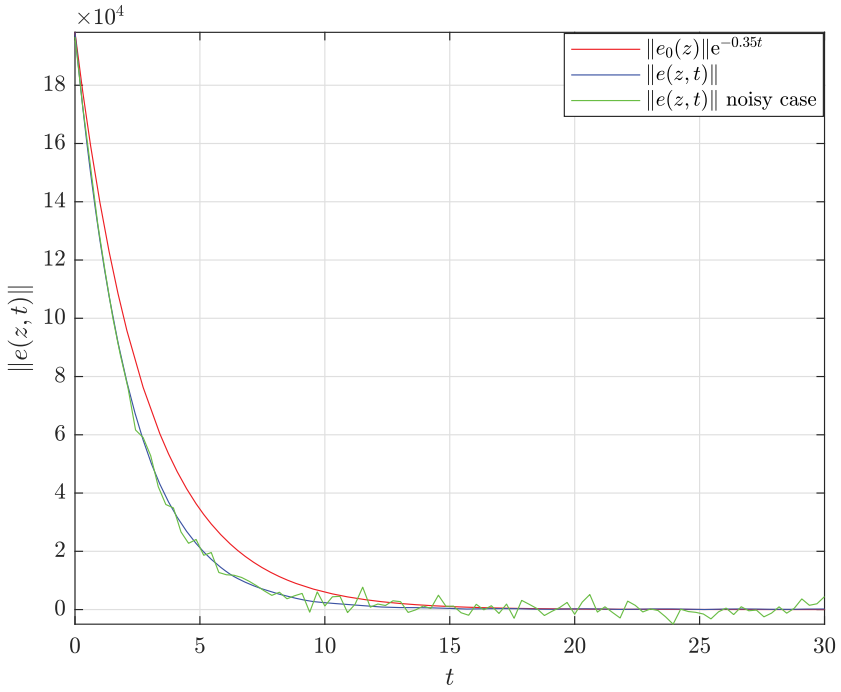

Figure 34 – Time evolution of the estimation error norm $\|e(z,t)\|$.

One of the main virtues of the SEIR distributed model based state estimation is to attain the monitoring of the pandemic throughout the host region which plays a fundamental role as warning system of the current epidemiological situation in each sub-population in contrast with state estimation techniques based on lumped SIR models such as (MARTÍNEZ-GUERRA; FLORES-FLORES, 2021). For instance, the evolution of the partial number of infected people $\bar{I}(t) = \bar{I}_a(t) + \bar{I}_s(t)$ and under treatment $\overline{U}(t)$ population along with their estimated profiles related to the sub-population centered at $(100, 55)$ are shown in Figure 35 considering the measurement of total under treatment and deceased population. Notice that these local estimates can be utilized to alert the local health infrastructure to take further actions.

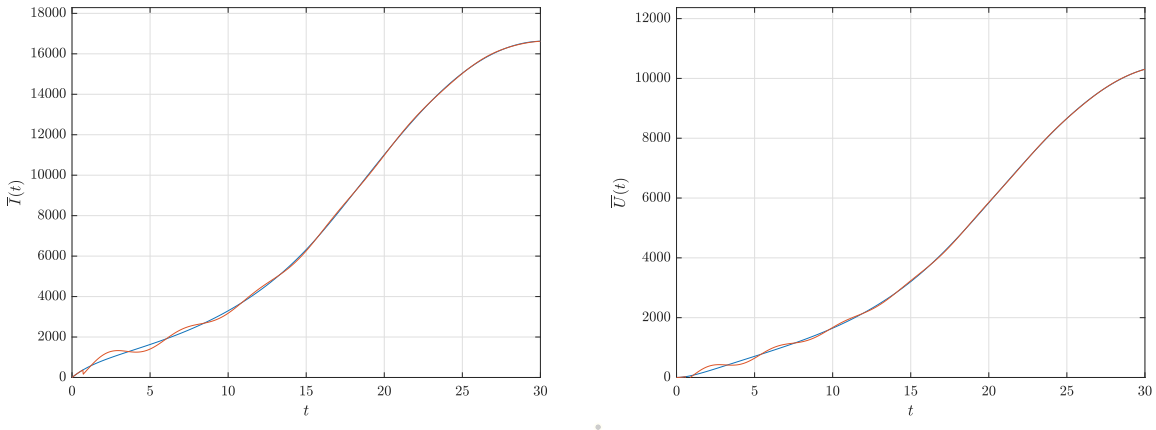

(a) $\overline{I}_a(t)$ and $\hat{\overline{I}}_a(t)$ (b) $\overline{U}(t)$ and $\hat{\overline{U}}(t)$

Figure 35 – Time evolution of the partial number of infected and under treatment people in the sub-population distribution centered at $(100, 55)$.

6.5 CONCLUDING REMARKS

In this chapter, a nonlinear Luenberger-like state observer was designed to estimate the compartmental variables of the generalized epidemiological SEIR model of COVID-19 spread proposed in (MAMMERI, 2020). The Lyapunov method has been applied to derive a set of LMI based conditions to ensure the local stability of the error dynamics which has been modeled as a Lure type system with a multivariable sector condition, thus the appropriate choice of the observer gains results from a SDP problem solution. The proposed technique is an attempt to set a non-conservative LMIs conditions through a polynomial parametrization of the decision variables where the integration by parts as well as the local checks, which is provided by embedding results on bounded domains as the Poincare inequality and the S-procedure for local stability analysis based on sector condition play a crucial role on this purpose. In this framework, the presence of bounded time variant parameters and incomplete measurement feedback may be tackled through the polytope analysis of the proposed LMIs which guarantees a robust convergence. Numerical experiments are presented to illustrate the method efficiency.

7 CONCLUSIONS

This thesis has addressed the state estimation problem for a certain class of transport-reaction systems described by semilinear PDE systems. Both early and late lumping approaches have been used to explore different design strategies. The core idea of the methodologies explored in this work has been to find sufficient conditions for ensuring the local exponential stability of the state estimation error dynamics under the assumption that the nonlinearity corresponding to the rate function is continuously differentiable and hence, locally Lipschitz. Particularly, this thesis is an attempt to provide a tractable framework for multi-state process having in domain distributed measurements. The proposed state estimation techniques significantly reduces the stability analysis complexity of the error dynamics by using local algebraic sector conditions to represent the error dynamics as a Lure system. It should be noticed that the addressed methodologies concerns a large class of semilinear PDE systems. Hereinafter a summary of the Thesis along with some comments and hints about the potential future research directions for the contribution of each Chapter are discussed:

- In Chapter 3 the orthogonal collocation method has been applied to derive a reduced-order finite dimensional approximate model by using lagrange interpolation and the roots of Jacobi polynomials as collocation nodes which also allowed us to apply an optimal location criteria of them in order to reduce the approximation error model. Then, an LMI based condition was proposed to design a nonlinear Luenberger-type observer. In addition, an offline sensor placement algorithm was also proposed to optimally allocate the measurement sensors in order to improve the estimation error convergence. An interesting topic for future generalization of the present results is to extend them for more computationally tractable reduction methods as the POD-Galerkin based method in which the derivation of the sector condition parameters related to the finite dimensional model deserves a more numerical attention due to the use of integral quadratures in the approximate model derivation.

- In Chapter 4 the state estimator design has been carried out by making reference to the spectral decomposition of the infinite dimensional description on Hilbert state space $\mathcal{H} = \mathbf{L}_2^{n_x}(0,1)$. The modal injection gain assignment that has been widely used for the stabilization of linear PDE systems allowed us to reduced the state estimation problem into the stabilization of a ODE system regarding the appropriate allocation of the slow modes of the dynamical system according to the local Lipschitz constants or the lower and upper bounds of the Jacobian matrix related to the nonlinear reaction function. Involving spatially dependent diffusion and advection coefficients into the proposed synthesis and its extension

to broader classes of PDE systems (e.g., high dimensional PDEs and PDEs with coupling of the advective an diffusive terms) are among the most interesting lines of future investigations.

- In Chapter 5 the Lyapunov method has been applied to derive a set of LMI based conditions aiming at designing a nonlinear Luenberger-type observer. The proposed methodology is an attempt to set a non-conservative approach through a polynomial parametrization of the decision variables. The use of results on bounded domains as the Wirtinger's inequality and the S-procedure for local stability analysis based on sector condition are also important to reduce the conservatism of the proposed approach. Our scope was to make these steps computationally tractable by formulating a semidefinite programming problem (SDP). The generalization of the proposed approach through the use of Lyapunov functionals of the form

$$V(e(z,t)) = \int_0^1 e^T(z,t)W_1(z)e(z,t) + \int_0^1 e^T(z,t)\int_0^1 W_2(z,y)e(y,t)dydz \quad (332)$$

addressed in (MEYER; PEET, Matthew M, 2016) in order to improve the stability analysis of PDE systems by adding more degrees of freedom (and hence to diminish the conservatism) in the Lyapunov functional is one of the the most interesting lines of future investigations.

The corresponding above mentioned techniques have been drawn in the light of a motivated exploitation of well recognized and widely used approaches in the literature of PDE systems theory. Thus, the state estimation problem was addressed in a unifying framework by combining: (i) model reduction techniques; (ii) semigroup theory; (iii) Lyapunov theory; and (iv) semidefinite and sum of squares programming.

In view of previous studies recorded in literature, the observer designed for these case studies represent important innovations, in the understanding of

- systematic design through the utilization of semidefinite programming tools for computing the parameters of the state observers;
- convergence behavior improvement through the sensor placement and the initial conditions optimization; and
- simple implementation.

These design features have been possible due to a fruitful combination of the above mentioned mathematical, system and computing tools, as well as analysis and design methods.

Finally in Chapter 6, some implications of the obtained design method in Chapter 5 in the perspective of bidimensional transport-reaction systems with application to the

estimation of the compartmental variables of the COVID-19 spread have been drawn yielding a set of LMI based conditions for the design of an exponential observer with a polynomial parameterized matrix as output injection.

Numerical simulations show the applicability of the suggested approaches to the considered classes of PDE systems, which were performed by means of Matlab and COMSOL software packages.

REFERENCES

A. VANDE WOUWER; POINT, Nicolas; PORTEMAN, Stephanie; REMY, Marcel. An approach to the selection of optimal sensor locations in distributed parameter systems. **Journal of process control**, Elsevier, v. 10, n. 4, p. 291–300, 2000.

A. VANDE WOUWER; ZEITZ, M. State estimation in distributed parameter systems. **CONTROL SYSTEMS, ROBOTICS AND AUTOMATION–Volume XIV: Nonlinear, Distributed, and Time Delay Systems-III**, EOLSS Publications, p. 92, 2009.

AÇIKMEŞE, Behçet; CORLESS, Martin. Observers for systems with nonlinearities satisfying incremental quadratic constraints. **Automatica**, Elsevier, v. 47, n. 7, p. 1339–1348, 2011.

ADAMS, RA. Sobolev Spaces, Academic Press. Inc, 1978.

ALHUMAIZI, Khalid. A moving collocation method for the solution of the transient convection–diffusion-reaction problems. **Journal of computational and applied mathematics**, Elsevier, v. 193, n. 2, p. 484–496, 2006.

ALIZADEH, Farid; HAEBERLY, Jean-Pierre A; OVERTON, Michael L. Primal-dual interior-point methods for semidefinite programming: convergence rates, stability and numerical results. **SIAM Journal on Optimization**, SIAM, v. 8, n. 3, p. 746–768, 1998.

ALONSO, Antonio A; KEVREKIDIS, Ioannis G; BANGA, Julio R; FROUZAKIS, Christos E. Optimal sensor location and reduced order observer design for distributed process systems. **Computers & chemical engineering**, Elsevier, v. 28, n. 1-2, p. 27–35, 2004.

ARCAK, Murat; KOKOTOVIĆ, Petar. Nonlinear observers: a circle criterion design and robustness analysis. **Automatica**, Elsevier, v. 37, n. 12, p. 1923–1930, 2001.

ARCEDE, Jayrold P; CAGA-ANAN, Randy L; MENTUDA, Cheryl Q; MAMMERI, Youcef. Accounting for Symptomatic and Asymptomatic in a SEIR-type model of COVID-19. **arXiv preprint arXiv:2004.01805**, 2020.

BACCOLI, Antonello; PISANO, Alessandro. Anticollocated backstepping observer design for a class of coupled reaction-diffusion PDEs. **Journal of Control Science and Engineering**, Hindawi Publishing Corp., v. 2015, p. 53, 2015.

BANKS, H Thomas; KUNISCH, Karl. **Estimation techniques for distributed parameter systems**. [S.l.]: Springer Science & Business Media, 2012.

BARTECKI, Krzysztof. A general transfer function representation for a class of hyperbolic distributed parameter systems. **International Journal of Applied Mathematics and Computer Science**, v. 23, n. 2, 2013.

BOUBAKER, Olfa; BABARY, Jean-Pierre; KSOURI, Mekki. Variable structure estimation and control of nonlinear distributed parameter bioreactors. In: IEEE. SMC'98 Conference Proceedings. 1998 IEEE International Conference on Systems, Man, and Cybernetics (Cat. No. 98CH36218). [S.l.: s.n.], 1998. P. 3770–3774.

BOYD, John P. **Chebyshev and Fourier spectral methods**. [S.l.]: Courier Corporation, 2001.

BOYD, Stephen; EL GHAOUI, Laurent; FERON, Eric; BALAKRISHNAN, Venkataramanan. **Linear matrix inequalities in system and control theory**. [S.l.]: SIAM, 1994.

BRENNER, Susanne C; SCOTT, L Ridgway; SCOTT, L Ridgway. **The mathematical theory of finite element methods**. [S.l.]: Springer, 2008. v. 3.

CASTILLO, Felipe; WITRANT, Emmanuel; PRIEUR, Christophe; DUGARD, Luc. Boundary observers for linear and quasi-linear hyperbolic systems with application to flow control. **Automatica**, Elsevier, v. 49, n. 11, p. 3180–3188, 2013.

CHAUDHURI, SYAMA P. Distributed optimal control in a nuclear reactor. **International Journal of Control**, Taylor & Francis, v. 16, n. 5, p. 927–937, 1972.

CHEN, Nanshan et al. Epidemiological and clinical characteristics of 99 cases of 2019 novel coronavirus pneumonia in Wuhan, China: a descriptive study. **The lancet**, Elsevier, v. 395, n. 10223, p. 507–513, 2020.

CHEN, Wanyi; TU, Fengsheng. Modal observability and detectability for infinite dimensional systems. **Applied Mathematics Letters**, Elsevier, v. 8, n. 2, p. 61–65, 1995.

CHEN, Yun; HE, Jia; MU, Yang; HUO, Ying-Chao; ZHANG, Ze; KOTSOPOULOS, Thomas A; ZENG, Raymond J. Mathematical modeling of upflow anaerobic sludge blanket (UASB) reactors: Simultaneous accounting for hydrodynamics and bio-dynamics. **Chemical Engineering Science**, Elsevier, v. 137, p. 677–684, 2015.

CURTAIN, Ruth; ZWART, Hans. **Introduction to infinite-dimensional systems theory: a state-space approach**. [S.l.]: Springer Nature, 2020. v. 71.

DANCKWERTS, Peter V. Continuous flow systems: distribution of residence times. **Chemical engineering science**, Elsevier, v. 2, n. 1, p. 1–13, 1953.

DAVIS, Philip J. **Interpolation and approximation**. [S.l.]: Courier Corporation, 1975.

DELATTRE, Cedric; DOCHAIN, Denis; WINKIN, Joseph. Observability analysis of nonlinear tubular (bio) reactor models: a case study. **Journal of Process Control**, Elsevier, v. 14, n. 6, p. 661–669, 2004.

DELATTRE, Cédric; DOCHAIN, Denis; WINKIN, Joseph. Sturm-Liouville systems are Riesz-spectral systems. **International Journal of Applied Mathematics and Computer Science**, v. 13, p. 481–484, 2003.

DEMETRIOU, Michael A. Robust sensor location optimization in distributed parameter systems using functional observers. In: IEEE. PROCEEDINGS of the 44th IEEE Conference on Decision and Control. [S.l.: s.n.], 2005. P. 7187–7192.

DOCHAIN, D. **Contribution to the analysis and control of distributed parameter systems: with application to (bio) chemical processes and robotics**. 1994. PhD thesis – CIACO.

DOESBURG, Hans van; DE JONG, WA. Transient behaviour of an adiabatic fixed-bed methanator—I: experiments with binary feeds of CO or CO2 in hydrogen. **Chemical Engineering Science**, Elsevier, v. 31, n. 1, p. 45–51, 1976.

EWING, RE; PILANT, MS; WADE, JG; WATSON, AT. Parameter estimation in petroleum and groundwater modeling. **IEEE Computational Science and Engineering**, Citeseer, v. 1, n. 3, p. 19–31, 1994.

FERRAGUT, Luis; ASENSIO, M Isabel; CASCÓN, José Manuel; PRIETO, D; RAMÍREZ, Joaquín. An efficient algorithm for solving a multi-layer convection–diffusion problem applied to air pollution problems. **Advances in Engineering Software**, Elsevier, v. 65, p. 191–199, 2013.

FEYO DE AZEVEDO, S; ROMERO-OGAWA, MA; WARDLE, AP. Modelling of tubular fixed-bed catalytic reactors: a brief review. **Chemical engineering research & design**, v. 68, n. 6, p. 483–502, 1990.

FINLAYSON, Bruce A. **Nonlinear analysis in chemical engineering**. [S.l.]: Bruce Alan Finlayson, 2003.

FINLAYSON, Bruce A. **The method of weighted residuals and variational principles**. [S.l.]: SIAM, 2013. v. 73.

FRIDMAN, Emilia. Observers and initial state recovering for a class of hyperbolic systems via Lyapunov method. **Automatica**, Elsevier, v. 49, n. 7, p. 2250–2260, 2013a.

FRIDMAN, Emilia. Observers and initial state recovering for a wave equation: an LMI approach. **IFAC Proceedings Volumes**, Elsevier, v. 46, n. 3, p. 337–342, 2013b.

FRIDMAN, Emilia; ORLOV, Yury. An LMI approach to H_∞ boundary control of semilinear parabolic and hyperbolic systems. **Automatica**, Elsevier, v. 45, n. 9, p. 2060–2066, 2009.

FRIEDLY, John C. **Dynamic behavior of processes**. [S.l.]: Prentice-Hall, 1972.

FUJII, Nobuo. Feedback stabilization of distributed parameter systems by a functional observer. **SIAM Journal on Control and Optimization**, SIAM, v. 18, n. 2, p. 108–120, 1980.

GAHLAWAT, Aditya; PEET, Matthew M. A convex sum-of-squares approach to analysis, state feedback and output feedback control of parabolic PDEs. **IEEE Transactions on Automatic Control**, IEEE, v. 62, n. 4, p. 1636–1651, 2016a.

GAHLAWAT, Aditya; PEET, Matthew M. Optimal state feedback boundary control of parabolic PDEs using SOS polynomials. In: IEEE. 2016 American Control Conference (ACC). [S.l.: s.n.], 2016b. P. 4350–4355.

GAY, David Henry. **Identification and control of distributed parameter systems by means of the singular value decomposition**. 1989. PhD thesis – The University of Wisconsin-Madison.

GOTTLIEB, David; ORSZAG, Steven A. **Numerical analysis of spectral methods: theory and applications**. [S.l.]: SIAM, 1977.

GUNDER, T; SEHLINGER, A; SKODA, R; MÖNNIGMANN, M. Sensor placement for reduced-order model-based observers in hydraulic fluid machinery. **IFAC-PapersOnLine**, Elsevier, v. 51, n. 13, p. 414–419, 2018.

HARDY, GH; LITTLEWOOD, JE; PÓLYA, G. **Inequalities**. [S.l.]: Cambridge: Cambridge University Press, 1970.

HUANG, Wenzhang; HAN, Maoan; LIU, Kaiyu. Dynamics of an SIS reaction-diffusion epidemic model for disease transmission. **Mathematical Biosciences & Engineering**, American Institute of Mathematical Sciences, v. 7, n. 1, p. 51, 2010.

JACOB, Birgit; PARTINGTON, Jonathan R. Admissibility of control and observation operators for semigroups: a survey. **Current trends in operator theory and its applications**, Springer, p. 199–221, 2004.

JADACHOWSKI, Lukas; MEURER, Thomas; KUGI, Andreas. Backstepping observers for linear PDEs on higher-dimensional spatial domains. **Automatica**, Elsevier, v. 51, p. 85–97, 2015.

JADACHOWSKI, Lukas; MEURER, Thomas; KUGI, Andreas. State estimation for parabolic PDEs with varying parameters on 3-dimensional spatial domains. **IFAC Proceedings Volumes**, Elsevier, v. 44, n. 1, p. 13338–13343, 2011.

KAMRAN, Niloofar Nasiri. **Sliding Mode Observers for Distributed Parameter Systems: Theory and Applications**. 2016. PhD thesis – Embry-Riddle Aeronautical University.

KATZ, Rami; FRIDMAN, Emilia. Constructive method for finite-dimensional observer-based control of 1-D parabolic PDEs. **Automatica**, Elsevier, v. 122, p. 109285, 2020.

KHALIL, Hassan K. **Nonlinear Systems (3rd edition)**. [S.l.]: Prentice Hall, 2002.

KIRCHER, Kevin J; ZHANG, K Max. Testing building controls with the BLDG toolbox. In: IEEE. 2016 American Control Conference (ACC). [S.l.: s.n.], 2016. P. 1472–1477.

KOTSUR, Maxim. Optimal control of distributed parameter systems with application to transient thermoelectric cooling. **Advances in Electrical and Computer Engineering**, Stefan cel Mare University of Suceava, v. 15, n. 2, p. 117–123, 2015.

LANGMUIR, Irving. THE VELOCITY OF REACTIONS IN GASES MOVING THROUGH HEATED VESSELS AND THE EFFECT OF CONVECTION AND DIFFUSION. **Journal of the American Chemical Society**, ACS Publications, v. 30, n. 11, p. 1742–1754, 1908.

LAO, Liangfeng; ELLIS, Matthew; ARMAOU, Antonios; CHRISTOFIDES, Panagiotis D. Economic model predictive control of parabolic PDE systems: Handling state constraints by adaptive proper orthogonal decomposition. In: IEEE. 53RD IEEE Conference on Decision and Control. [S.l.: s.n.], 2014. P. 2758–2763.

LAUER, Stephen A; GRANTZ, Kyra H; BI, Qifang; JONES, Forrest K; ZHENG, Qulu; MEREDITH, Hannah R; AZMAN, Andrew S; REICH, Nicholas G; LESSLER, Justin. The incubation period of coronavirus disease 2019 (COVID-19) from publicly reported confirmed cases: estimation and application. **Annals of internal medicine**, American College of Physicians, v. 172, n. 9, p. 577–582, 2020.

LE FLOCH, Caroline; KARA, Emre Can; MOURA, Scott. PDE modeling and control of electric vehicle fleets for ancillary services: A discrete charging case. **IEEE Transactions on Smart Grid**, IEEE, v. 9, n. 2, p. 573–581, 2016.

LEFÈVRE, L; DOCHAIN, Denis; DE AZEVEDO, S Feyo; MAGNUS, Alphonse. Optimal selection of orthogonal polynomials applied to the integration of chemical reactor equations by collocation methods. **Computers & Chemical Engineering**, Elsevier, v. 24, n. 12, p. 2571–2588, 2000.

LIU, Bai-Nan; BOUTAT, Driss; LIU, Da-Yan. Backstepping observer-based output feedback control for a class of coupled parabolic PDEs with different diffusions. **Systems & Control Letters**, Elsevier, v. 97, p. 61–69, 2016.

LIU, Ya-Qiang; WANG, Jun-Wei; SUN, Chang-Yin. Observer-based output feedback compensator design for linear parabolic PDEs with local piecewise control and pointwise observation in space. **IET Control Theory & Applications**, IET, v. 12, n. 13, p. 1812–1821, 2018.

LIU, Zhihua; MAGAL, Pierre; SEYDI, Ousmane; WEBB, Glenn. Predicting the cumulative number of cases for the COVID-19 epidemic in China from early data. **arXiv preprint arXiv:2002.12298**, 2020.

LOFBERG, Johan. YALMIP: A toolbox for modeling and optimization in MATLAB. In: IEEE. 2004 IEEE international conference on robotics and automation (IEEE Cat. No. 04CH37508). [S.l.: s.n.], 2004. P. 284–289.

LONG, Youwei; WANG, Shugang; WANG, Jihong; ZHANG, Tengfei. Mathematical model of heat transfer for a finned tube cross-flow heat exchanger with ice slurry as cooling medium. **Procedia Engineering**, Elsevier, v. 146, p. 513–522, 2016.

LOPEZ-GOMEZ, ID; ESTRADA, O; OSSWALD, T. Modeling and simulation of polymer processing using the radial functions method. **Wak Zeitschrift Kunststofftechnik**, v. 3, n. 2, 2007.

LOTFI, El Mehdi; MAZIANE, Mehdi; HATTAF, Khalid; YOUSFI, Noura. Partial differential equations of an epidemic model with spatial diffusion. **International Journal of Partial Differential Equations**, Hindawi, v. 2014, 2014.

MAIDI, Ahmed; CORRIOU, Jean-Pierre. PDE control of heat exchangers by input-output linearization approach. In: ADVANCED Analytic and Control Techniques for Thermal Systems with Heat Exchangers. [S.l.]: Elsevier, 2020. P. 367–386.

MAMMERI, Youcef. A reaction-diffusion system to better comprehend the unlockdown: Application of SEIR-type model with diffusion to the spatial spread of COVID-19 in France. **arXiv preprint arXiv:2005.03499**, 2020.

MARKO, L; MENNEMANN, J-F; JADACHOWSKI, L; KEMMETMÜLLER, W; KUGI, A. Early-and late-lumping observer designs for long hydraulic pipelines: Application to

pumped-storage power plants. **International Journal of Robust and Nonlinear Control**, Wiley Online Library, v. 28, n. 7, p. 2759–2779, 2018.

MARTÍNEZ-GUERRA, Rafael; FLORES-FLORES, Juan Pablo. An algorithm for the robust estimation of the COVID-19 pandemic's population by considering undetected individuals. **Applied Mathematics and Computation**, Elsevier, v. 405, p. 126273, 2021.

MAVKOV, Bojan; WITRANT, Emmanuel; PRIEUR, Christophe. Distributed control of coupled inhomogeneous diffusion in tokamak plasmas. **IEEE Transactions on Control Systems Technology**, IEEE, v. 27, n. 1, p. 443–450, 2017.

MEYER, Evgeny; PEET, Matthew M. A Convex Approach for Stability Analysis of Coupled PDEs using Lyapunov Functionals. **arXiv preprint arXiv:1602.06986**, 2016.

MEYER, Evgeny; PEET, Matthew M. Stability analysis of parabolic linear PDEs with two spatial dimensions using Lyapunov method and SOS. In: IEEE. 2015 54th IEEE Conference on Decision and Control (CDC). [S.l.: s.n.], 2015. P. 1884–1890.

MIRANDA, Ramón; CHAIREZ, Isaac; MORENO, Jaime. Observer design for a class of parabolic PDE via sliding modes and backstepping. In: IEEE. VARIABLE Structure Systems (VSS), 2010 11th International Workshop on. [S.l.: s.n.], 2010. P. 215–220.

MIRÓN, Jesús; GONZÁLEZ, MªP; PASTRANA, Lorenzo; MURADO, MA. Diauxic production of glucose oxidase by Aspergillus niger in submerged culture: A dynamic model. **Enzyme and Microbial Technology**, Elsevier, v. 31, n. 5, p. 615–620, 2002.

MITCHELL, Andrew Ronald; GRIFFITHS, David Francis. The finite difference method in partial differential equations. **A Wiley-Interscience Publication**, 1980.

MOURA, Scott; BENDTSEN, Jan; RUIZ, Victor. Observer design for boundary coupled PDEs: Application to thermostatically controlled loads in smart grids. In: IEEE. 52ND IEEE conference on decision and control. [S.l.: s.n.], 2013. P. 6286–6291.

NESTEROV, Yurii; NEMIROVSKII, Arkadii. **Interior-point polynomial algorithms in convex programming**. [S.l.]: SIAM, 1994.

NGUYEN, Philipp; TENNO, Robert. Modelling and control of a flash evaporator through ODE system representation in PDEs form. In: IEEE. 2016 12th IEEE

International Conference on Control and Automation (ICCA). [S.l.: s.n.], 2016. P. 317–322.

OLIVEIRA, Ricardo CLF; PERES, Pedro LD. Stability of polytopes of matrices via affine parameter-dependent Lyapunov functions: Asymptotically exact LMI conditions. **Linear algebra and its applications**, Elsevier, v. 405, p. 209–228, 2005.

OMOSEBI, AO; IGBOKOYI, AO. Boundary effect on pressure behavior of Power-Law non-Newtonian fluids in homogeneous reservoirs. **Journal of Petroleum Science and Engineering**, Elsevier, v. 146, p. 838–855, 2016.

PAPACHRISTODOULOU, Antonis; ANDERSON, James; VALMORBIDA, Giorgio; PRAJNA, Stephen; SEILER, Peter; PARRILO, Pablo A. **Sum of squares optimization toolbox for MATLAB user's guide**. [S.l.]: University of Oxford, 2013.

PAPACHRISTODOULOU, Antonis; PEET, Matthew Monnig. On the analysis of systems described by classes of partial differential equations. In: IEEE. PROCEEDINGS of the 45th IEEE Conference on Decision and Control. [S.l.: s.n.], 2006. P. 747–752.

PARK, HM; CHO, DH. The use of the Karhunen-Loeve decomposition for the modeling of distributed parameter systems. **Chemical Engineering Science**, Elsevier, v. 51, n. 1, p. 81–98, 1996.

PARRILO, Pablo A. Semidefinite programming relaxations for semialgebraic problems. **Mathematical programming**, Springer, v. 96, n. 2, p. 293–320, 2003.

PARRILO, Pablo A. **Structured semidefinite programs and semialgebraic geometry methods in robustness and optimization**. [S.l.]: California Institute of Technology, 2000.

PARULEKAR, Satish J; RAMKRISHNA, Doraiswami. Tubular reactor stability revisited without the Danckwerts boundary conditions. **Chemical engineering science**, Elsevier, v. 39, n. 3, p. 455–469, 1984.

PAYNE, Lawrence E; WEINBERGER, Hans F. An optimal Poincaré inequality for convex domains. **Archive for Rational Mechanics and Analysis**, Springer, v. 5, n. 1, p. 286–292, 1960.

PAZY, Amnon. **Semigroups of linear operators and applications to partial differential equations**. [S.l.]: Springer Science & Business Media, 2012. v. 44.

POPOV, VM. Absolute stability of nonlinear systems of automatic control. **Automation and Remote Control**, v. 22, n. 8, p. 857–875, 1962.

RAJAEI, Arman; RAEISZADEH, Mahsa; AZIMI, Vahid; SHARIFI, Mojtaba. State estimation-based control of COVID-19 epidemic before and after vaccine development. **Journal of Process Control**, Elsevier, v. 102, p. 1–14, 2021.

RAY, WH. **Advanced process control, Series in chemical engineering**. [S.l.]: Butterworth, Boston, 1981.

ROCHA-CÓZATL, Edmundo; MORENO, Jaime A. Dissipative design of unknown input observers for systems with sector nonlinearities. **International Journal of Robust and Nonlinear Control**, Wiley Online Library, v. 21, n. 14, p. 1623–1644, 2011.

SANATKAR, Mohammad Reza; WHITE, Warren N; NATARAJAN, Balasubramaniam; SCOGLIO, Caterina M; GARRETT, Karen A. Epidemic threshold of an SIS model in dynamic switching networks. **IEEE Transactions on Systems, Man, and Cybernetics: Systems**, IEEE, v. 46, n. 3, p. 345–355, 2015.

SCHAUM, A; MEURER, T; MORENO, J. Dissipativity-based observer design for a class of coupled. In: 2ND IFAC Workshop on Control of Systems Modeled by Partial Differential Equations (CPDE). [S.l.: s.n.]. P. 99–104.

SCHAUM, Alexander; MEURER, Thomas; MORENO, Jaime A. Dissipative observers for coupled diffusion–convection–reaction systems. **Automatica**, Elsevier, v. 94, p. 307–314, 2018.

SCHAUM, Alexander; MORENO, Jaime A; FRIDMAN, Emilia; ALVAREZ, Jesus. Matrix inequality-based observer design for a class of distributed transport-reaction systems. **International Journal of Robust and Nonlinear Control**, Wiley Online Library, v. 24, n. 16, p. 2213–2230, 2014.

SÉRO-GUILLAUME, Olivier; RAMEZANI, Sepehr; MARGERIT, Jonathan; CALOGINE, Didier. On large scale forest fires propagation models. **International Journal of Thermal Sciences**, Elsevier, v. 47, n. 6, p. 680–694, 2008.

SMYSHLYAEV, Andrey; KRSTIC, Miroslav. Backstepping observers for a class of parabolic PDEs. **Systems & Control Letters**, Elsevier, v. 54, n. 7, p. 613–625, 2005.

STEWART, WE; SØRENSEN, JP. **Collocation and Parameter Estimation in Chemical Reaction Engineering**. [S.l.]: New York: John Wiley, 1980.

STURM, Jos F. Using SeDuMi 1.02, a MATLAB toolbox for optimization over symmetric cones. **Optimization methods and software**, Taylor & Francis, v. 11, n. 1-4, p. 625–653, 1999.

TSUBAKINO, Daisuke; HARA, Shinji. Backstepping observer design for parabolic PDEs with measurement of weighted spatial averages. **Automatica**, Elsevier, v. 53, p. 179–187, 2015.

TUCSNAK, Marius; WEISS, George. **Observation and control for operator semigroups**. [S.l.]: Springer Science & Business Media, 2009.

VANDENBERGHE, Lieven; BOYD, Stephen. Semidefinite programming. **SIAM review**, SIAM, v. 38, n. 1, p. 49–95, 1996.

VAZQUEZ, Rafael; KRSTIC, Miroslav; CORON, Jean-Michel. Backstepping boundary stabilization and state estimation of a $2\times$ 2 linear hyperbolic system. In: IEEE. 2011 50th IEEE conference on decision and control and european control conference. [S.l.: s.n.], 2011. P. 4937–4942.

VAZQUEZ, Rafael; SCHUSTER, Eugenio; KRSTIC, Miroslav. Magnetohydrodynamic state estimation with boundary sensors. **Automatica**, Elsevier, v. 44, n. 10, p. 2517–2527, 2008.

VIDYASAGAR, Mathukumalli. **Nonlinear systems analysis**. [S.l.]: SIAM, 2002.

VILLADSEN, John; MICHELSEN, Michael L. Solution of differential equation models by polynomial approximation(Book). **Englewood Cliffs, N. J., Prentice-Hall, Inc., 1978. 460 p**, 1978.

VILLADSEN, JV; STEWART, Warren E. Solution of boundary-value problems by orthogonal collocation. **Chemical Engineering Science**, Elsevier, v. 22, n. 11, p. 1483–1501, 1967.

VRIES, D; KEESMAN, KJ; ZWART, H. A Luenberger observer for an infinite dimensional bilinear system: a UV disinfection example. **IFAC Proceedings Volumes**, Elsevier, v. 40, n. 20, p. 667–672, 2007.

WANG, Jun-Wei; LIU, Ya-Qiang; SUN, Chang-Yin. Luenberger Observer Design for State Estimation of a Linear Parabolic Distributed Parameter System with Discrete Measurement Sensors. In: 12TH World Congress on Intelligent Control and Automation. [S.l.: s.n.], 2016. P. 1123–1128.

WANG, Yan; RAJAMANI, Rajesh; BEVLY, David M. Observer design for differentiable lipschitz nonlinear systems with time-varying parameters. In: IEEE. 53RD IEEE Conference on Decision and Control. [S.l.: s.n.], 2014. P. 145–152.

WEEKMAN JR, Vern W. Kinetics and dynamics of catalytic cracking selectivity in fixed-bed reactors. **Industrial & Engineering Chemistry Process Design and Development**, ACS Publications, v. 8, n. 3, p. 385–391, 1969.

WINKIN, Joseph J; DOCHAIN, Denis; LIGARIUS, Philippe. Dynamical analysis of distributed parameter tubular reactors. **Automatica**, Elsevier, v. 36, n. 3, p. 349–361, 2000.

WU, Fen; YILDIZOGLU, Suat E. Distributed parameter-dependent modeling and control of flexible structures, 2005.

WU, Huai-Ning; WANG, Hong-Du; GUO, Lei. Finite dimensional disturbance observer based control for nonlinear parabolic PDE systems via output feedback. **Journal of Process Control**, Elsevier, v. 48, p. 25–40, 2016.

XING, Xueyan; LIU, Jinkun. PDE modelling and vibration control of overhead crane bridge with unknown control directions and parametric uncertainties. **IET Control Theory & Applications**, Wiley Online Library, v. 14, n. 1, p. 116–126, 2020.

XU, Xiaodong; DUBLJEVIC, Stevan. The state feedback servo-regulator for countercurrent heat-exchanger system modelled by system of hyperbolic PDEs. **European Journal of Control**, Elsevier, v. 29, p. 51–61, 2016.

YANG, Hongjun; LIU, Jinkun; LAN, Xu. Observer design for a flexible-link manipulator with PDE model. **Journal of Sound and Vibration**, Elsevier, v. 341, p. 237–245, 2015.

YANG, Yu; DUBLJEVIC, Stevan. Linear matrix inequalities (LMIs) observer and controller design synthesis for parabolic PDE. **European Journal of Control**, Elsevier, v. 20, n. 5, p. 227–236, 2014.

YEBI, Adamu; AYALEW, Beshah. Partial differential equation-based process control for ultraviolet curing of thick film resins. **Journal of Dynamic Systems, Measurement, and Control**, American Society of Mechanical Engineers Digital Collection, v. 137, n. 10, 2015.

ZEMOUCHE, Ali; BOUTAYEB, Mohamed; BARA, G Iulia. Observer Design for Nonlinear Systems: An Approach Based on the Differential Mean Value Theorem. In: IEEE. PROCEEDINGS of the 44th IEEE Conference on Decision and Control. [S.l.: s.n.], 2005. P. 6353–6358.

ZHOU, Peng et al. A pneumonia outbreak associated with a new coronavirus of probable bat origin. **nature**, Nature Publishing Group, v. 579, n. 7798, p. 270–273, 2020.

APPENDIX A – CLASSICAL ORTHOGONAL POLYNOMIALS

In mathematics, the classical orthogonal polynomials are the most widely used orthogonal polynomials: the Hermite polynomials, Laguerre polynomials, Jacobi polynomials (including as a special case the Gegenbauer polynomials, Chebyshev polynomials, and Legendre polynomials).

Jacobi polynomials

The N-th order Jacobi polynomial $\mathbf{P}_N^{(\alpha,\beta)}$ on the space interval $[z_l, z_r]$ is defined by the orthogonal relation

$$\int_{z_l}^{z_r} (z-z_l)^{\beta}(z_r-z)^{\alpha}\mathbf{P}_j^{(\alpha,\beta)}(z)\mathbf{P}_N^{(\alpha,\beta)}(z)dz = 0, \quad j = 0, ..., N-1. \tag{333}$$

It can be seen from (333) that Jacobi polynomials are orthogonal. α and β denote weightings on the left end point z_l and right end point z_r, respectively. $\alpha = 1$ if z_l is included as an interpolation point, otherwise $\alpha = 0$. β is selected in the same way regarding the right end z_r.

For $(\alpha, \beta) = (0, 0)$, $\mathbf{P}_N^{(0,0)}$ reduces to the Legendre polynomials. For $(\alpha, \beta) = (\pm\frac{1}{2}, \pm\frac{1}{2})$, $\mathbf{P}_N^{(\pm\frac{1}{2},\pm\frac{1}{2})}$ reduces to the the Chebyshev polynomials (of the second and first kind, respectively). The Jacobi polynomials with $\alpha = \beta$ are called the Gegenbauer polynomials.

A power series representation $\mathbf{P}_N^{(\alpha,\beta)}$ can be written as

$$\mathbf{P}_N^{(\alpha,\beta)} = \sum_{i=0}^{N} (-1)^{N-i}\gamma_i z^i \tag{334}$$

where γ_i is calculated iteratively,

$$\gamma_i = \frac{N-i+1}{i}\frac{N+i+\alpha+\beta}{i+\beta}\gamma_{i-1} \tag{335}$$

in which $\gamma_0 = 1$ and $i = 1, ..., N$.

It has been providing, e.g., (VILLADSEN, John; MICHELSEN, 1978), that $\mathbf{P}_N^{(\alpha,\beta)}$ has N real and distinct zeros z_j,

$$z_l < z_j < z_r, \quad j = 1, ..., N. \tag{336}$$

A detailed numerical determination of the zeros of Jacobi polynomials can also be found in (VILLADSEN, John; MICHELSEN, 1978).

Remark A.1. *A classical choice of collocation points in the orthogonal collocation method is to take them as zeros of orthogonal polynomials, usually from the N-th order Jacobi polynomial* $\mathbf{P}_N^{(\alpha,\beta)}$.

Choosing zeros of classical orthogonal polynomials as collocation points makes orthogonal collocation approximations able to integrate exactly polynomials up to order $2N - 1$ *by means of quadrature formula (GAY, 1989), which actually is the maximum order of accuracy reachable with such* N*-th order approximations. In this sense, this choice can be considered as optimal, and, in practice, it provides results comparable with those obtained from Galerkin's method.*

APPENDIX B – HILBERT SPACES AND OPERATOR THEORY

Definition B.1. *Let $\mathcal{H}$ be a linear space over the real field $\mathbb{R}$. If for any pair $x_1,\ x_2 \in \mathcal{H}$ is defined a map $\langle\cdot,\cdot\rangle : \mathcal{H}\times\mathcal{H}\to\mathbb{R}$ with the properties*

- $\langle x_1, x_2\rangle = \langle x_2, x_1\rangle$*;*
- $\langle \alpha x_1 + \beta x_2, x_3\rangle = \alpha\langle x_1, x_3\rangle + \beta\langle x_2, x_3\rangle,\ \alpha,\ \beta \in \mathbb{R}$ *and* $x_3 \in \mathcal{H}$*;*
- $\langle x_1, x_1\rangle \geq 0$ *and* $\langle x_1, x_1\rangle = 0$ *if and only if* $x_1 = 0$*,*

then $\langle\cdot,\cdot\rangle$ is called a scalar product on $\mathcal{H}$. By the scalar product the norm

$$\|x\| = \sqrt{\langle x, x\rangle},\ \forall x \in \mathcal{H} \tag{337}$$

is defined. In addition, the Schwarz inequality

$$|\langle x_1, x_2\rangle| \leq \|x_1\|\|x_2\|$$

is valid. A Banach space with a scalar product and the norm defined by (337) *is called a Hilbert space.*

Lebesgue square integrable vector valued functions

The space $\mathcal{H} = \mathbf{L}_2^{n_x}(\Omega)$ is the Hilbert space of square integrable real vector valued functions $x : \Omega \subset \mathbb{R}^{n_z} \to \mathbb{R}^{n_x}$, which is equipped with an inner product generated by its norm

$$\langle x,x\rangle = \int_\Omega x^T(\mathrm{z})x(\mathrm{z})d\Omega < \infty \tag{338}$$

where $d\Omega = d\mathrm{z}_1 \ldots d\mathrm{z}_{n_z}$.

The basic example is when $\Omega = (a, b) \subset \mathbb{R}$ and $n_x = 1$, i.e,

$$\mathbf{L}_2(a,b) = \left\{ x : (a,b)\to\mathbb{R} : \left(\int_a^b x^2(z)dz\right)^{\frac{1}{2}} < \infty \right\}. \tag{339}$$

Sobolev spaces for scalar functions

The Sobolev space for $\mathcal{H} = \mathbf{W}^{1,2}(\Omega)$ is the Hilbert space, often denoted by $H^1(\Omega)$, defined as

$$\mathbf{W}^{1,2}(\Omega) = \left\{ x \in \mathbf{L}_2(\Omega) : D^\alpha x \in \mathbf{L}_2(\Omega)\ \forall\ |\alpha| \leq 1 \right\}. \tag{340}$$

Definition B.2. *A linear operator $\mathcal{T}$ is a map $\mathcal{T} : D(\mathcal{T}) \subset \mathcal{H}_1 \to \mathcal{H}_2$ such that for all $x_1,\ x_2 \in \mathcal{D}(\mathcal{T})$ and scalar α, it holds that*

$$\mathcal{T}(x_1 + x_2) = \mathcal{T}x_1 + \mathcal{T}x_2,$$
$$\mathcal{T}(\alpha x_1) = \alpha \mathcal{T}x_1.$$

Definition B.3. *Let $\mathcal{T}$ be a linear operator from $\mathcal{D}(\mathcal{T}) \subset \mathcal{H}_1$ to $\mathcal{H}_2$. $\mathcal{T}$ is a bounded linear operator if there exists a real number c such that for all $x \in \mathcal{D}(\mathcal{T})$*

$$\|Tx\|_{\mathcal{H}_2} \leq c\|x\|_{\mathcal{H}_1}.$$

Definition B.4. *Let $\mathcal{T}$ be a bounded linear operator from $\mathcal{D}(\mathcal{T}) \subset \mathcal{H}_1$ to $\mathcal{H}_2$. We define its norm, $\|\mathcal{T}\|$, by*

$$\|\mathcal{T}\| = \sup_{x \in \mathcal{D}(\mathcal{T})} \frac{\|\mathcal{T}x\|_{\mathcal{H}_2}}{\|x\|_{\mathcal{H}_1}},\quad x \neq 0.$$

A consequence of the previous definition is that $\|\mathcal{T}x\|_{\mathcal{H}_2} \leq \|\mathcal{T}\|\|x\|_{\mathcal{H}_1}$.

Definition B.5. *If $\mathcal{H}_1$ and $\mathcal{H}_2$ are normed linear spaces, we define the normed linear space $\mathcal{L}(\mathcal{H}_1, \mathcal{H}_2)$ to be the space of bounded linear operators from $\mathcal{H}_1$ to $\mathcal{H}_2$ with $D(T) = \mathcal{H}_1$. For the special case that $\mathcal{H}_1 = \mathcal{H}_2$ we denote $\mathcal{L}(\mathcal{H}_1, \mathcal{H}_1)$ by $\mathcal{L}(\mathcal{H}_1)$.*

Definition B.6. *Assume that the domain of the linear operator $\mathcal{A}$, $\mathcal{D}(\mathcal{A}) \subset \mathcal{H}$, is dense in $\mathcal{H}$. Then the adjoint operator $\mathcal{A}^* : D(\mathcal{A}^*) \subset \mathcal{H} \to \mathcal{H}$ of $\mathcal{A}$ is defined as $\langle \mathcal{A}x_1, x_2\rangle = \langle x_1, \mathcal{A}^*x_2\rangle$, where $x_2 \in D(\mathcal{A}^*)$ and $\mathcal{A}^*x_2 = x_2^*$.*

Definition B.7. *We say that a densely defined, linear operator $\mathcal{A}$ is symmetric if for all $x_1,\ x_2 \in \mathcal{D}(\mathcal{A})$*

$$\langle \mathcal{A}x_1, x_2\rangle = \langle x_1, \mathcal{A}x_2\rangle.$$

A symmetric operator is selfadjoint if $\mathcal{D}(\mathcal{A}^*) = \mathcal{D}(\mathcal{A})$.

Definition B.8. *A self-adjoint operator $\mathcal{A}$ on the Hilbert space $\mathcal{H}$ is nonnegative if*

$$\langle \mathcal{A}x, x\rangle \geq 0,\ \forall x \in \mathcal{D}(\mathcal{A});$$

$\mathcal{A}$ is positive if

$$\langle \mathcal{A}x, x\rangle > 0,\ \forall x \in \mathcal{D}(\mathcal{A})\ x \neq 0;$$

and $\mathcal{A}$ is coercive if there exists an $\epsilon > 0$ such that

$$\langle \mathcal{A}x, x\rangle \geq \epsilon\|x\|^2,\ \forall x \in \mathcal{D}(\mathcal{A}).$$

APPENDIX C – INSTRUMENTAL RESULTS

In this appendix, we present some statements and results used for the development of this thesis.

Definition C.1. *Let $x,\ \hat{x} \in \mathbb{R}^n$. We define by $Co(x, \hat{x})$ the convex hull of the set $\{x,\ \hat{x}\}$, i.e.*

$$\mathrm{Co}(x, \hat{x}) = \left\{\theta x + (1-\theta)\hat{x} :\ \theta \in [0, 1]\right\}. \tag{341}$$

Lemma C.1. *(Differential mean value theorem (ZEMOUCHE et al., 2005))*
Let the function $r(x) : \mathbb{R}^n \to \mathbb{R}$ differentiable with respect to x and let $x,\ \hat{x}$ be two elements in $\mathbb{R}^n$. Then, there is an element $\breve{x} \in Co(x, \hat{x})$, such that:

$$r(x) - r(\hat{x}) = \nabla r(\breve{x})(x - \hat{x}) \tag{342}$$

where $\nabla r = \begin{bmatrix} \partial_{x_1} r & \cdots & \partial_{x_n} r \end{bmatrix}$.

Lemma C.2. *(Wirtinger's inequality (HARDY et al., 1970))*
Let $x \in \mathbf{W}^{1,2}([a, b])$ be a scalar function with $x(a) = 0$ or $x(b) = 0$, then the following inequality holds

$$\int_a^b x^2(z)dz \leq \frac{4(b-a)^2}{\pi^2} \int_a^b \left(\frac{dx}{dz}(z)\right)^2 dz. \tag{343}$$

Lemma C.3. *(Poincaré–Wirtinger inequality (ADAMS, 1978))*
Let Ω be an open bounded Lipschitz connected subset in $\mathbb{R}^n$. Then there exists a constant C_Ω, depending only on Ω, such that for every function $x \in W^{1,2}(\Omega)$

$$\int_\Omega (x(\mathbf{z}) - m_x)^2\, d\Omega \leq C_\Omega \int_\Omega |\nabla_{\mathbf{z}} x(\mathbf{z})|^2 d\Omega. \tag{344}$$

where

$$m_x = \frac{1}{|\Omega|} \int_\Omega x(\mathbf{z}) d\Omega. \tag{345}$$

is the mean value of x over Ω, with $|\Omega|$ standing for the Lebesgue measure of the domain Ω.

Remark C.1. *The Poincaré constant C_Ω depends on the geometry of the domain Ω. Particularly, if Ω is a bounded, convex, Lipschitz domain with diameter d, then the Poincaré constant is at most d/π (PAYNE; WEINBERGER, 1960).*

Lemma C.4. *(Schur Complement lemma (BOYD, S. et al., 1994)) Consider the matrix*

$$M = \begin{bmatrix} A & B \\ C & D \end{bmatrix} \tag{346}$$

with D, a non-singular (invertible) matrix. The matrix

$$S = A - BD^{-1}C \tag{347}$$

is called the Schur complement of D in M. If M is a symmetric definite matrix then $M > 0$ *is equivalent to*

$$D > 0 \quad \textit{and} \quad S = A - BD^{-1}C > 0. \tag{348}$$

The S-procedure for quadratic forms and strict inequalities

Let $T_0, ..., T_p \in \mathbb{R}^{n\times n}$ be symmetric matrices. We consider the following condition on $T_0, ..., T_p$:

$$\zeta^T T_0 \zeta > 0 \ \ \forall\ \zeta \neq 0 \quad \text{such that} \quad \zeta^T T_i \zeta \geq 0,\ \ i = 1, ...,\ \ p. \tag{349}$$

It is obvious that if there exists scalars $\tau_i \geq 0$, $i = 1, ..., p$ such that

$$T_0 - \sum_{i=1}^{p} \tau_i T_i > 0 \tag{350}$$

then (349) holds. It is a nontrivial fact that when $p = 1$, the converse holds, provided that there is some ζ_0 such that $\zeta_0^T T_1 \zeta_0 > 0$. Note that (350) is an LMI in the variables T_0 and $\tau_i \geq 0$, $i = 1, ..., p$.

APPENDIX D – INTEGRATION BY PARTS

In this thesis, we will restrict ourselves to the use of equalities generated through the use of the technique known as integration by parts. In its most general form, this equality is defined by the following, where for a vector field $\mathbf{u}$ and a scalar function v defined in the closure of an open solid region $\Omega \in \mathbb{R}^{n_z}$. $\partial\Omega$ denotes the boundary of the region Ω and $\mathbf{n}$ is the outward normal vector to this boundary.

$$\int_{\Omega} \mathbf{u} \cdot \nabla v d\Omega = \int_{\partial\Omega} v\mathbf{u} \cdot \mathbf{n} d\partial\Omega - \int_{\Omega} v\nabla \cdot \mathbf{u} d\Omega. \tag{351}$$

The case $\mathbf{u} = \nabla u$, where $u \in C^2(\Omega)$, is known as the first of Green's identities:

$$\int_{\Omega} \nabla u \cdot \nabla v d\Omega = \int_{\partial\Omega} v\Delta u \cdot \mathbf{n} d\partial\Omega - \int_{\Omega} v\Delta u d\Omega. \tag{352}$$

INTEGRATION BY PARTS OF QUADRATIC FORMS

For the Lyapunov convergence assessment, we are interested in integrals related to quadratic forms of the state vector and its first or second derivative.

We consider first the one-dimensional integral

$$\int_a^b e^T(z)\tilde{\mathcal{V}}(z)\partial_z e(z)dz = \sum_{i,j}^{n} \int_a^b e_i(z)\nu_{ij}(z)\partial_z e_j(z)dz \tag{353}$$

with $\tilde{\mathcal{V}} : [a, b] \to \mathbb{R}^{n\times n}$. Thus, integrating by parts the terms of the summation, it is easy to show that

$$\int_a^b e^T(z)\left(\tilde{\mathcal{V}}(z) + \tilde{\mathcal{V}}^T(z)\right)\partial_z e(z)dz = e^T(z)\tilde{\mathcal{V}}(z)e(z)\Big|_a^b - \int_a^b e^T(z)\partial_z\tilde{\mathcal{V}}(z)e(z)dz. \tag{354}$$

If $\mathcal{V} : [a, b] \to \mathbb{S}^n$, then we have

$$\int_a^b e^T(z)\tilde{\mathcal{V}}(z)\partial_z e(z)dz = \frac{1}{2}e^T(z)\tilde{\mathcal{V}}(z)e(z)\Big|_a^b - \frac{1}{2}\int_a^b e^T(z)\partial_z\tilde{\mathcal{V}}(z)e(z)dz. \tag{355}$$

Similarly the one-dimensional integral

$$\int_a^b e^T(z)\tilde{D}(z)\partial_z^2 e(z)dz = \sum_{i,j}^{n} \int_a^b e_i(z)\tilde{d}_{ij}(z)\partial_z^2 e_j(z)dz. \tag{356}$$

with $\tilde{D} : [a, b] \to \mathbb{R}^n$. Thus, its integration by parts yields

$$\int_a^b e^T(z)\tilde{D}(z)\partial_z^2 e(z)dz = e^T(z)\tilde{D}(z)\partial_z e(z)\Big|_a^b - \int_a^b \partial_z e^T(z)\tilde{D}(z)\partial_z e(z)dz - \int_a^b e^T(z)\partial_z\tilde{D}(z)\partial_z e(z)dz. \quad (357)$$

If $\tilde{D} : [a, b] \to \mathbb{S}^n$, we can apply the identity in (355) into the last term of the right side of (357), thus we obtain

$$\int_a^b e^T(z)\tilde{D}(z)\partial_z^2 e(z)dz = e^T(z)\tilde{D}(z)\partial_z e(z)\Big|_a^b - \frac{1}{2}e^T(z)\partial_z\tilde{D}(z)e(z)\Big|_a^b + \frac{1}{2}\int_a^b e^T(z)\partial_z^2\tilde{D}(z)e(z)dz - \int_a^b \partial_z e^T(z)\tilde{D}(z)\partial_z e(z)dz. \quad (358)$$

In bidimensional systems, we are interested in the integral

$$\int_\Omega e^T(\mathbf{z})\tilde{D}(\mathbf{z})\Delta e(\mathbf{z})d\Omega = \sum_{i,j}^n \int_\Omega e_i(\mathbf{z})\tilde{d}_{ij}(\mathbf{z})\Delta e_j(\mathbf{z})d\Omega. \quad (359)$$

Applying Green's first identity in the right side of (359), it yields

$$\sum_{i,j}^n \int_\Omega e_i(\mathbf{z})\tilde{d}_{ij}(\mathbf{z})\Delta e_j(\mathbf{z})d\Omega = \sum_{i,j}^n \Big(\int_{\partial\Omega} e_i(\mathbf{z})\tilde{d}_{ij}(\mathbf{z})\nabla e_j(\mathbf{z})\cdot\mathbf{n}dl - \int_\Omega \tilde{d}_{ij}(\mathbf{z})\nabla e_i(\mathbf{z})\cdot\nabla e_j(\mathbf{z})d\Omega\Big) + \frac{1}{2}\int_\Omega e_i(\mathbf{z})\Delta\tilde{d}_{ij}(\mathbf{z})e_j(\mathbf{z})d\Omega - \frac{1}{2}\int_{\partial\Omega} e_j(\mathbf{z})\nabla\tilde{d}_{ij}(\mathbf{z})e_i(\mathbf{z})\cdot\mathbf{n}dl. \quad (360)$$

For Neumann boundary conditions $\Delta e\cdot\mathbf{n}\Big|_{\partial\Omega} = 0$

$$\int_\Omega e^T(\mathbf{z})\tilde{D}(\mathbf{z})\Delta e(\mathbf{z})d\Omega = \frac{1}{2}\int_\Omega e^T(\mathbf{z})\Delta\tilde{W}(\mathbf{z})e(\mathbf{z})d\Omega - \int_\Omega (\mathrm{vec}\nabla e(\mathbf{z}))^T\left[I_2\otimes\tilde{W}(\mathbf{z})\right](\mathrm{vec}\nabla e(\mathbf{z}))\,d\Omega. \quad (361)$$